Dynamics and Morphodynamic Implications of

Chute Channels in Large, Sand-Bed Meandering Rivers

Michael C. Grenfell

Doctor of Philosophy in Geography

College of Life and Environmental Sciences

UNIVERSITY OF
EXETER

July 2012

Dynamics and Morphodynamic Implications of
Chute Channels in Large, Sand-Bed Meandering Rivers

Submitted by Michael Cyril Grenfell

to the University of Exeter

as a thesis for the degree of Doctor of Philosophy

in Geography in the College of Life and Environmental Sciences

July 2012

This thesis is available for Library use on the understanding that it is copyright material and that no quotation from the thesis may be published without proper acknowledgement.

I certify that all material in this thesis which is not my own work has been identified, and that no material has previously been submitted and approved for the award of a degree by this or any other University.

....

Michael Cyril Grenfell

ABSTRACT

Chute channel formation is a key process in the transition from a single-thread meandering to a braided channel pattern, but the physical mechanisms driving the process remain unclear. This research combines GIS and spatial statistical analyses, field survey, Delft3D hydrodynamic and morphodynamic modelling, and Pb-210 alpha-geochronology, to investigate controls on chute initiation and stability, and the role of chute channels in the planform dynamics of large, sand-bed meandering rivers. Sand-bed reaches of four large, tropical rivers form the focus of detailed investigations; the Strickland and Ok Tedi in Papua New Guinea, the Beni in Bolivia, and the lower Paraguay on the Paraguay/Argentina border. Binary logistic regression analysis identifies bend migration style as a key control on chute channel initiation, with most chute channels forming at bends that are subject to a rapid rate of extension (elongation in a direction perpendicular to the valley axis). Bend extension rates are shown to track variation in potential specific stream power, such that reaches and sub-reaches of the rivers studied fit within a planform continuum expressed though increasing bend extension rates and chute initiation frequency, and driven by increasing stream power relative to bedload calibre.

Field observations of point bar geomorphology and vegetation dynamics illustrate the importance of rapid bend extension in forming wide sloughs between scroll bars that are aligned with the direction of over-bar flow, and in breaking the continuity of vegetation encroachment on point bars. Bathymetric surveys and Delft3D simulations for the Strickland River provide insight into flow and sediment division at bifurcate meander bends. Coupled with GIS analyses, these simulations show that stable chute channels have higher gradient advantages than chute channels subject to infill, but that upstream and downstream changes in bend orientation can also influence chute stability. The process of bend extension is typically associated with an increase in the chute gradient advantage, further elucidating the role of bend migration style in chute

stability. At the reach scale, rivers with higher sediment loads (Qs/Q) are characterised by higher rates of chute infill.

Strickland River floodplain sedimentation rates derived through Pb-210 alpha-geochronology are substantially higher adjacent to single-thread bends than adjacent to bifurcate bends, potentially due to an observed increase in channel capacity (and reduction in floodplain inundation frequency) associated with bend bifurcation. Further research is needed to determine whether this observation is significant in light of high uncertainty in the spatial variability of sedimentation rate estimates, but the data presented highlight a need for carefully considered stratified sampling approaches in floodplain coring campaigns, and illustrate the complexity of possible sediment dispersal mechanisms, and associated ecological responses.

GIS analysis of the response of the Ok Tedi in Papua New Guinea to direct addition of mine tailings elucidates interplay between channel steepening due to the propagation of a tailings sediment slug, and mid-channel bar formation induced by the increased sediment load, with associated topographic forcing of bend and chute development. A temporal pattern of increased chute initiation frequency on the Ok Tedi mirrors the inter- and intra-reach spatial pattern of chute initiation frequency on the Paraguay, Strickland and Beni Rivers, where increased stream power is associated with increased bend extension and chute initiation rates. The process of chute formation is shown to be rate-dependent, and the threshold value of bend extension for chute initiation is shown to scale with reach-scale stream power, reminiscent of slope-ratio thresholds in river avulsion. However, Delft3D simulations suggest that chute formation can exert negative feedback on shear stress and bank erosion in the adjacent mainstem bifurcate, such that the process of chute formation is also rate-limiting. Chute formation is activated iteratively in space and time in response to changes in river energy, selectively targeting sites of greatest change, and thereby mediating the river response.

LIST OF CONTENTS

LIST OF TABLES

LIST OF FIGURES

meander bend Str54.

ACKNOWLEDGEMENTS

Nambawan lik-lik wopa biscuit deserve special mention; I'm not sure what they put in those biscuits, but it is remarkable how many days one can survive eating little else!

I am grateful to Dave Pennyfather and Geoff Pickup for providing various geographic data for the Fly, Strickland and Ok Tedi, and to Porgera Mining for providing Strickland flow data. John Lewin kindly offered to read a draft of the second chapter, and provided excellent feedback and encouragement. Tom Dunne provided insightful feedback on a presentation of some of my early results, and both Tom and John's interest in this work has been a source of inspiration.

My research was funded primarily by the University of Exeter, through a graduate fellowship. Fieldwork in Papua New Guinea was funded by the American National Science Foundation Margins Source-to-Sink Research Programme. Support for accommodation at the American Geophysical Union Fall Meeting in December 2011 was provided by the British Society for Geomorphology. I would like to thank these organisations for their support. Finally, I would like to thank NASA for opening their Landsat data archives to the public domain. This action has significantly advanced the study of large rivers that are difficult to cover in the field, and this thesis would have been a lot lighter without NASA's free provision of Landsat imagery!

CHAPTER 1

Introduction

1.1. Large Rivers Research

Large rivers play a globally significant role in transferring fluid and particulate matter from continental sources to distant intra-continental or oceanic sinks (Gupta, 2007; Guyot and Walling, 2009). Potter (1978) was the first to attempt to explicitly distinguish 'large' rivers from the rest, in a study of fluvial sand dispersal and sandstone geology. Lacking extensive discharge and sediment load data (given the date of the study), Potter (1978) suggested that large rivers are those with lengths exceeding 1000 km, and drainage basin areas exceeding 100 000 km^2, but argued that discharge was probably the most fundamental single rank criterion. Annual average water discharge is currently most commonly used to rank the World's largest rivers (e.g. Meade, 1996; Gupta, 2007), but river length, drainage basin area, and suspended sediment and solute loads are also considered in many ranking systems.

Inclusion of these other parameters is important because rivers in particular geo-climatic settings, although not high-ranking in terms of discharge, supply globally significant volumes of sediment to the ocean (Milliman and Meade, 1983; Milliman and Syvitski, 1992; Milliman, 1995; Milliman and Farnsworth, 2011). For example, rivers draining the island of New Guinea (land surface area ~ 800 000 km^2) discharge approximately the same amount of sediment annually as the combined estimated loads of all rivers draining North America (land surface area ~ 25 000 000 km^2; Milliman, 1995). A single, standard definition for 'large rivers' has not been sought, as large rivers research has gained momentum in recent years more as a way of thinking about and investigating fluvial systems, than as a rank-specific, scale-constrained path of inquiry. Nonetheless, large rivers possess several key defining characteristics.

First, large rivers are important components of continental- and sub-continental-scale landforms (Gupta, 2007). They integrate the hydrological response of very large areas, such that changes in their behaviour in response to global change provide an important indicator of changes in the hydrological response of the Earth system (Blum, 2007; Guyot and Walling, 2009). However, it is seldom possible to fully disentangle effects of global (e.g. climate) change from those brought about by direct anthropogenic alteration of catchment conditions (Walling and Fang, 2003; Blum, 2007), partly because the magnitude and extent of alteration has been so great, and partly through a lack of understanding of large river processes (Gupta, 2002; 2007).

Large rivers also integrate the effects of earth surface processes at very large scales, and therefore play a fundamental role in landscape evolution, and in material fluxes from continental interiors to sedimentary basins (Blum, 2007). Some large rivers are associated with fluxes of water, sediment and solutes large enough to play a significant role in global biogeochemical cycles (Sinha and Friend, 2007). For example, recent studies have shown that the burial of carbon on continents, notably within floodplain deposits of large rivers, is an order of magnitude greater than the burial of carbon in the oceans (Aufdenkampe *et al.*, 2011).

Second, due to their great length, many large rivers flow across a range of environments, alternating between rock-cut and alluvial reaches, and are subject to morphological and behavioural adjustments at each transition (Gupta, 2002; 2007). Thus, large rivers are commonly polyzonal; different reaches integrate signals from different physiographic regions, each of which may be subject to a different magnitude and direction of change in discharge and sediment supply over time (Blum, 2007). As a result, large rivers often have complex Quaternary histories, with different modes of change in the uplands, lowlands and at the mouth (Gupta, 2002). Event-scale hydrological responses in large rivers may be damped by extended flood travel times (Guyot and

Walling, 2009), but longer-term shifts in flood magnitude and frequency are surprisingly rapidly transferred through large basins, relative to the timescales required to transfer changes in sediment supply (Blum, 2007). Aggregation and buffering processes that operate in large river basins can dampen or remove signals of increasing sediment flux, and thereby complicate the link between upstream and downstream response to environmental change (Thorne, 2002; Walling, 2006).

Third, large rivers play a central role in hydropower generation, interbasin water transfers, transportation, agricultural production (irrigation) and mining, fisheries, domestic water consumption, and tourism (Latrubesse *et al.*, 2009). Thus, large rivers are exposed to problems of multiple and often conflicting uses, and pressures and impacts on the World's large rivers have increased greatly in recent years as a consequence of their exploitation to meet the needs of a growing World population (Sinha and Friend, 2007; Lu and Jiang, 2009; Vienna Declaration, 2011). In addition, large rivers typically flow through international basins, so that anthropogenic impacts on large rivers are transboundary in nature, and are therefore difficult to mitigate (Gupta, 2007).

Fourth, large river floodplains and megafans host a large proportion of the World's tropical rainforests and globally significant wetland systems such as El Pantanal (e.g. Assine and Soares, 2004; Assine and Silva, 2009) and the Okavango Swamps (McCarthy and Ellery, 1998), and are associated with high species richness due to their size, varied age structure and habitat complexity. Flood pulse dynamics associated with large river-wetland systems in the tropics (e.g. Junk *et al.*, 1989; Junk, 1999) introduce hydrological seasonality to otherwise relatively unseasonal (climatically) environments, and thereby fundamentally shape ecological interactions (Sparks, 1995). However, the benefits of large rivers to economic productivity have been accompanied by impairment to ecosystems and biodiversity (e.g. Sparks, 1995; Vörösmarty *et al.*, 2010).

Humans have simultaneously increased sediment transport by global rivers through catchment land degradation and soil erosion, yet reduced the flux of sediment reaching the coasts largely due to sand-mining and retention in reservoirs (Syvitski *et al.*, 2005). It is estimated that 25 to 30 % of the total global sediment flux is intercepted by reservoirs (Vörösmarty *et al.*, 2003), and over half of the World's large river systems are affected by impoundment (Nilsson *et al.*, 2005), and evidence declining sediment loads (Walling and Fang, 2003; Lu and Chen, 2008). Many large rivers terminate in large, long-lived deltas which have played a major role in basin filling in both deep and shallow waters (Potter, 1978), and disruption of sediment supply to these and other coastal environments by reservoir construction has broad ecological and environmental consequences that are not yet fully understood (Vörösmarty *et al.*, 2003; Lu and Chen, 2008).

Finally, large rivers are difficult environments to investigate, requiring heavy reliance on temporally-stuttered observation windows provided by satellite imagery, protracted, logistically-challenging field campaigns (Thorne, 2002; Gupta, 2002; 2007), and novel approaches to data collection and spatial integration of the heterogeneity contained within their large drainage basins (Guyot and Walling, 2009). As a consequence, less is known about the hydrology, geomorphology, sedimentology, and ecology of large rivers, than small rivers that are easier to cover in the field, model, and manage (Gupta, 2007). This in itself provides strong motivation for large rivers research.

In addition, large rivers have played a defining role in the development and fate of ancient civilisations (Gupta, 2002; 2007; Schumm, 2005), have served as navigation pathways for modern exploration (Gupta, 2007), drive large-scale natural hazards such as floods, bank erosion and rapid channel migration (Latrubesse *et al.*, 2009), and will play a defining role in the future of a large proportion of the World's population (Sinha and Friend, 2007; Vienna Declaration, 2011). It is therefore critical that we advance our understanding of these globally significant landscape systems.

1.2. Planform Dynamics of Alluvial Rivers

Channel Planform Classification

'River channel planform' refers to the channel pattern as viewed from above, at a scale of tens of bar or meander lengths (Kleinhans, 2010). Spatial and temporal variation and transitions in channel planform have captivated geomorphologists for over a century (e.g. Lokhtin, 1897), as it has long been recognised that planform dynamics provide insight into river behaviour and river responses to internal and external change (Schumm, 1985). Changes in planform therefore provide an indicator of change that if correctly interpreted may prove a valuable river management tool (Brierley and Fryirs, 2005). There have been four broad approaches to investigating and explaining river planform; i) qualitative classifications, based primarily on image analysis, ii) empirical discriminations based on slope, discharge, stream power, shear stress, sediment load, and/or sediment calibre, iii) experimental attempts at creating particular planform types, and iv) physics-based predictors of bar pattern or branching intensity. In addition, there have been several general reviews of approaches, and attempts at synthesising and reinterpreting existing data (e.g. Schumm, 1985; Ferguson, 1987; Alabyan and Chalov, 1998; Kleinhans, 2010).

Qualitative river morphology/planform classifications provide a common language for communication among researchers (Eaton *et al.*, 2010). Their application and value is perhaps best summarised by Brierley and Fryirs (2005: 12): "In making inferences from system-specific information, cross-reference is made to theoretical and empirical relationships to explain system behaviour and predict likely future conditions", and therefore qualitative classifications offer "a conceptual tool with which to read and interpret landscapes". Qualitative classifications generally draw on empirical and experimental work, providing syntheses of forms that may be useful in certain management contexts, but provide limited insight into the underlying physical controls on planform change, and the morphodynamics associated with particular patterns (Eaton *et al.*, 2010). As a point of departure, a simple, qualitative summary of

the basic channel planform types recognised in the literature is provided in Figure 1.1, and this is followed by a more detailed review of planform definitions, and qualitative, empirical, experimental, and physics-based approaches to investigating planform controls. The review excludes distributive multiple-channel patterns such as those found on deltas, where channel branching is not often accompanied by re-joining (e.g. Edmonds and Slingerland, 2008).
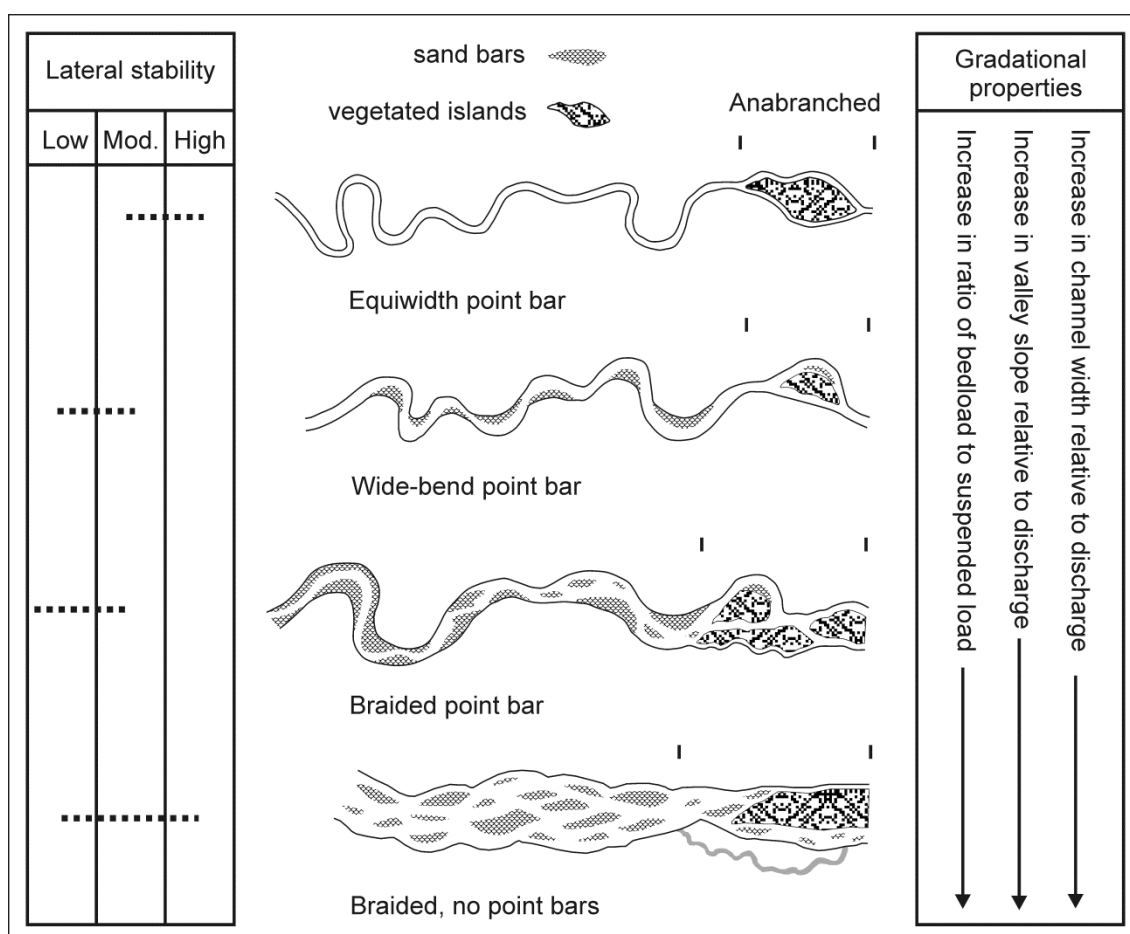
Figure 1.1: A general, simplified qualitative classification of river channel planform, based on planimetric pattern and temporal dynamics (modified from Brice, 1982). This classification scheme is largely consistent with the recent empirical/physics-based discriminant functions of Kleinhans and van den Berg (2011).

At the simplest level, channel patterns may be distinguished as either single-thread or multiple-thread. Single-thread channels may be either straight or sinuous, and either laterally stable or actively migrating across a floodplain

(Figure 1.2). A channel sinuosity (P) of 1.5 (channel length divided by valley-axis length) is traditionally used to distinguish between low (P < 1.5) and high (P > 1.5) sinuosity channels (Leopold and Wolman, 1957; Begin, 1981), with straight channels having a sinuosity of ~ 1. Straight channels are rare in nature, and are often set within some sort of structural grain that inhibits bank erosion. Thus, unless restricted from doing so, rivers tend to adopt a planform other than straight. The term 'meandering' has been loosely applied in the past to refer to both laterally stable and actively migrating high-sinuosity channels, but herein applies only to actively migrating high-sinuosity channels set within alluvial floodplains (as in the case of Kleinhans and van den Berg, 2011). Individual branches within some multiple-thread channel types may also be described in terms of their sinuosity and lateral mobility (Nanson and Knighton, 1996), although their overall classification would remain multiple-thread.
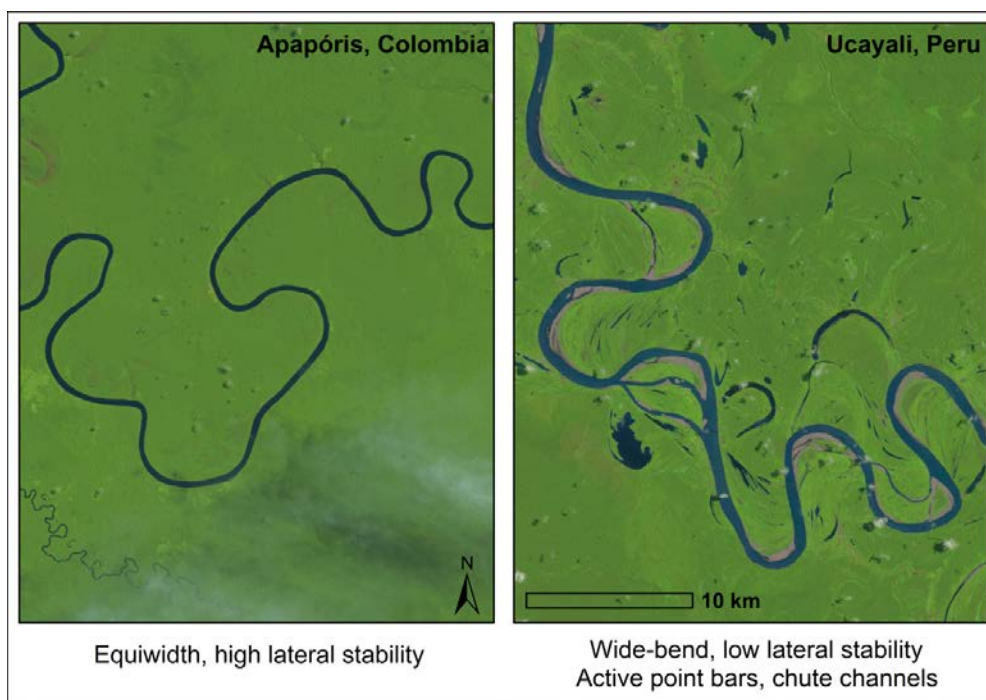
Figure 1.2: 'Landsatlook' Landsat 7 ETM+ false-colour composites showing single-thread channel patterns. The sinuous, equiwidth pattern of the laterally-stable Apapóris River in Colombia contrasts sharply with the wide-bend/chute pattern of the Ucayali River in Peru. The Ucayali has a prominently-scrolled floodplain, and unvegetated point bars, indicative of active lateral migration. Image source: USGS Global Visualisation Viewer.

Multiple-thread channels may be either braided or anabranching (Figure 1.3). Nanson and Knighton (1996: 218) define anabranching as "a system of multiple channels characterised by vegetated or otherwise stable alluvial islands that divide flows at discharges up to nearly bankfull". Key distinctions between braiding and anabranching are that the islands of anabranching networks persist for decades or centuries, are well-vegetated and have relatively stable banks, and are of a similar elevation to that of the surrounding floodplain, whereas the islands of braided networks typically comprise sediment bars that may only be exposed at low to moderate flows, and consist of poorly consolidated and sparsely vegetated material that is mobile at sub-decadal timescales (Nanson and Knighton, 1996). Anastomosing channels are considered a subset of the anabranching class, traditionally used to describe low-energy anabranching channels set within highly cohesive or densely-vegetated banks, such that individual branches have little to no lateral mobility (Ellery *et al.*, 1993; Knighton and Nanson, 1993; Makaske, 2001).

Anabranching in Alluvial Rivers

Early investigations into the cause of anabranching by Richards *et al.* (1993) and Knighton and Nanson (1993) agreed on two key points now supported by a large (and growing) body of research, i) anabranching rivers do not fit comfortably within empirical meandering-braided channel pattern continua (discussed further in a following section), and ii) avulsion driven by aggradation is a key mechanism of anabranch formation. Anabranching channel networks typically comprise one primary channel that is dominant in terms of bedload transport, and several secondary channels (incomplete avulsions) that may assume a primary role if aggradation of the primary channel switches the dominant transport thread (Richards *et al.*, 1993; Jerolmack and Mohrig, 2007; Jerolmack and Paola, 2007; Kleinhans *et al.*, 2008).

Jerolmack and Mohrig (2007) demonstrated that avulsion frequency in aggrading settings scales with the time required for channel bed sedimentation to produce a deposit equal to one channel depth, and that anabranching may

only be maintained in environments undergoing bed aggradation rates that are rapid compared with lateral channel migration rates. This finding supports the suggestion by Knighton and Nanson (1993) that anabranch formation should be favoured in settings where the rate of sediment supply exceeds the transport capacity of the channel, and (in the case of anastomosing channels) resistant banks limit lateral channel migration that could provide space for excess sediment storage in lateral accretion deposits (e.g. point bars). These findings are in turn supported by Makaske *et al.* (2009), and Kleinhans *et al.* (2012), who suggest that anabranching channels are characterised by a disequilibrium flow-sediment feed, but that frequent avulsion is a consequence of bed aggradation progressing more rapidly than levee accretion in laterally-stable channels.

In a comprehensive review of the causes and characteristics of anabranching rivers, Nanson and Knighton (1996) suggest that a semi-permanent system of multiple channels offers a means of concentrating flow and maximizing bedload transport in settings where there is little or no opportunity to increase gradient. Huang and Nanson (2007) demonstrated that an increase in the number of channels in an anabranching network may produce a proportional decrease in flow efficiency, but flow efficiency may be significantly increased by a reduction in channel width, which occurs during the development of vegetated alluvial islands or between-channel ridges. Huang and Nanson (2007) concluded that this interplay between the formation of new channels and adjustments to channel geometry during island development is able to balance river energy where longitudinal slope adjustments are impeded. It is within this theoretical context that Latrubesse (2008) framed the tendency for mega-rivers (rivers with mean annual discharges greater than 17 000 m^3 s^{-1}) to develop anabranching patterns. Following Huang and Nanson (2007), Latrubesse (2008) suggested that because mega-rivers have very low slopes (<0.00015 m m^{-1}) through hundreds of kilometres upstream of the ocean, but high discharge and sediment loads, transport may be hydraulically forced by island deposition, which reduces channel width and maximizes flow depth and velocity.
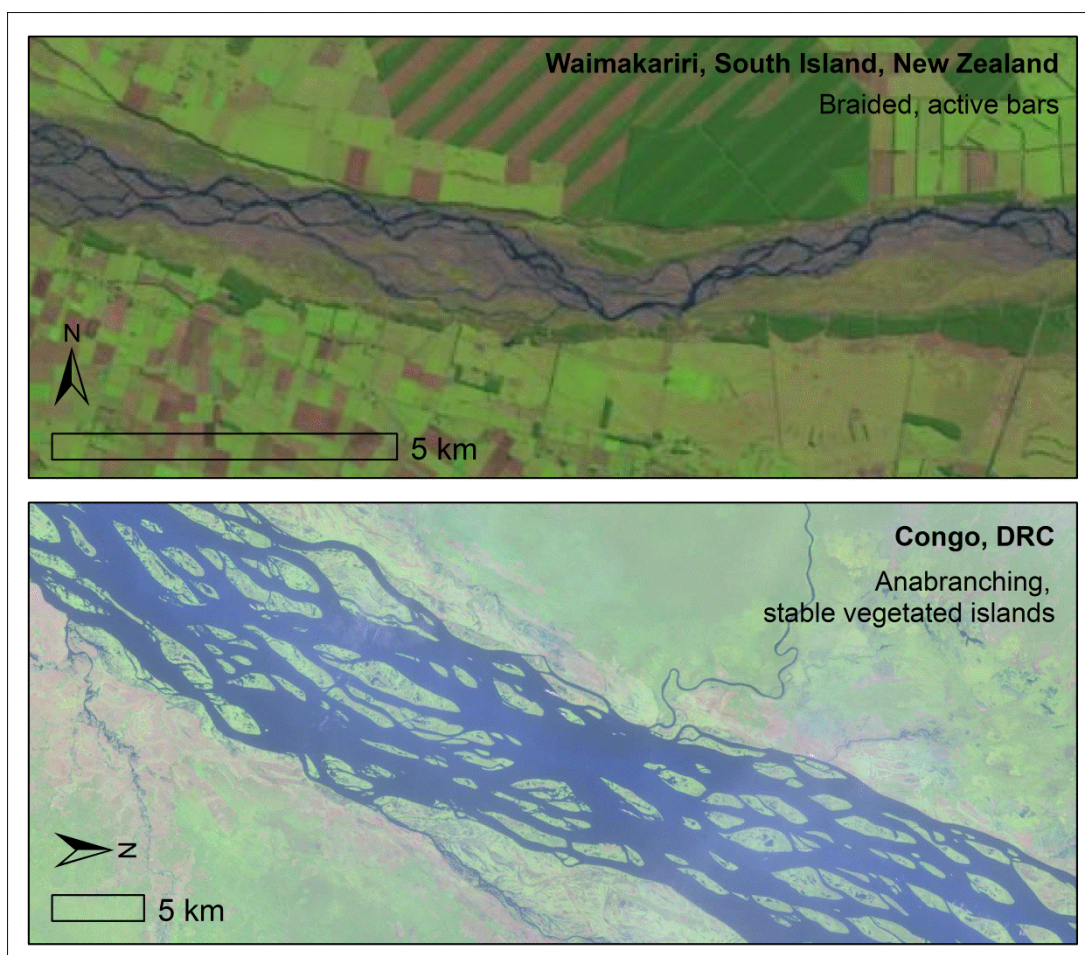
Figure 1.3: 'Landsatlook' Landsat 7 ETM+ false-colour composites showing multiple-thread channel patterns. Bar stability, due largely to vegetation growth, distinguishes the anabranching Congo River in the Democratic Republic of Congo from the braided Waimakariri River on the South Island of New Zealand.

The Meandering-Braided Channel Pattern Continuum

From the outset, empirical discrimination between meandering and braided channel patterns was viewed as a complex problem (e.g. Lane, 1957), acknowledging that no two-variable approach would ever capture the full diversity of controls on pattern characteristics and transitions (Eaton *et al.*, 2010). Nonetheless, two-variable empirical discriminations have achieved successful distinction between meandering and braided patterns, and although the physical basis of these relations has been challenged on several counts, the empirical approach has not been abandoned, and has evolved constantly in response to ongoing critique (e.g. Kleinhans and van den Berg, 2011). The first attempts at empirical discrimination plotted mean annual discharge (Lane,

1957), or bankfull discharge (Leopold and Wolman, 1957), against channel slope. Since these variables depend strongly on channel pattern, or in the case of mean annual discharge, are not considered to fundamentally shape channel hydraulic geometry, these early discriminant functions were revised by subsequent research. However, perhaps the single most significant contribution of the early work of Leopold and Wolman (1957) was the recognition that meandering and braided patterns plot on a continuum, without hard thresholds (Begin, 1981; Ferguson, 1987), an idea that is now generally accepted (Figure 1.4).
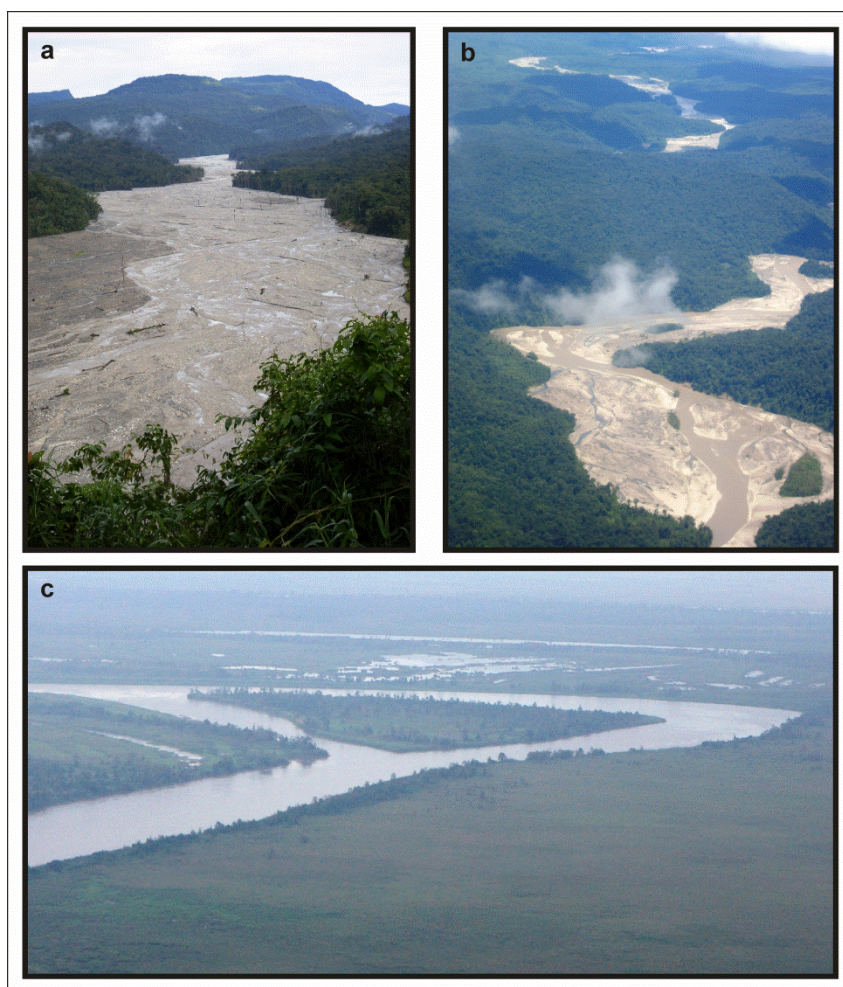
Figure 1.4: The meandering-braided channel pattern continuum illustrated in Papua New Guinea rivers. The pattern of the Ok Tedi River transitions from 'braided, no point bars' (a) to 'braided point bar' (c), and ultimately develops a pattern similar to that of the sand-bed Strickland River (wide-bend point bar, with stable chute channels, c). The role of chute channel initiation and stability in such planform transitions is a focus of this thesis.

Ferguson (1987: 131) summarised the findings of the original discriminant functions of Lane (1957) and Leopold and Wolman (1957), and the experimental analysis of channel pattern that followed these empirical analyses, by Schumm and Khan (1972): "Taken together, these papers are generally agreed to show, firstly, that for any given discharge and bed material there is one threshold slope above which channels will meander and another, higher one above which they will braid; and secondly, that the critical slope decreases with increasing discharge." Begin (1981) attempted to frame these inverse slope-discharge thresholds in terms of relative shear stress, while others provided an interpretation based on specific stream power (e.g. Carson, 1984), suggesting that braided rivers have higher energy than meandering rivers. However, Carson (1984) and Ferguson (1987) emphasised the importance of sedimentary controls on channel pattern, suggesting that planform pattern may be influenced to a great extent by the amount and calibre of bed sediment supplied to a channel, and the composition of channel banks (e.g. Schumm, 1963).

Sedimentary controls on channel pattern have been most extensively studied in laboratory flumes (for a review, see Howard, 2009). In attempting to develop a meandering channel in flume experiments, Friedkin (1945) found that developing point bars would become dissected by chute channels as the thalweg in the cross-over zone of meander trains shoaled, and a braided pattern would result. Experiments by Schumm and Khan (1972) showed that by introducing fine sediment with the flow, alternate bars may be stabilised, leading to thalweg scour and maintenance of a low sinuosity, predominantly single-thread channel. Subsequent experimental research has shown that a single-thread actively-meandering channel is difficult to establish in flume experiments, and requires i) cohesive bank material and/or vegetation to stabilise bars and banks, allow meander bends to increase in amplitude, limit channel widening that leads to flow instability and mid-channel bar deposition, and limit chute formation (e.g. Gran and Paola, 2001; Peakall *et al.*, 2007; Tal and Paola, 2007; 2010), and ii) a high suspended sediment load to increase developing bar and bank elevations and fill chute channels as they form

(Braudrick *et al.*, 2009). In addition, banks must not be so cohesive that migration is prevented altogether, resulting in planform ossification (Peakall *et al.*, 2007).

To address the earlier criticism levelled at empirical discriminant functions, van den Berg (1995) sought measures of slope and stream power that were relatively independent of planform, for 228 river reaches from around the World. Following Carson (1984), valley slope was used instead of channel slope (which is dependent on sinuosity). Van den Berg (1995) used bankfull discharge or, where such data were available, mean annual flood discharge, in a regime relationship for the prediction of channel width. Different exponents were used for sand-bed (Eq. 1.1) and gravel-bed (Eq. 1.2) rivers, based on a review of literature. Predicted width and valley slope were used to determine 'potential' specific stream power (ω_v), given by:

Sand-bed rivers:

$$\omega_v = 2.1 \, S_v \, \sqrt{Q} \; (\text{kW m}^{-2}) \qquad\qquad (1.1)$$

Gravel-bed rivers:

$$\omega_v = 3.3 \, S_v \, \sqrt{Q} \; (\text{kW m}^{-2}) \qquad\qquad (1.2)$$

Where;
S_v is valley slope (m m^{-1});
Q is bankfull or mean annual flood discharge (van den Berg, 1995).

River pattern stability was then represented by the product of ω_v and channel bedload D_{50}, and van den Berg (1995) found the discriminator between predominantly braided and predominantly meandering (ω_{bm}) at $900 D_{50}^{\,0.42}$. This finding was confirmed by Bledsoe and Watson (2001) using logistic regression analysis.

Lewin and Brewer (2001; 2003) took exception to the broad application of a regime-based estimate of width developed for single-thread rivers, and argued that its effect in the case of braided rivers is to raise specific stream power considerably (thus falsely improving discrimination). In addition, Lewin and Brewer (2001: 337) suggested that van den Berg's (1995) approach "obscures the complexity of processes which underlie the patterning of river planforms", especially large-scale bedform development and stability. In reply, van den Berg and Bledsoe (2003) agreed with much of Lewin and Brewer's (2001) critique, but argued that it was 'off the mark', since discriminant functions by design do not aim to describe the complexity of processes underlying planform pattern, but can only provide a rough indication of the pattern that may develop given a change in extrinsic or intrinsic drivers (and that therein lies their value).

Most recently, Kleinhans and van den Berg (2011) extended the empirical analysis of van den Berg (1995), and provided a comparison with physics-based predictions of bar pattern and braiding intensity (after Struiksma *et al.*, 1985; Crosato and Mosselman, 2009), recognising that the presence and nature of bars combined with the nature and rates of floodplain formation and bank erosion most meaningfully define channel pattern (in agreement with Lewin and Brewer, 2001; 2003). A simple, quasi-physical explanation for the meandering-braided channel pattern continuum emerges from this work (Kleinhans and van den Berg, 2011: 721): "Increasing potential-specific stream power implies more energy to erode banks and indeed correlates to channels with high width–depth ratio. Bar theory predicts that such rivers develop more bars across the width" (and are therefore characterised by higher braiding intensity).

1.3. Chute Channels in Meandering Rivers

Thus, the meandering-braided channel pattern continuum is a planform manifestation of excess available river energy; a balance between the energy of flow (commonly quantified as unit steam power or shear stress), and dynamic

resistance due to bed material calibre and bank strength. Single-thread meandering rivers plot in part of the continuum defined by low excess available river energy, while braided rivers plot in part of the continuum defined by high excess available river energy. It is likely that empirical discrimination of channel pattern has now reached its logical conclusion (this was suggested by Thorne, 1997, prior to the critique of Lewin and Brewer, 2001; 2003), and further advances are required in the physical elucidation of mechanisms of planform change (Lewin and Brewer, 2001; 2003). Importantly, Kleinhans and van den Berg (2011) found that planform patterns that are transitional between single-thread meandering and braided occur where chute channel formation is prolific, in keeping with the results of several experimental studies (e.g. Peakall *et al.*, 2007; Braudrick *et al.*, 2009). It is therefore critical that we advance our understanding of the process(es) of chute formation in meandering rivers.

A complete understanding of chute formation requires several paths of inquiry. First, it is important to understand triggering mechanisms for chute initiation, which may only be resolved probabilistically (e.g. Howard, 1996). A fundamental question in this regard is whether bends with particular planform characteristics and hydraulic geometry are more susceptible to chute initiation than others. Some insight has been provided (e.g. Howard, 1996; Micheli and Larsen, 2010), but for a narrow subset of river types. Second, it is important to understand bifurcation dynamics governing the division of flow and sediment following chute initiation, and hence the stability of chute channels, as previously studied for braided river bifurcations (e.g. Bolla Pittaluga *et al.*, 2003), and avulsions (e.g. Slingerland and Smith, 1998; Edmonds and Slingerland, 2008; Kleinhans *et al.*, 2008). An improved understanding of triggering mechanisms for chute initiation, coupled with an understanding of chute-mainstem bifurcation dynamics, will improve the predictive capacity of 1D meander migration models (e.g. Parker *et al.*, 2010) that can test ideas about river-floodplain evolution over long timescales.

Finally, a complete understanding of meandering-braided channel pattern transitions requires analysis of feedback effects of chute formation and chute cutoff on the physical drivers of channel planform change. Fundamental questions in this regard are to what extent chute formation and chute cutoff have a mediating effect on channel sinuosity and slope (e.g. Camporeale *et al.*, 2008), whether chute formation represents a mechanism of self-organisation in meandering rivers (e.g. Stølum, 1996; Hooke, 2007), and whether chute formation exerts feedback effects on bar development and floodplain sedimentation processes in the vicinity of the channel that may reinforce or impede channel planform change. The aim and primary research questions to be addressed in this thesis follow. The thesis focuses on large, sand-bed meandering rivers, which are poorly understood in comparison with small gravel-bed rivers, and gravel-bed rivers in general, which have been a particular focus of past research on chute formation.

1.4. Thesis Aim and Primary Research Questions

Aim: To understand the role of chute channels in the planform dynamics of large, sand-bed meandering rivers.

The thesis seeks to address the following three fundamental questions, within the context of large, sand-bed meandering rivers:

1. What controls chute initiation?

2. What controls chute stability?

3. What are the morphodynamic implications of chute channels?

1.5. Thesis Structure

Each of the chapters that follow this introduction is presented as a self-contained body of work (except the final, concluding chapter), addressing one or more of the primary research questions listed in Section 1.4. Included in each chapter is a review of literature relevant to the question(s) addressed, methods of data collection and analysis, results, discussion and conclusions.

Chapter 2 deals with the initiation and stability of chute channels from the broad, empirical perspective of spatial statistical analysis, and includes a detailed account of the regional physiographic settings of the rivers studied. Chapter 3 deals in greater detail with physical controls on chute stability, drawing on Delft3D simulations based on channel bathymetric data collected during a month-long field campaign in Papua New Guinea. Chapter 4 considers the implications of chute formation for overbank sedimentation and near-channel floodplain dynamics, revisiting and extending a published dataset of floodplain sedimentation rates from the Strickland River, Papua New Guinea.

Chapter 5 considers the implications of chute formation for meandering river planform dynamics, drawing extensively on understanding gained from the analyses presented in Chapters 2 to 4, and extending these analyses with additional data. Chapter 5 thus provides an overall conceptual synthesis of the research. Chapter 6 provides a concluding summary of key research outcomes, and offers a research forecast for large river processes. References for all chapters are presented in a single list at the end of the thesis.

CHAPTER 2

Chute Channel Dynamics in Large, Sand-Bed Meandering Rivers

2.1. Introduction

Early pioneering studies of large meandering rivers identified a prevalence of meander bends at which channel bifurcation by chute formation had resulted in the establishment of stable 'chute cutoff islands' (Blake and Ollier, 1971; Fly-Strickland Dispersal System, Papua New Guinea), or 'towheads' (Fisk, 1944, 1947; Mississippi River, USA, Russell, 1954; Meander River, Anatolia). Fisk (1947) and Blake and Ollier (1971) noted a tendency for chute and mainstem bifurcates to remain simultaneously active, such that the chutes conveyed permanent flow, and co-evolved with the mainstem for decades. Relatively long-lived chute channels are also known from the Calamus River, Nebraska (Bridge *et al.*, 1986), and the Sacramento River, California (Micheli and Larsen, 2010).

The formation of these 'bifurcate meander bends' (Figure 2.1) is an intellectually alluring phenomenon; their initiation in large, tropical meandering rivers appears contrary to the findings of experimental studies that suggest that chute formation should be suppressed in rivers with cohesive, well-vegetated channel banks (Schumm and Khan, 1972; Smith, 1998; Gran and Paola, 2001; Tal and Paola, 2007; 2010) and a high suspended sediment load (Ashmore, 1991; Peakall *et al.*, 2007; Braudrick *et al.*, 2009). High bank strength should limit channel widening and associated flow instability that leads to mid-channel bar deposition and braiding. Bar stabilisation (most notably by vegetation growth) should limit bar dissection by chute channels, and a high suspended sediment load should fill topographic lows as they form (see Howard, 2009, for a review).
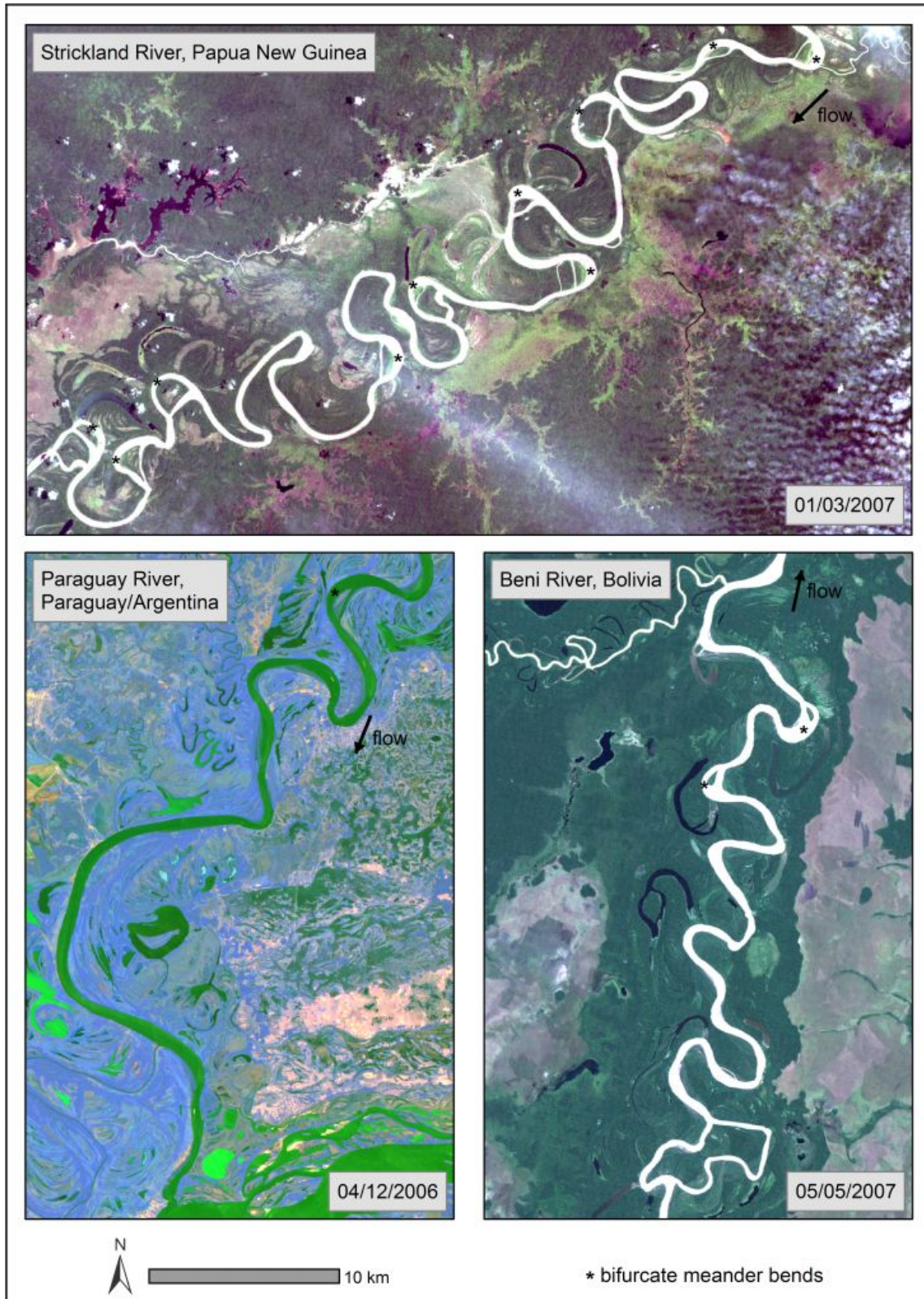
Figure 2.1: Bifurcate meander bends in large, sand-bed meandering rivers.

Understanding the stability of bifurcate meander bends may yield insight into controls on chute cutoff, considered here to occur only if the mainstem branch of the bifurcation becomes hydraulically disconnected by sedimentation, and the chute captures all flow (e.g. Constantine *et al.*, 2010a). As a first step toward understanding the dynamics and morphodynamic implications of bifurcate meander bends, and with a view toward providing observational insight that may assist process-based approaches to understanding chute formation, this chapter aims to determine whether it is possible to predict chute channel initiation in large, sand-bed meandering rivers, based on attributes of channel planform character and dynamics, and examines controls on chute initiation and stability.

The presence, and in some cases prevalence of bifurcate meander bends suggests a transitional planform pattern, and associated transitional processes. Although empirical discriminations of channel planform have been criticised for failing to elucidate underlying physical controls on planform change, and for using variables that are not entirely independent of planform (Carson, 1984; Lewin and Brewer, 2001; 2003), little exception is taken with the notion that meandering and braided channel patterns form a morphological continuum (first noted by Leopold and Wolman, 1957), with transient thresholds separating forms (Begin, 1981; Ferguson, 1987). Thus, transitional patterns and transitional processes should be anticipated (Ferguson, 1987). The meandering-braided continuum is a planform manifestation of excess available river energy; a balance between the energy of flow (commonly quantified as unit steam power or shear stress), and dynamic resistance due to bed material calibre and bank strength (Kleinhans, 2010). Single-thread meandering rivers plot in part of the continuum defined by low excess available river energy, while braided rivers plot in part of the continuum defined by high excess available river energy.

However, the most recent contribution to the suite of discriminant functions that followed the work of Leopold and Wolman (1957), that by Kleinhans and

van den Berg (2011), identifies the broadest range of transitional patterns yet, including 'meandering channels with scrolls', and 'moderately braided and meandering channels with scrolls and chutes', and is supported by a physics-based predictor of bar pattern. The empirical/physics-based discrimination of Kleinhans and van den Berg (2011) is anticipated in Brice's (1975) qualitative distinction between actively meandering channels of the class 'single-phase, wider at bends, chutes common', and those of the class 'single-phase, wider at bends, chutes rare'. It is also largely allied with the results of experimental studies which suggest that chute channel formation is a key process in the transition from a single-thread meandering to a braided pattern (Friedkin, 1945; Schumm and Khan, 1972; Ashmore, 1991; Ferguson, 1993).

Unfortunately, physical controls on the process of chute formation remain poorly understood, impeding numerical simulation efforts aimed at developing a predictive understanding of the processes of chute formation and chute cutoff (Seminara, 2006; Camporeale *et al.*, 2008; Bolla Pittaluga *et al.*, 2009; Frascati and Lanzoni, 2009), and the role of chute cutoff in channel planform dynamics (Hooke, 2007; Camporeale *et al.*, 2008). Larsen *et al.* (2006) used a sinuosity threshold to simulate cutoff events on the Sacramento, but the only detailed attempt to incorporate chute cutoff in a 1D meander migration model remains that of Howard (1996). Howard (1996) reasoned that the probable timing and location of chute cutoff might be predicted based on the magnitude of near-bank velocity at a potential breach point, and attributes of channel planform and floodplain relief, including the distance across and gradient advantage of a potential chute path, the floodplain elevation of a potential chute path, and the bifurcation angle between the mainstem and potential chute. To quantify exponents of these model terms, Howard (1996) drew largely on the work of Lewis and Lewin (1983), to date one of the most comprehensive studies of meander cutoff ever undertaken, although limited to gravel-bed rivers within a narrow geographic focus.

The principal underlying assumption of Howard's (1996) approach was that chute cutoff would be favoured at bends with particular characteristics, an assumption tested by Micheli and Larsen (2010) for the Sacramento River. Micheli and Larsen (2010) found that bends subject to chute cutoff had higher values of sinuosity and entrance angle, and lower values of curvature, than single-thread bends, and suggested that threshold values of these attributes exist that may enable prediction of chute formation, but that these values are likely to vary with valley slope. This suggestion is supported by the observations of Tower (1904) and Lewis and Lewin (1983); that chute channels form more frequently in steeper river reaches, where stream power and shear stress are likely to be higher (also recall Kleinhans and van den Berg, 2011). Micheli and Larsen (2010) argue that bend geometry determines whether or not a bend is primed for cutoff (perhaps akin to the notion that aggradation primes channels for crevassing and avulsion; Slingerland and Smith, 1998), but that the nature and timing of floods largely determine the timing of cutoff (after Hooke, 2008). The approach followed in this study is similar to that of Micheli and Larsen (2010), but differs primarily in its use of binary logistic regression analysis to test the significance of different attributes of planform character and dynamics in chute initiation, and in its focus on large, sand-bed meandering rivers, for which few detailed analyses of chute formation exist.

2.2. Mechanisms of Chute Formation in Meandering Rivers

The formation of a chute channel at a meander bend typically requires some mechanism to force flow over a developing point bar, or over-bank across a meander bend, with subsequent scour and incision (Johnson and Paynter, 1967; Peakall *et al*., 2007). One process by which this may occur involves stalling or shoaling of bedload sheets or unit bars, associated with an increase in bend amplitude and sinuosity, and concomitant decrease in channel slope and capacity (Carson, 1986; Ashmore, 1991; Peakall *et al*., 2007). This process may be enhanced by local channel blockages caused by engineering works (Thompson, 2003), ice dams (Gay *et al*., 1998), woody debris (Keller and Swanson, 1979), or

the passage of sediment slugs eroded from a bend upstream (Ashmore, 1991), and changes in bend orientation induced by the blockages or by channel impingement against cohesive valley fill (Lewin and Brindle, 1977). The diversion of flow into a chute channel may further reduce mainstem capacity such that shoaling at the bifurcation point is enhanced, with positive feedback effects on flow diversion into the chute (Pinter *et al.*, 2004).

Chute channel formation may occur through enlargement of a pre-existing topographic low (e.g. a slough between adjacent unit bars, Bridge and Demicco, 2008), or through headward erosion initiated at a point of flow re-entry at the downstream edge of the point bar (Hooke, 1995; Gay *et al.*, 1998). An alternative mechanism of chute formation was proposed by Constantine *et al.* (2010b) for large rivers with uniform floodplain topography (e.g. the Sacramento and the Missouri), involving the initiation and downstream propagation of a niche or 'embayment' within the cutbank. Embayments were observed to form at the point of maximum bend curvature (and bank shear stress) in the cutbank upstream of bends ultimately subject to cutoff. Both this mechanism involving embayment formation and downstream propagation, and the mechanism involving headcut erosion described in detail by Gay *et al.* (1998), are incisional processes that may act on well-established inner-bank floodplain (Figure 2.2, a, b), and as such are affected by reductions in floodplain surface roughness and root-hold through removal of natural vegetation, and are strongly correlated with flood events (Constantine *et al.*, 2010b; Micheli and Larsen, 2010).

Both Seminara (2006) and Bolla Pittaluga *et al.* (2009) hint at the possibility of bend widening and island formation driving the process of chute formation, the latter following the analysis of Repetto *et al.* (2002) of channel widening and flow expansion leading to stable mid-channel bar formation in straight channels (see also Luchi *et al.*, 2010a; 2010b). Bifurcation by mid-channel bar formation is known from braided rivers (Ferguson, 1993), but is considered a less common mechanism of braiding development than bar dissection by chute incision (Ashmore, 1991).
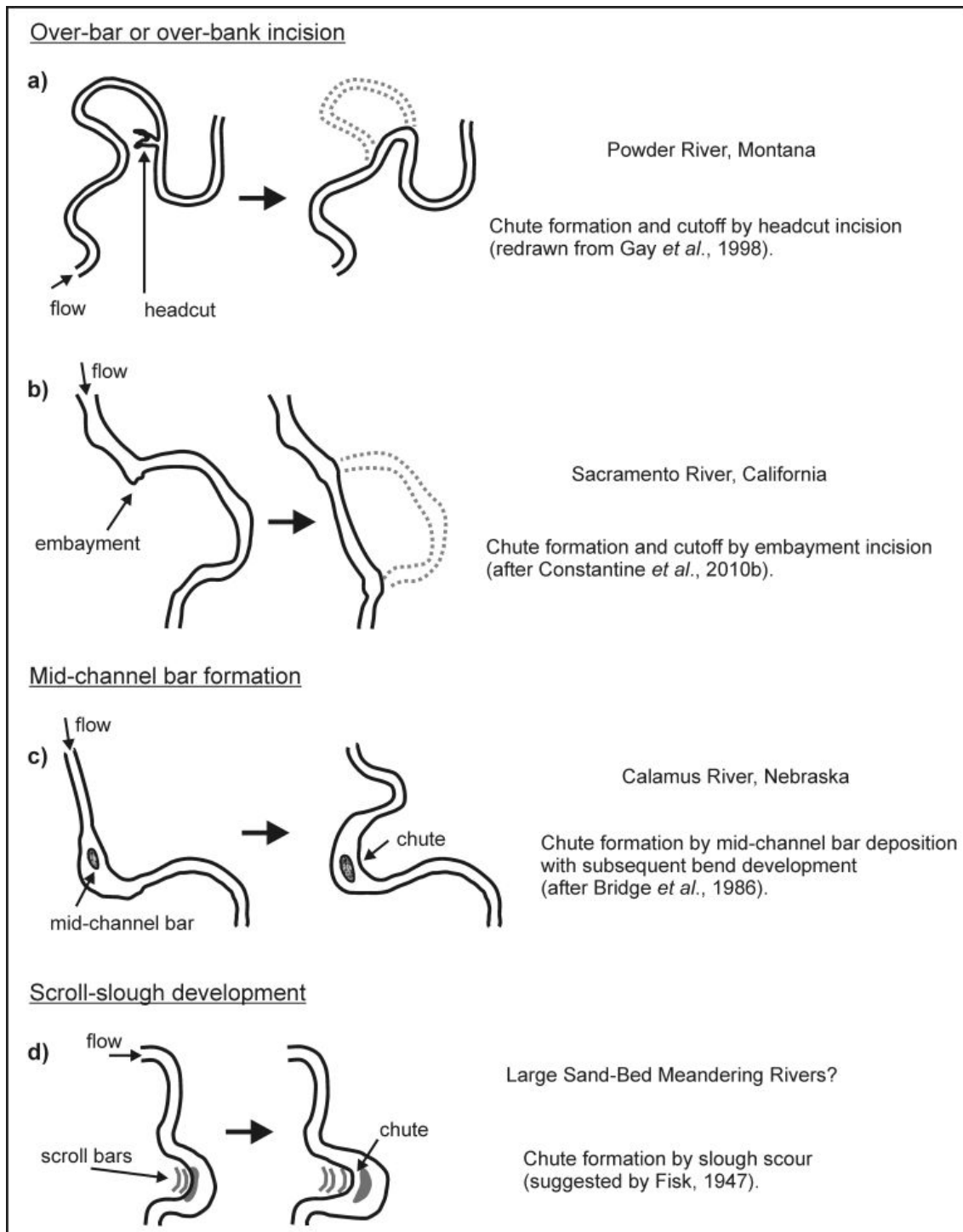
Figure 2.2: Mechanisms of chute formation (and chute cutoff) in meandering rivers. Mechanisms (a) and (b) are more common in gravel bed rivers, while mechanisms (c) and (d) are more common in sand-bed rivers. Chute formation by mid-channel bar formation (c), and by scroll-slough development (d), are the main focus of this thesis.

Bridge *et al.* (1986) describe chute formation on the Calamus River as occurring by mid-channel bar formation, with subsequent bank erosion and bend development (Figure 2.2, c). This mechanism differs from the incisional mechanisms described in that it is driven initially by deposition. Chute cutoff occurs on the Calamus when a change in flow orientation at a bend entrance favours the chute, and the mainstem begins to infill (Bridge *et al.*, 1986).

A final potential mechanism that has not been well documented involves scroll-slough development (Figure 2.2, d). Scour and enlargement of sloughs to form chute channels is implied in the work of Fisk (1947), but the underlying physical controls on scroll-slough formation, and associated chute formation, are poorly understood. Nanson and Croke (1992) suggest three possible mechanisms of scroll bar formation: i) iterative accretion of transverse sand bars on a point bar, which are subsequently capped by overbank sediment and preferentially vegetated, ii) focused deposition of suspended sediment in a flow-separation envelope over the point bar, or in the lee of debris stranded on the point bar at the inner-bank apex, and iii) formation of a chute channel between the inner bank and adjacent point bar. The lattermost mechanism generates circularity in explanation, and indicates that in rivers with scroll bars (e.g. many large, sand-bed meandering rivers), chute formation and scroll-slough formation may be mutually-dependent processes, and that the key to understanding their formation is to understand the mechanism by which inner-bank attachment of bars is broken (e.g. Peakall *et al.*, 2007). Bridge and Demicco (2008) suggest that rapid and intermittent meander migration would lead to the deposition of distinct unit bars on the point bar, whereas slow and continuous migration would lead to sheet-like deposition, in general agreement with Hickin and Nanson's (1975) observations that scroll bars develop a wider spacing and form more frequently as the rate of channel migration increases. It is hoped that the analysis presented in this chapter will shed more light on this mechanism of chute formation.

2.3. River Locations and Physiographic Settings

Alluvial sand-bed reaches of three large, tropical meandering rivers with varied physiographic settings were selected for analysis. Overall, the climatic setting of these rivers is similar (Barros *et al.*, 2004; Gautier *et al.*, 2007; Aalto *et al.*, 2008). Each reach has bifurcate meander bends, but initial image analysis indicated that the magnitude and frequency of bend bifurcation differed among rivers, and it was considered that investigating the reason for these differences would provide useful insight into controls on chute initiation and stability. An additional advantage of the selected reaches is that slope, bedload calibre, and water and suspended sediment discharge data of comparable quality are available for each. Brief descriptions of regional climate, geology and tectonics, hydrology, and sediment load are presented here, to establish key points of comparison.

Strickland River, Papua New Guinea
The Strickland River drains part of the Papuan Fold Belt comprising the highland central spine of the island of New Guinea, a feature subject to active uplift driven by convergence of the Australian and Pacific Plates (see Davies, 2009, for a summary of the geological and tectonic setting). Peaks approach 4000 m in elevation near the river's source, and throughout the headwaters the terrain is steep and highly dissected, and underlying lithology weak and highly deformed (Davies, 2009). This geological setting, coupled with a warm, wet tropical climate, results in frequent landsliding, and concomitant high sediment delivery to the river's headwaters (Pickup *et al.*, 1981). Rainfall seasonality in the highlands is generally low, and drought only occurs in association with intense El Ninō events (Pickup *et al.*, 1981; Dietrich *et al.*, 1999).

The Strickland drops sharply to an extensive lowland surface at ~100 m amsl, the Fly-Digoel Shelf, which it traverses for ~250 km, trending south then southwest to its confluence with the Fly River (the Everill Junction) at ~6 m amsl. The entire lowland drainage network, including the Strickland River and

floodplains, and its lowland tributaries, cut into this surface in response to pre-Holocene tectonic and eustatic adjustments that remain poorly understood (Blake and Ollier, 1971; Dietrich *et al.*, 1999). The result is a highly dissected plateau with ~65 m relief in the north, and ~8 m relief toward the Everill Junction (Blake and Ollier, 1971).

The Strickland study reach extends from the gravel-sand transition, ~100 km down-valley to the Everill Junction (Figure 2.3). The average channel slope for this reach is ~0.0001 (Lauer *et al.*, 2008, SRTM data), average valley slope is ~0.0002, average annual total water discharge is 98144 Mm^3 (mean annual discharge 3110 m^3 s^{-1} gauged just upstream of the Everill Junction), and average annual total suspended sediment discharge for the reach is 70-80 Mt (Dietrich *et al.*, 1999). The Strickland River is characterised by low variation in water discharge, and may be in flood 40% of the time (Parker *et al.*, 2008). As a result, bankfull discharge is only slightly higher than the mean annual discharge, and is estimated at 3300 m^3 s^{-1} (Lauer *et al.*, 2008). As anticipated by Pickup *et al.* (1984) and Dietrich *et al.* (1999), floodplain sedimentation is approximately balanced by erosion due to meander migration at a reach-average rate of ~5 m a^{-1} (Aalto *et al.*, 2008), such that there is little to no net retention of sediment in the lowland floodplains. The median bed material calibre (D_{50}) for the reach is 0.2 mm (Lauer *et al.*, 2008).

Paraguay River, Paraguay/Argentina

The Paraguay River rises on the Parecis Plateau of the Brazilian Shield, Mato Grosso, and forms part of the border between Paraguay and Brazil, and Paraguay and Argentina, on route to its confluence with the Paraná. A reach of the lower Paraguay River was chosen for analysis, extending from immediately downstream of Asunción at ~65 m amsl, trending southwest, to the Paraguay-Paraná River confluence at ~50 m amsl (Figure 2.3). Floodplains of the study reach are bounded to the west by Quaternary sediments of the Chaco-Pampa Plain, and to the east by an area of Jurassic-Cretaceous tholeiitic (subalkaline) basalts and siliceous sandstones (Iriondo, 1993; Drago and Amsler, 1998).
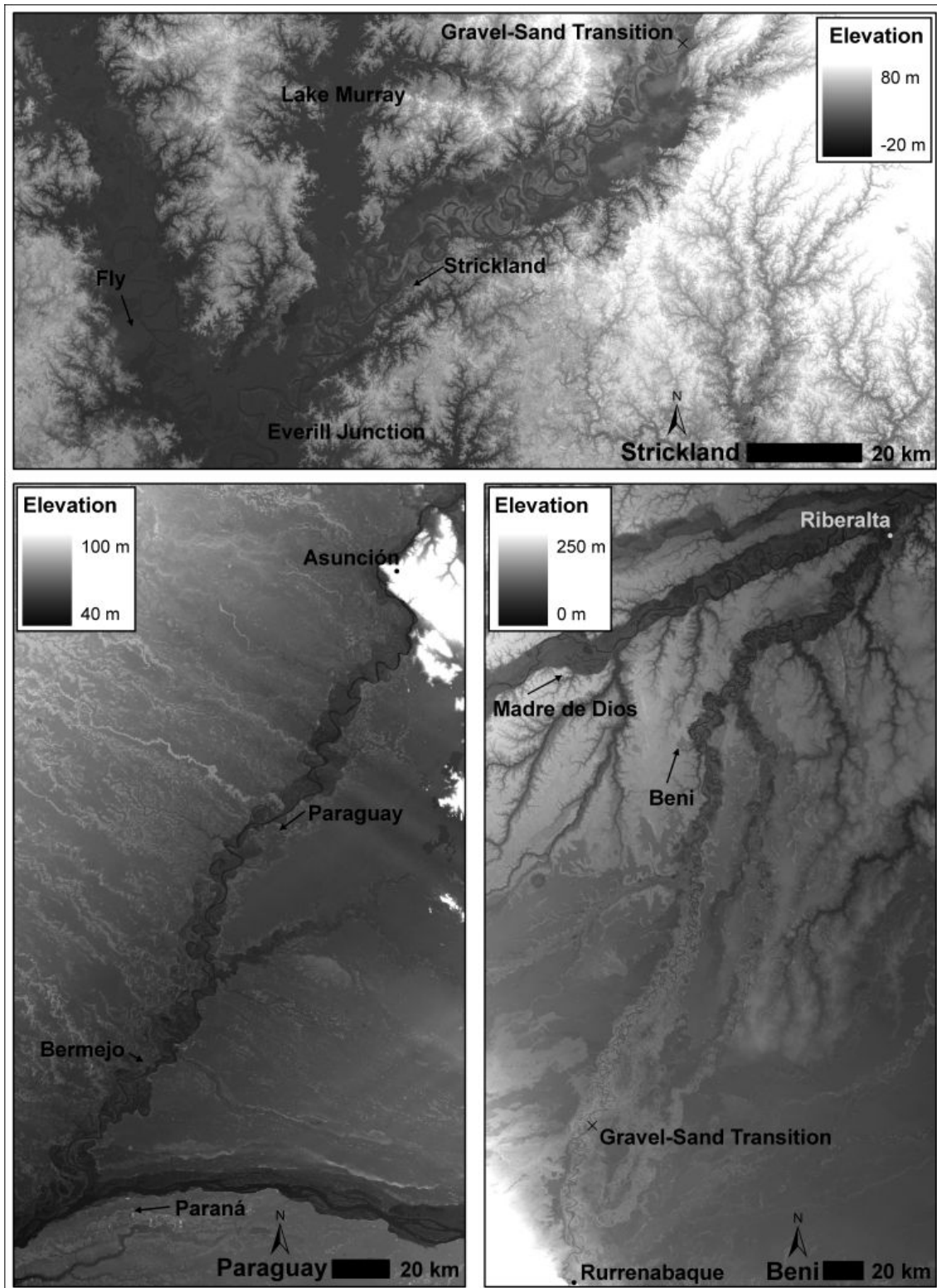
Figure 2.3: Study-reach SRTM digital elevation models for the Strickland, Paraguay, and Beni Rivers. Arrows adjacent to river names indicate the direction of flow. SRTM data source: CGIAR-CSI.

The eastern floodplain margin of the reach is fault-bounded (Iriondo, 1993), forming a raised terrace that spans the entire reach length. The average channel slope for the reach is ~0.00003 (Drago and Amsler, 1998), which equates to a valley slope of ~0.000045. SRTM data indicate a break in valley slope immediately downstream of the Bermejo confluence (valley slope upstream of Bermejo ~0.00003, valley slope downstream of Bermejo ~0.00005).

Upstream of this reach, the Paraguay River flows through a back-bulge depozone of the Central Andean foreland basin system hosting one of the World's largest wetlands, the megafan-floodplain complex El Pantanal (Horton and DeCelles, 1997; Assine and Soares, 2004; Assine and Silva, 2009). This fluvial disconnect and substantial sediment trap reduces the sediment load of the Paraguay downstream (Drago and Amsler, 1998; Assine and Silva, 2009), such that more than 80 % of the study reach has a relatively low average annual total suspended sediment discharge (~9 Mt, Drago and Amsler, 1988; Amsler and Drago, 2009). This increases markedly to ~70 Mt as the Bermejo River enters the Paraguay, draining the Argentinean Andes to the west (Drago and Amsler, 1988; Amsler and Drago, 2009). Sediment discharge figures are based on measurements made during the period of the year with maximum sediment transport, and thus slightly over-estimate average annual total suspended sediment discharge (Drago and Amsler, 1988; Amsler and Drago, 2009). The median bed material calibre (D_{50}) for the reach is 0.25 mm (Drago and Amsler, 1998).

Although El Pantanal mediates sediment supply to the lower Paraguay, the effect of the wetland complex on water discharge is less significant, as many of the major historical discharge events recorded at Asunción originated downstream of the Pantanal outlet (Barros et al., 2004). Average annual total water discharge downstream of the Bermejo confluence is 122633 Mm^3 (mean annual discharge 3886 m^3 s^{-1} gauged at Puerto Bermejo on the Paraguay; Krepper et al., 2006). The mean annual flood discharge at Puerto Bermejo is 4198 m^3 s^{-1} (Krepper et al., 2006). The Bermejo augments Paraguay flow by ~17 %

(Amsler and Drago, 2009), such that upstream of the Bermejo confluence, average annual total water discharge is ~101836 Mm^3 (mean annual discharge 3227 m^3 s^{-1}), and mean annual flood discharge ~3486 m^3 s^{-1}. Both water and sediment discharge of the Bermejo have increased markedly since the 1970s (Amsler and Drago, 2009), due to increased rainfall in the river's catchment (García and Vargas, 1996; 1998).

Beni River, Bolivia

The Beni River drains a high-elevation semi-arid swath of the Central Andean Cordillera, where peaks reach 6000 m amsl, as well as a large area of sub-Andean tropical humid forest (Aalto *et al.*, 2002). Crustal shortening and thickening within the Central Andean Cordillera since the Late Cretaceous-Palaeocene formed an orogenic wedge and, to the east, a cratonic retroarc foreland basin system (Horton and DeCelles, 1997). Topographic loading by the wedge drives a flexural pattern of subsidence – rise – subsidence that is manifest in foredeep – forebulge – back-bulge settings with distinct structural and sediment thickness characteristics at depth (Horton and DeCelles, 1997), and distinct valley surface slopes (Aalto, 2002; Gautier *et al.*, 2007).

From the foot of the piedmont at Rurrenabaque (~200 m amsl) to its confluence with the Mamore (~115 m amsl) to form the Madeira River, the Beni traverses the entire foreland basin system, trending northeast through the foredeep and forebulge, and east through the back-bulge (Aalto *et al.*, 2002). The Beni study reach extends from the gravel-sand transition near the head of the foredeep to the Beni-Madre de Dios River confluence near Riberalta (Figure 2.3). The average valley slope through the foredeep is ~0.0002, through the forebulge it is ~0.00007, and through the back-bulge it is ~0.0001 (Aalto, 2002, DGPS data; Gautier *et al.*, 2007, DGPS data).

Average annual total water discharge at the head of the reach is 64693 Mm^3 (mean annual discharge 2050 m^3 s^{-1} gauged at Angosto del Bala, near Rurrenabaque; Guyot, 1993), and immediately upstream of the Madre de Dios

confluence it is 90570 Mm^3 (mean annual discharge 2870 m^3 s^{-1} gauged at Portachuelo, near Riberalta; Guyot, 1993). Bankfull discharge for the reach is estimated at 7000 m^3 s^{-1} (Gautier *et al.*, 2007). Average annual total suspended sediment discharge at Angosto del Bala is 192 Mt, and at Portachuelo it is 100 Mt (Guyot, 1993). Distal floodplain sedimentation within the foreland basin occurs in discrete, episodic pulses linked to rapid-rise floods during La Niña events (Aalto *et al.*, 2003). Aalto *et al.* (2002) calculated a net transfer of 8 Mt a^{-1} of sediment from floodplain to channel, generated through rapid meander migration, and estimated a net retention of 98 Mt a^{-1} within the lowland basin by integrating measured floodplain sedimentation rates (Pb-210 alpha-geochronology) and floodplain-channel exchange during meander migration (in approximate agreement with the difference in gauged sediment loads; Guyot, 1993). The median bed material calibre (D_{50}) for the reach is 0.1 mm (Guyot *et al.*, 1999).

2.4. Methods

Image Acquisition and Preparation

Georeferenced multispectral image data for the past ~40 years were sourced for each of the rivers under investigation, using NASA's Warehouse Inventory Search Tool (EOSDIS, 2009), and the USGS Global Visualisation Viewer (EROS, 2009). Cloud-free images were sought at time intervals that were relatively comparable between rivers, resulting in a time step between images of approximately ten years (Table 2.1). Simple RGB false-colour composites were generated in ArcGIS from the three visible bands in each image dataset. Image resolutions varied from 79 m (Multi-Spectral Scanner, NASA Landsat 1-3, 4 and 5), to 30 m (Thematic Mapper, NASA Landsat 4, 5 and 7), to 15 m (Advanced Spaceborne Thermal Emission and Reflection Radiometer, NASA EOS-AM1). Composite images were clipped to the reach under investigation, then georeferenced relative to one another to improve the overlay accuracy.

Measurement of Channel Planform Characteristics and Dynamics

First, following the approach of Aalto *et al*. (2008), channel bank lines were digitised in ArcGIS for each image year, by tracing the contact between channel (including water and exposed, unvegetated bars) and vegetated floodplain, easily distinguished due to marked differences in reflectance. Field observations indicate that stoloniferous channel-fringing vegetation in the tropics (e.g. *Phragmites karka* in Papua New Guinea) rapidly colonises exposed sediment, and grows to heights that exceed bankfull elevation by over 3 m. Delineating banklines on this basis prevents inconsistency associated with fluctuations in stage. Channel centrelines were derived automatically from each pair of bank lines using a generalisation utility in ArcInfo.

Table 2.1: Summary of image sources used in the analysis.

River Name	Images			
Strickland	1972	1990/93	2002	2007
	MSS, 79 m	TM, 30 m	ASTER, 15 m	TM, 30 m
Paraguay	1975	1986	1999	2006
	MSS, 79 m	TM, 30 m	TM, 30 m	TM, 30 m
Beni	1975	1986	1997	2007
	MSS, 79 m	TM, 30 m	TM, 30 m	TM, 30 m

Second, each channel centreline was divided into a series of points spaced half a channel width apart, using editor and data management utilities in ArcInfo. Geographic coordinates (x, y) for the point strings were exported for use in a spreadsheet. An algorithm was used to calculate local curvature between consecutive points, and inflection points separating individual meander bends were identified where local curvature changed sign. The meander bends thus identified formed the basis of subsequent spatial data collection, and the unit of statistical analyses. Images were examined to record the presence of chute channels, in order to trace the history of chute initiation and infilling for each bend. Stable chutes were identified as those observed at a bend in three or more

successive images (i.e. that persisted for approximately 20 years or more), chute initiation was indicated by observation of a chute where none had existed in the previous image, and chute infilling was indicated by disappearance of a chute (due to vegetation encroachment) where one had been observed in the previous image. For each chute channel identified, chute-mainstem bifurcation angles were calculated at the point of intersection of chute and mainstem centrelines, and chute gradient advantages were calculated as the ratio of mainstem centreline length (bifurcation to confluence) to chute centreline length.

Third, the radius of curvature of each bend (bend-average curvature, see Crosato, 2009) was determined by mathematically fitting a circle to the point data using a solver that minimised the average difference in distance between a circle centre-point and five points on the bend centreline (arranged evenly around the bend apex). Bend radii of curvature were normalised by reach-average channel width. In addition, for the purpose of comparison with the results of Micheli and Larsen (2010), the centreline point string data were used to calculate bend sinuosities and entrance angles (angle between a line connecting inflection points of a bend and a tangent to the centreline at the upstream inflection point of the bend, after Micheli and Larsen, 2010).

Fourth, centreline overlay graphics were used to classify migration style for each bend at each time interval (each pair of successive images), following a system developed by Hooke (1977; 1984), and found to be appropriate for the rivers under investigation. Illustrated in Figure 2.4 (definitions after Hooke, 1977; 1984; Rohrer, 1984), the most common styles of meander migration observed were *extension* (displacement of a bend perpendicular to valley axis trend), *translation* (displacement of a bend in the direction of the valley axis trend), *rotation* (contortional, arcuate displacement of a bend in the directional of the valley axis trend), and *expansion* (enlargement of a bend on all sides). Since translation and rotation both essentially involve movement in the direction of the valley axis trend, these migration styles were grouped as one in the statistical analyses.

Bend migration style is an outcome of several inter-related factors, including centrifugal and convective hydraulic accelerations induced by upstream and local curvature and bed topography, and backwater effects originating downstream (summarised by Furbish, 1991), and the alluvial heterogeneity of the floodplain environment (summarised by Ferguson, 1975). Measurement of bend migration style follows the hypothesis that the direction and rate of outer bank erosion at a bend partly determines how much space is available at the inner bank for point bar deposition, and the potential topographic expression of the point bar, and partly determines the alignment of lineations within a point bar (such as sloughs adjacent to scroll bars) relative to the direction of over-bar flow, all of which should have implications for chute channel formation (see, for example, Howard, 1996).
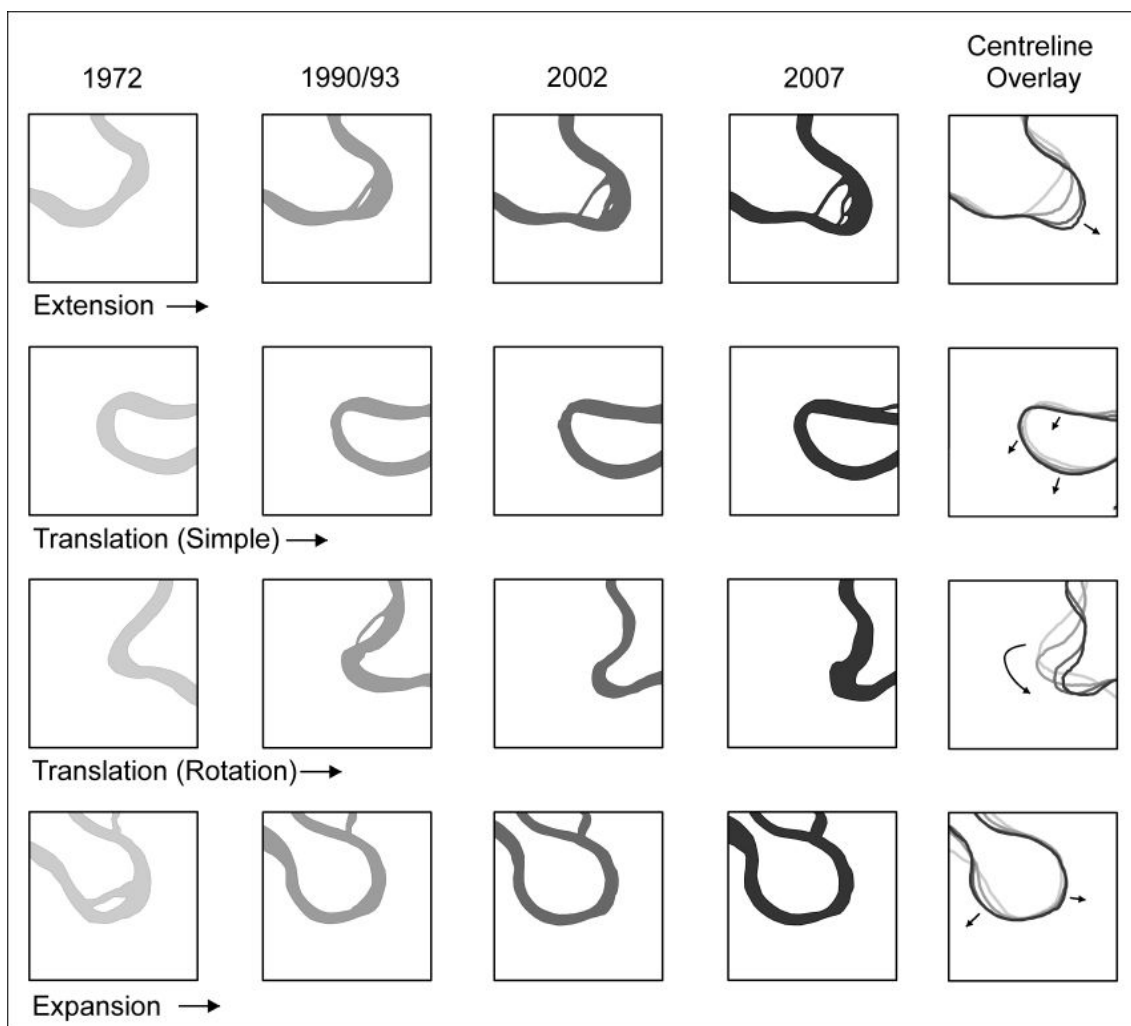
Figure 2.4: Bend migration style classification scheme (after Hooke, 1977; 1984).

Fifth, as illustrated in Figure 2.5, centrelines from successive image years were intersected, using an overlay analysis in ArcInfo, to derive polygons of centreline displacement. Meander migration rates were calculated for each migration style by dividing displacement polygon areas by their centreline lengths (half the polygon perimeter), and then by the time interval between successive images, giving a rate in $m^2\ m^{-1}\ a^{-1}$ ($m\ a^{-1}$). These measurements were normalised by reach-average channel width, to allow comparison among different rivers. This centreline-overlay method has been applied in several studies of large rivers (e.g. Aalto *et al.*, 2008, Micheli and Larsen, 2010), but displacement rates have not previously been apportioned by migration style in the manner described here.
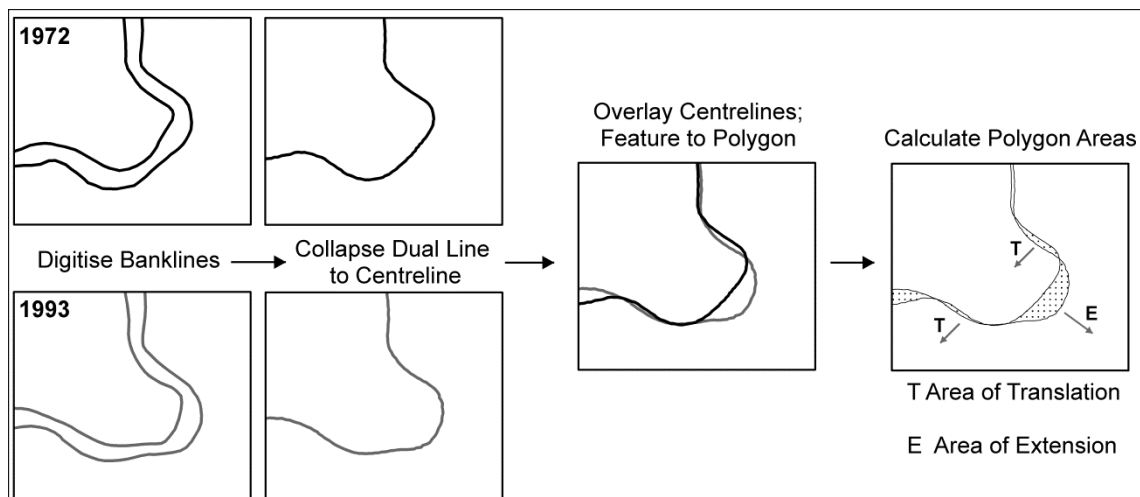
Figure 2.5: Method used to calculate bend displacement polygon areas in ArcInfo.

Analysis of Error

The same method used to calculate migration rates was used to determine error in migration rate measurements. This involved digitising bank lines for a set of open-water oxbow lakes, clearly visible in each image, then deriving and intersecting centrelines to calculate displacement (after Aalto *et al.*, 2008). Approximately one oxbow lake per 30 km active channel length was selected for error analysis, a density governed by availability of oxbows that had not been breached by the main stem during the period of image analysis, nor had

been subject to substantial (shape-changing) input of clastic sediment. Oxbows selected were spaced as evenly as possible throughout each reach under investigation.

Table 2.2: Estimated error in migration rate measurements due to image overlay offsets and digitising inconsistencies. Note: For illustrative purposes, error estimates are presented as a proportion of the average bend migration rate, but it is acknowledged that there is greater uncertainty in migration rate measurements for slowly-migrating bends than for rapidly-migrating bends. Where there is no apparent migration, the uncertainty is ~ 1 pixel.

River Name	Image Period	Average Bend Migration Rate (channel widths)	Error (+/-) (channel widths)	Error (+/-) (%)
Strickland	1972-1990 (Lower Reach)	0.027	0.003	12.26
	1972-1993 (Upper Reach)	0.019	0.002	10.36
	1990-2002 (Lower Reach)	0.033	0.004	13.20
	1993-2002 (Upper Reach)	0.031	0.006	19.05
	2002-2007 (Full Reach)	0.019	0.004	22.27
Paraguay	1975-1986	0.013	0.002	14.54
	1986-1999	0.009	0.001	8.62
	1999-2006	0.008	0.001	14.26
Beni	1975-1986	0.041	0.010	23.88
	1986-1997	0.035	0.002	4.60
	1997-2007	0.033	0.001	4.48

This method accounts for image offsets following georeferencing, as well as error associated with user interpretation of bank lines at different image resolutions during digitising. Displacement of oxbows follows similar planes to the displacement of the active channel, and since bank lines of the oxbows were more difficult to identify than those of the active channel, where contrasts in reflectance were starker, the displacement likely represents maximum possible error (Aalto *et al.*, 2008). Furthermore, the offsets are internally consistent in that

relative differences in the displacement of individual bends are accurately reflected, although the magnitude of displacement may not be absolutely accurate. Estimates of error are summarised in Table 2.2 – the average error for the entire dataset is +/- 13 % (i.e. +/- 0.65 m a^{-1} on a migration rate of 5 m a^{-1}). The process of digitising vector banklines from raster imagery involves generalising the channel edge at the contact between channel and vegetated floodplain (developing a smooth contour from a stair-cased edge), adding additional minor error to the analysis. Overall, the method of calculating migration rates is able to distinguish, with high certainty, between bends migrating slowly and bends migrating rapidly, a primary requirement of subsequent statistical analysis.

Binary Logistic Regression Analysis

Rather than investigating whether it is possible to predict chute presence/absence at a bend, statistical analysis centred on investigating whether it is possible to predict chute initiation at a bend, with a view to identifying the underlying drivers and accounting for bend development history. In statistical terms, the primary goal of this investigation was to determine the possibility of predicting membership of one of two categorical outcomes; the null case of no chute initiation at a bend (0), versus the case of chute initiation at a bend (1), based on continuous predictor variables (the measured attributes of channel planform character and dynamics, Table 2.3). Binary logistic regression serves this goal.

Since categorical data violate the assumption of linearity of linear regression models, this is overcome in logistic regression models by applying a logarithmic transformation, or 'logit' (Berry and Feldman, 1985). The test is used to predict the probability of an outcome given known values of predictor variables, in a multiple regression environment (see Bledsoe and Watson, 2001, for an application in fluvial geomorphology, and Field, 2009, for a simplified explanation). The forced entry method in SPSS was used in this analysis, and for each variable that had a statistically significant effect on the model outcome,

both Cox and Snell (1989) and Nagelkerke (1991) estimates of R^2 are presented to determine key predictors (those with statistically significant values of R^2 that explain the most variance in the model).

Table 2.3: Attributes of bend planform characteristics and dynamics used in the binary logistic regression analysis.

	Categorical Outcome Variable
	Whether a Chute Forms at a Bend or Not, During the Full Analysis Period
	Continuous Predictor Variables (Bend Attributes)
1	Average Curvature (R:w)
2	Minimum Curvature (R:w)
3	Maximum Curvature (R:w)
4	Average Entrance Angle (°)
5	Minimum Entrance Angle (°)
6	Maximum Entrance Angle (°)
7	Average Sinuosity
8	Minimum Sinuosity
9	Maximum Sinuosity
10	Average Rate of Extension (Channel Widths a^{-1})
11	Average Rate of Translation (Channel Widths a^{-1})
12	Average Rate of Expansion (Channel Widths a^{-1})
13	Average Rate of Total Migration, All Styles Combined (Channel Widths a^{-1})

Assumption Testing

Linearity: The first assumption of logistic regression is that the relationship between continuous predictors and the logit of the outcome variable is linear. This assumption is violated if the interaction term between a predictor and its log transformation is significant (Hosmer and Lemeshow, 1989). In this analysis, there were no significant interaction terms, indicating that the assumption of linearity is valid.

Independence of errors: The second assumption of logistic regression is that cases of data are not related. It would therefore be incorrect to use measurements of predictor variables for the same bend at different points in time (e.g. bend entrance angle for each measurement period), as this would lead to over-dispersion (Field, 2009). This analysis used average, and in some cases, minimum and maximum values of predictor variables for each bend for the full analysis period (e.g. bend average entrance angle = [entrance angle at 1972 + entrance angle at 1990/93 + entrance angle at 2002 + entrance angle at 2007]/4).

Multicollinearity: The third assumption of logistic regression is that there are no significant correlations between predictor variables. This is tested in SPSS using normal multiple linear regression with collinearity diagnostics. For each river, the linear regression model tolerance values, and the variance proportions of the collinearity diagnostics suggested collinearity between average, minimum and maximum values of curvature (R:w), sinuosity and entrance angle, as might have been expected. On this basis, the analysis was repeated using single descriptor values for curvature (R:w), sinuosity and entrance angle (i.e. average values only, then minimum values only, then maximum values only).

2.5. Results

Bend-Scale Controls on Chute Channel Initiation
The binary logistic regression analysis revealed that only one predictor has a statistically significant effect for each river: 'Average rate of extension' (computed R^2 values and odds ratios are summarised in Table 2.4). In terms of predicting chute initiation at a bend, the average rate of extension of a bend alone accounts for 37-54 % of the variation in the Strickland data (54 bends), 36-58 % of the variation in the Paraguay data (45 bends), and 30-44 % of the variation in the Beni data (114 bends). Odds ratios >1 indicate that as the extension rate of a bend increases, the likelihood of chute initiation at the bend increases. Overall, the average rate of extension of bends subject to chute initiation is 3 times greater than that of bends not subject to chute initiation on

the Strickland, 4 times greater on the Beni, and 22 times greater on the Paraguay. Equations 2.1 to 2.3 describe the probability of chute initiation at a bend for each river as a function of average rate of bend extension, based on regression model estimates. $P(y)$ is the probability of chute channel initiation at a bend, and x is the average rate of extension of the bend, in units of average channel width. Unfortunately, because these probability functions are based on decadal-scale average rates of bend extension, they could not be used to predict the probability of chute initiation during bend development in a 1D meander migration model, but may be used to test chute-initiation rules such as those developed by Howard (1996).

Table 2.4: Results of the binary logistic regression analysis.

River Name	R^2 (Cox and Snell, 1989)	R^2 (Nagelkerke, 1991)	Odds Ratio
Strickland	0.37	0.54	1.07
Paraguay	0.36	0.58	8.12
Beni	0.30	0.44	1.33
Predictor: Average Rate of Extension			$p < .01$

Strickland;

$$P(y) = \frac{1}{1+e^{-(-11.11+108.29x)}} \qquad (2.1)$$

Paraguay;

$$P(y) = \frac{1}{1+e^{-(-2.65+520.18x)}} \qquad (2.2)$$

Beni;

$$P(y) = \frac{1}{1+e^{-(-3.11+73.97x)}} \qquad (2.3)$$

A comparison of summary statistics for single-thread and bifurcate meander bends suggests that although the effect of other measured planform attributes on chute initiation is not significant in terms of the logistic regression, there are

at least consistent differences between single-thread and bifurcate bends (Table 2.5). On average, bifurcate bends have lower curvature (R:w), but a higher bend entrance angle and sinuosity, than single-thread bends, a finding consistent with the results of Micheli and Larsen (2010) for the gravel-bed Sacramento River.

In addition, values of these attributes from the present study for bifurcate bends occupy a narrower range than is the case for single-thread bends (except for entrance angle and sinuosity in the Beni data). The difference in standard deviation of curvature values is most pronounced, and may track an R:w range favourable to rapid meander migration (e.g. Hickin and Nanson, 1984; Furbish, 1988; Crosato, 2009). The curvature results are also similar to those of Lewis and Lewin (1983), who found that most cutoffs (of any kind, although chutes were most commonly observed) occurred at bends with R:w of 2 to 3.
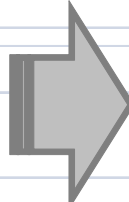
Reach-Scale Controls on Chute Channel Initiation and Stability
A comparison of physiographic data for all rivers (Table 2.6), along with reach-scale descriptive statistics for bend migration (Table 2.7) and bifurcation (Table 2.8) provides broader context for the identified bend-scale controls on chute initiation, and yields valuable insight into chute stability. Firstly, there are substantial differences in slope and average annual suspended sediment load (described by the relationship Qs/Q) among rivers, and within individual river reaches. Mutual variation in slope and sediment load is evident in all cases (higher sediment loads are associated with higher slopes, Table 2.6), but no general causal relationship is suggested. The Paraguay has the lowest slope and sediment load overall, but values of these variables downstream of the Bermejo confluence approach those of the Strickland. The Beni has a roughly equivalent slope to the Strickland through the foredeep and back-bulge, but a lower slope through the forebulge, illustrating the strong effect of tectonics on slope in this setting. However, the sediment load of the Beni is substantially higher than that of the Strickland and Paraguay, even at Riberalta after ~100 Mt sequestration to floodplain fill (Guyot, 1993; Aalto *et al.*, 2002).

Table 2.5: Comparison of descriptive statistics for Curvature (R:w), entrance angle and sinuosity, for cases in which bends are single-thread, and cases in which bends are partitioned by chute channels. Attribute values are associated with individual observations of bend planform in each image. The total number of cases is not divisible by the number of bends because some bends are cut off during the analysis period.

Strickland			
Single-Thread Cases (n = 142)			
	Curvature (R:w)	Entrance Angle (°)	Sinuosity
Mean	2.78	52.61	1.52
StDev	1.41	23.15	0.40
Bifurcate Cases (n = 66)			
	Curvature (R:w)	Entrance Angle (°)	Sinuosity
Mean	2.55	63.71	1.66
StDev	0.78	20.09	0.29
Paraguay			
Single-Thread Cases (n = 130)			
	Curvature (R:w)	Entrance Angle (°)	Sinuosity
Mean	3.02	53.64	1.52
StDev	1.71	20.41	0.33
Bifurcate Cases (n = 50)			
	Curvature (R:w)	Entrance Angle (°)	Sinuosity
Mean	2.95	61.12	1.54
StDev	0.92	12.34	0.27
Beni			
Single-Thread Cases (n = 342)			
	Curvature (R:w)	Entrance Angle (°)	Sinuosity
Mean	2.63	56.08	1.74
StDev	1.31	24.77	0.73
Bifurcate Cases (n = 69)			
	Curvature (R:w)	Entrance Angle (°)	Sinuosity
Mean	2.16	71.30	2.24
StDev	0.74	27.01	1.29
Note: 'case' refers to one bend in one image.			

Table 2.6: Reach-scale and within-reach variation in slope, average annual water (Q) and suspended sediment (Qs) discharge, and average annual sediment load (Qs/Q) data for the rivers studied.

Strickland	Reach Average		
Valley Slope	0.0002		
Water Discharge, Q (Mm^3 a^{-1})	98144		
Suspended Sediment Discharge, Qs (Mt a^{-1})	70 - 80		
Ratio Qs:Q (kg m^{-3})	0.71 - 0.82		
Paraguay	Upstream of Bermejo	Downstream of Bermejo	
Valley Slope	0.00003	0.00005	
Water Discharge, Q (Mm^3 a^{-1})	101836	122633	
Suspended Sediment Discharge, Qs (Mt a^{-1})	9	70	
Ratio Qs:Q (kg m^{-3})	0.09	0.57	
Beni	Foredeep	Forebulge	Back-Bulge
Valley Slope	0.0002	0.00007	0.0001
	Rurrenabaque		Riberalta
Water Discharge, Q (Mm^3 a^{-1})	64693		90570
Suspended Sediment Discharge, Qs (Mt a^{-1})	192		100
Ratio Qs:Q (kg m^{-3})	2.97		1.10

Overall rates of bend migration track the differences in slope and discharge (stream power, discussed later) between rivers, with the Beni bends migrating most rapidly, and the Paraguay bends least rapidly (Table 2.7, row 8). Strickland bends migrate by extension to a greater extent and at a greater rate (in comparison to the rate of translation) than the other rivers, and by translation to the least extent, while the opposite is the case for the Paraguay (rows 2-5). Aalto *et al*. (2008) also noted an increase in channel length in their

analysis of reach-scale channel migration of the Strickland, and ascribed this to channel elongation through extension. Rates of bend expansion are much lower than those of other styles of migration (row 7). Bend expansion is more common on the Beni than on the other rivers (row 6), and the extent to which Beni bends migrate by extension and translation is more similar than for the other rivers (rows 2 and 4). Differences in migration style may be partly related to interactions with infilled oxbow lakes (clay plugs), which have the potential to deflect or impede cutbank erosion, and thereby alter migration style (e.g. Fisk, 1947, Figure 2.6).

Table 2.7: Summary statistics describing trends in migration style and rates of bend migration for the rivers studied.

	Migration Statistics	Strickland	Paraguay	Beni
1	Number of bends analysed	54	45	115
2	Percentage of bends subject to extension	70	24	54
3	Average bend extension rate	0.0155	0.0022	0.0168
4	Percentage of bends subject to translation	48	84	68
5	Average bend translation rate	0.0076	0.0077	0.0166
6	Percentage of bends subject to expansion	7	9	18
7	Average bend expansion rate	0.0011	0.0003	0.0029
8	Average total migration rate	0.0242	0.0101	0.0363
Note: migration rates are in channel widths per year.				

Table 2.8: Summary statistics describing chute channel initiation and stability in the rivers studied.

	Chute Statistics	Strickland	Paraguay	Beni
1	Total number of chute channels observed	32	21 (5)	42 (30)
2	Chute:bend ratio	0.59	0.47 (0.71)	0.36 (0.50)
3	Chute:bend ratio (initiation only)	0.26	0.20 (0.57)	0.25 (0.42)
4	Percentage stable chute-mainstem bifurcations	63	67 (40)	33 (33)
5	Percentage chute infills	28	24 (40)	57 (80)
6	Number of chute cutoffs	1	0	1
7	Average chute-mainstem bifurcation angle for stable bifurcations (°)	71.77	62.13	50.28
8	Average chute-mainstem bifurcation angle for chute infills (°)	43.92	45.48	39.73
9	Average chute gradient advantage for stable bifurcations	1.67	1.41	1.56
10	Average chute gradient advantage for chute infills	1.17	1.13	1.27

Beni: values in brackets represent foredeep.

Paraguay: values in brackets represent reach downstream of Bermejo confluence.

More detailed analysis of the migration of individual bends sheds some light on the mechanisms of chute formation involved (Figure 2.6). More than 95 % of all chutes that formed during the imagery analysis period initiated at chord locations (close to the inner-bank apex, terminology after Lewis and Lewin, 1983), on bends that were wider through the apex than at inflections (Figure 2.6, A). This location suggests formation as a component of scroll-slough development, where rapid migration results in wide scroll-slough spacing providing an efficient conduit for flow (Hickin and Nanson, 1975). During their formation, scroll bars may generate a convergent pattern of secondary currents that moves suspended sediment from the sloughs toward the scroll apexes, so that the bars become emergent even at moderate flows (Nanson, 1980), and prominent chute channels result. Stable chute channels on these rivers do not

form by scour of sloughs located further from the inner-bank apex within vegetated floodplain. A less common mechanism of chute formation involves mid-channel bar deposition in a widened, straight reach, with subsequent bend extension (described by Bridge *et al*., 1986, Figure 2.2, c, Figure 2.6, B).
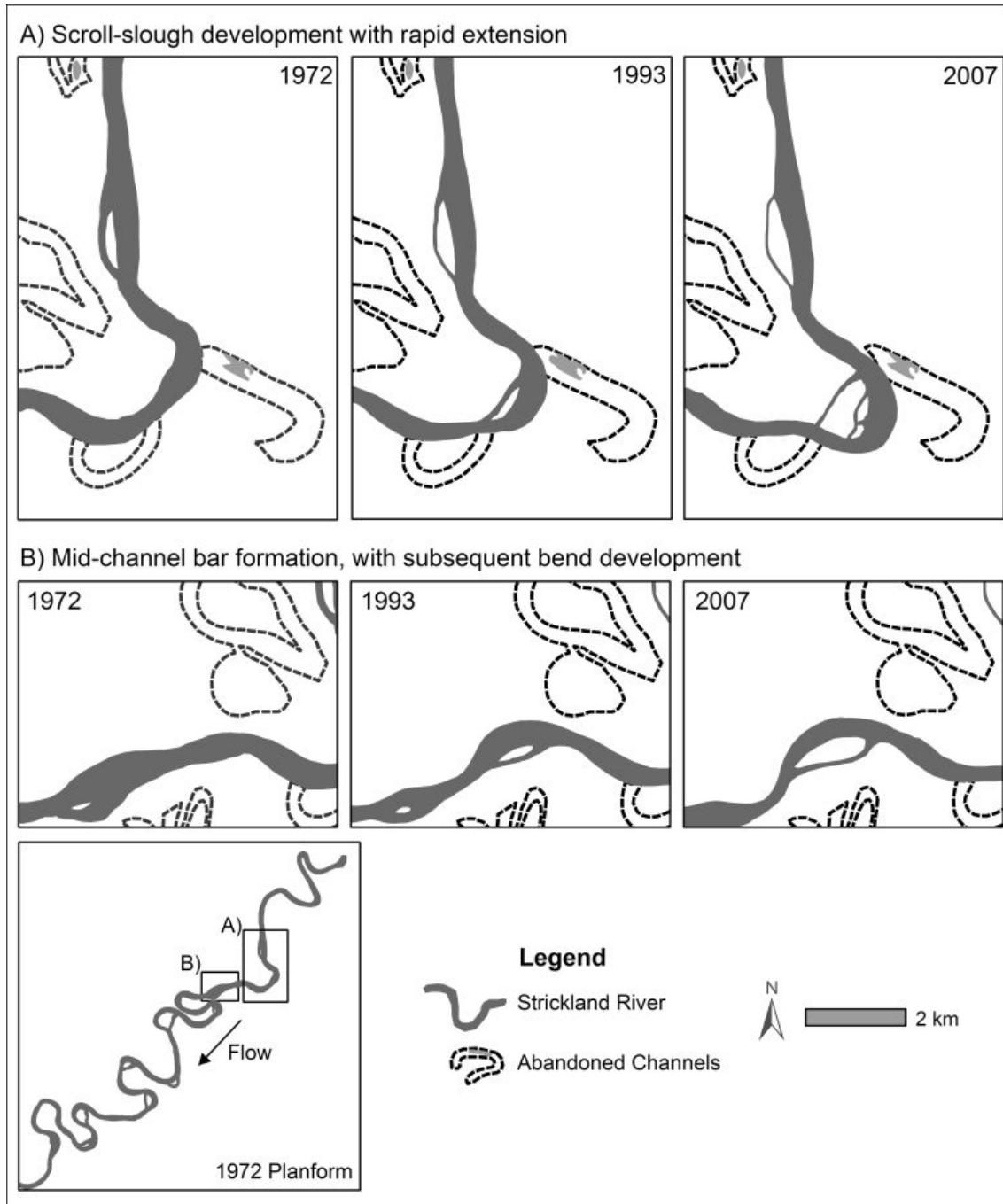
Figure 2.6: Mechanisms of chute formation observed in the large, sand-bed meandering rivers studied.

Consistent with the relationship between extension and chute initiation identified by the binary logistic regression analysis, the Strickland has more chute channels (Table 2.8, row 2), and a greater rate of chute initiation (row 3) than the other rivers. Sub-reaches within the Paraguay and Beni with the highest slope (i.e. downstream of the Bermejo confluence on the Paraguay, and the Beni foredeep), have more chute channels (row 2, values in brackets), and greater than reach-average rates of chute initiation (row 3, values in brackets). The effect of sediment load on chute stability is indicated by a substantially lower frequency of stable bifurcate bends (row 4), and substantially higher incidence of chute infill (row 5) on the Beni in relation to the other rivers. Most notably, 80 % of chutes in the Beni foredeep infill during the analysis period, a phenomenon also reflected in the Paraguay data downstream of the Bermejo confluence (higher rates of chute initiation, but also a higher incidence of chute infill, row 5, values in brackets).

Complete chute cutoff is an exceedingly rare event on these large, sand-bed meandering rivers (Table 2.8, row 6), and one of two outcomes is most likely once a chute channel initiates: i) chute infill, maintaining a single-thread bend planform, or ii) formation of a stable, bifurcate meander bend. It is not uncommon to observe bifurcate bend geometry in abandoned channels as well, the overall horseshoe planform of which implicates neck cutoff as the dominant process by which bends are excised in this setting. The data for chute-mainstem bifurcation angle (rows 7 and 8), and chute gradient advantage (rows 9 and 10) may provide some explanation as to why certain chute channels infill, and others form stable bifurcations; for all rivers, stable chute-mainstem bifurcations have higher bifurcation angles (rows 7 and 8), and greater chute gradient advantages (rows 9 and 10) than those subject to chute infill.

It is noted that the images provide temporally-isolated windows on river activity; dynamics are inferred by changes evident from one image to the next, and any change that occurs outside the observation windows is not recorded. Thus, chutes that initiate immediately after the capture date of one image, but

infill before the capture date of the next image are not recorded. This results in a slight bias toward the recording of relatively stable chutes, such that observations of chute initiation more accurately reflect the formation of chutes that persist at least for several floods, and the results meld controls on chute stability and chute initiation. This has the disadvantage of clouding insight into triggering mechanisms for chute initiation, but the advantage of providing holistic insight into controls on the overall process of chute formation; from initiation, through evolution, to fate.

2.6. Discussion

Using bedload calibre data and estimates of bankfull discharge or mean annual flood provided in the 'River Locations and Physiographic Settings' section of this chapter, it is possible to plot the rivers studied within the empirical discriminant functions of Kleinhans and van den Berg (2011, Figure 2.7). In accordance with the data presented for river migration rates (Table 2.7) and chute formation (Table 2.8), the rivers (and sub-reaches) generally fit within the appropriate classes distinguished by Kleinhans and van den Berg (2011). The Paraguay upstream of the Bermejo confluence (1 in Figure 2.7) plots within the range of meandering channels with scrolls, while the Paraguay downstream of the Bermejo (3 in Figure 2.7) plots at the transition from meandering channels with scrolls to moderately braided and meandering channels with scrolls and chutes. The Strickland (6 in Figure 2.7) and the Beni as a whole (5 in Figure 2.7) plot at the transition from moderately braided and meandering channels with scrolls and chutes to highly braided channels, while the Beni foredeep (7 in Figure 2.7) plots within the range of highly braided channels (this misclassification is discussed further below). Also included in Figure 2.7 are data for the lower- and upper-middle Fly River (2 and 4 in Figure 2.7, respectively). Although the lower-middle Fly plots within the range of meandering channels with scrolls, it is considered to be 'impounded' by backwater effects of the larger Strickland River, and has an appreciably lower

slope and suspended load than the Strickland, very little bedload, and virtually immeasurable rates of meander migration (Dietrich *et al.*, 1999).
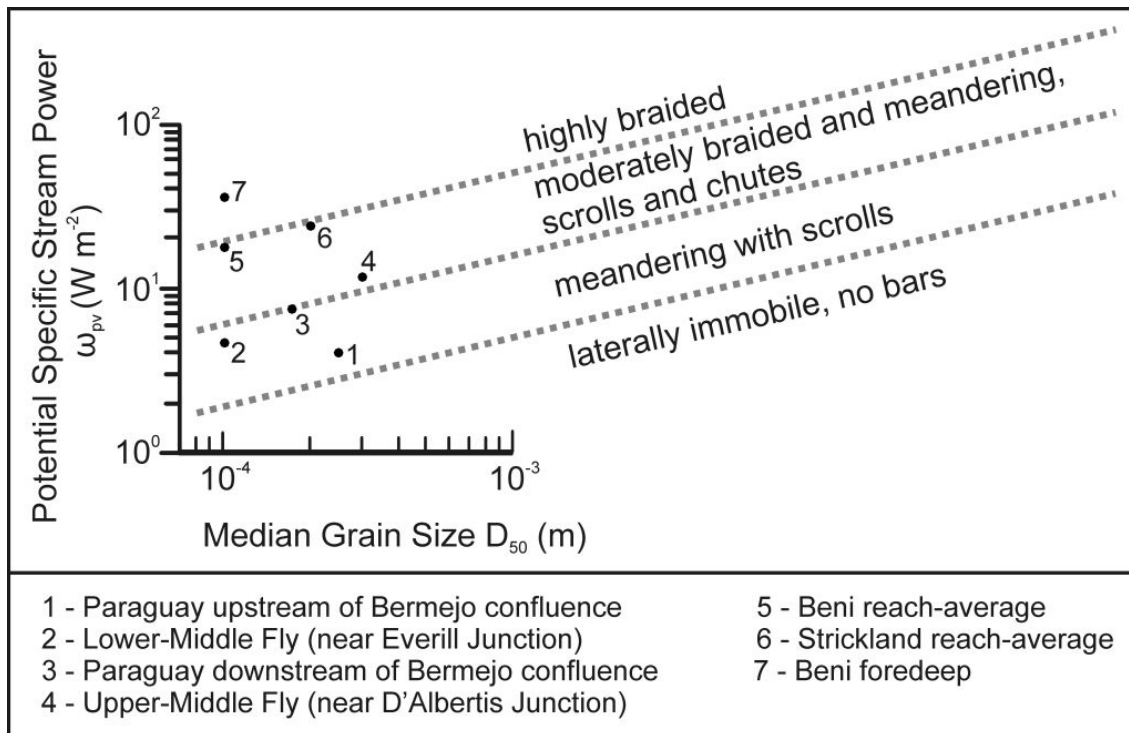
Figure 2.7: Study reaches and sub-reaches plotted within the empirical planform continuum of Kleinhans and van den Berg (2011), wherein potential specific stream power is related to valley gradient and predicted width. Data sources are given in the 'River Locations and Physiographic Settings' section of this paper. Data for the Fly are included for comparison with the Strickland (see Dietrich *et al.*, 1999; Lauer *et al.*, 2008).

Since the rivers studied are similar in terms of bedload calibre, the planform continuum plotted in Figure 2.7 largely reflects the effect of increasing potential specific stream power on channel activity and pattern, and the remainder of this discussion draws on additional data presented in this chapter to advance the understanding of why this may be the case. Differences in potential specific stream power are largely related to slope in the case of sub-reach comparison, and to the combination of slope and discharge in the case of inter-reach comparison, and are manifest in different bend extension rates (Table 2.7). Brice (1975) observed that active meanders tend to be wider at bends than at crossover points, as is the case for all rivers in this study. This widening is most

likely an outcome of rapid outer-bank erosion that in the short term outpaces inner-bank deposition (see Parker *et al.*, 2010), such that scroll bars develop a wider spacing (Hickin and Nanson, 1975), and a gap is maintained between the point bar/scroll-slough complex and the inner bank (e.g. Peakall *et al.*, 2007; Braudrick *et al.*, 2009). It must be emphasised that scroll bar formation is not in itself a driver of chute formation, otherwise rivers such as the Beatton in Canada (e.g. Hickin, 1974) and the Klip in South Africa (Tooth *et al.*, 2002) would have chutes. Although the Beatton and Klip form scroll bars, they migrate slowly due to low stream power, and meander bends are excised almost exclusively by neck cutoff.

Detailed observation of the developmental pathway of bends subject to rapid extension provides a conceptual model for understanding why and how this type of migration (above others) favours the initiation and stability of chute channels during scroll-slough development (Figure 2.8). The bend shown is from the Strickland River, but the sequence of change illustrated is typical of most bends in this study subject to rapid extension. First, migration by extension favours positive alignment of scroll-slough topography with the downstream direction of flow diversion across the developing point bar/scroll-slough complex (Figure 2.9, a). The direction of bend movement may be traced by the alignment of scroll bars and sloughs (Hickin and Nanson, 1975; 1984), and at extending bends, sloughs form parallel to the inner-bend apex, providing a direct flow path between bend limbs as extension progresses. In contrast, translation generally results in scroll-slough development that is parallel to the bend limbs and perpendicular to the flow path across the bend neck (Figure 2.9, b).

At the simplest level, these chute channels need 'space' to form within the inner-bank part of the bend, and bar topography conducive to channelling flow, conditions provided by rapid bend extension. Drawing on the literature, one may speculate that rapidly extending bends of sand-bed meandering rivers are vulnerable to dissection by chute channels because point bar development and

associated thalweg shoaling of bedload sheets and unit bars diverts flow into prominent, positively-aligned sloughs (Carson, 1986; Ashmore, 1991; Peakall *et al.*, 2007). Similarly, in gravel-bed rivers rapid extension may limit the topographic expression of point bars, rendering them vulnerable to dissection (Schumm and Khan, 1972; Ashmore, 1991; Howard, 1996).
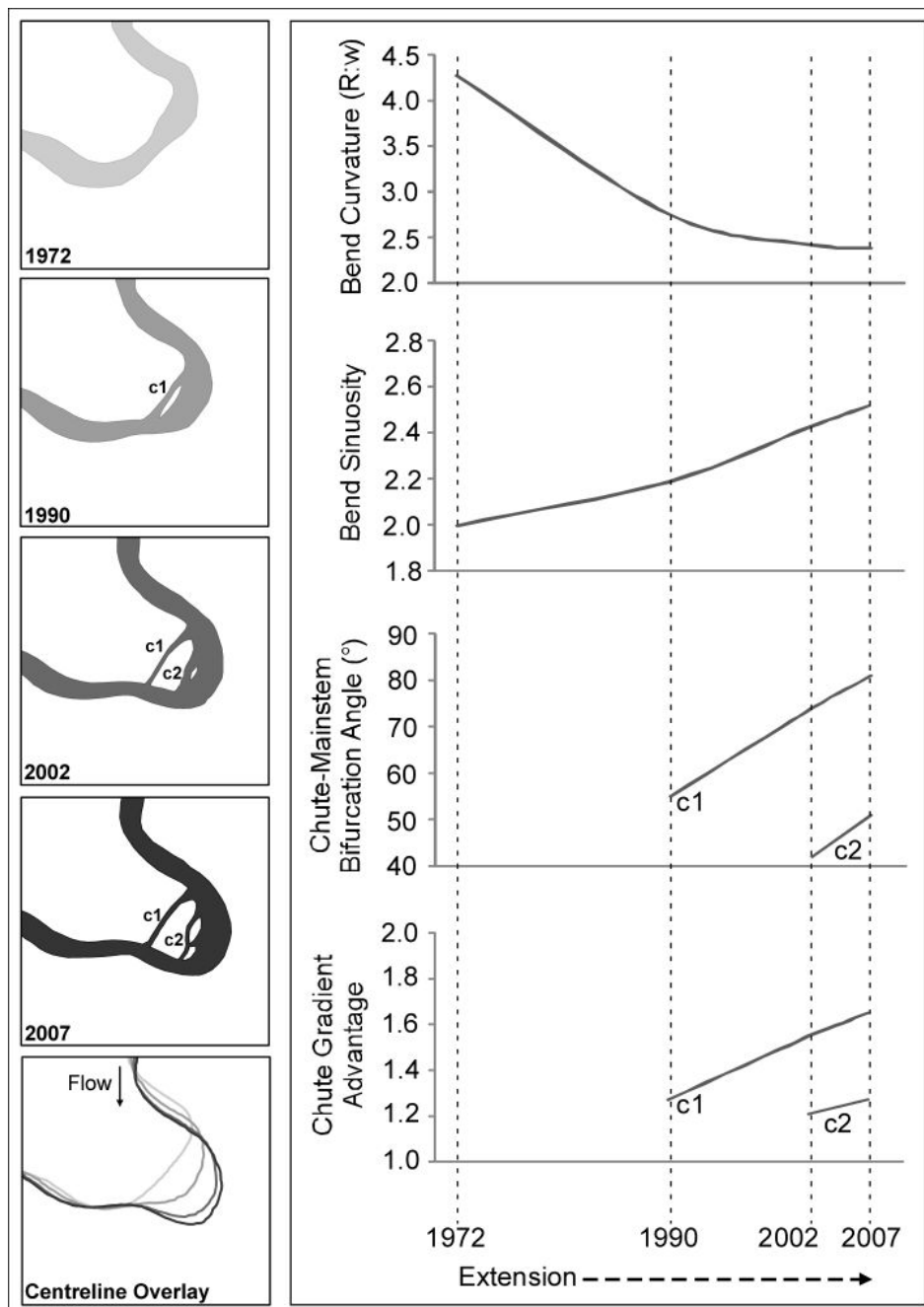
Figure 2.8: The developmental pathway typical of bends undergoing rapid extension, illustrating the formation of stable chute channels, and measured changes in bend apex average curvature (R:w), sinuosity, chute-mainstem bifurcation angle, and chute gradient advantage.
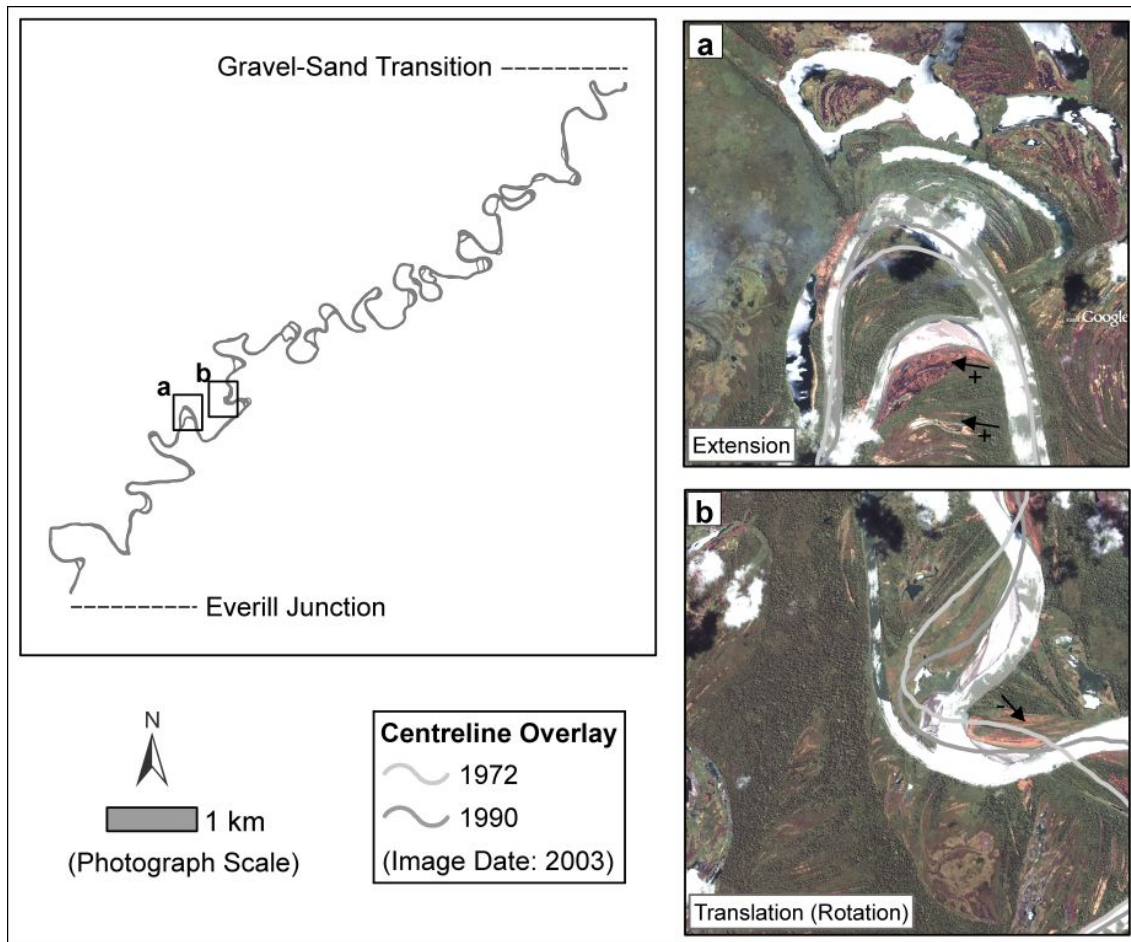
Figure 2.9: Meander bends of the Strickland River, Papua New Guinea, showing alignment of ridge/slough topography during bend migration by extension (a), and translation (rotational-type, b). Bends that undergo extension form ridges and sloughs that are positively-aligned with the downstream direction of flow over the developing point bar (arrow+), while bends subject to translation form ridges and sloughs aligned perpendicular to the downstream direction of flow over the point bar (arrow-). Note: no cases of scour and reactivation of old sloughs far from the active point bar were observed during image analyses – chutes form during active scroll-slough development. Image source: GeoEye, available through Google Earth Pro.

Second, immediately after initiation, chute channels in sandy point bars are vulnerable to infill due to the low bifurcation angle and low gradient advantage associated with their chord location (Figure 2.8), conditions which favour a rapid influx of sediment. An analysis of oxbow lake infilling on the Sacramento River by Constantine *et al*. (2010a) demonstrated that a low diversion angle between a chute channel and newly-forming oxbow lake results in greater oxbow sedimentation than a high diversion angle. Simulations using the Multi-

Dimensional Surface Water Modelling System (MD-SWMS) of the US Geological Survey, predicted flow separation within the entrance of abandoned bends with high diversion angles, which would favour rapid bedload accretion at the bend entrance, leading to rapid isolation of the mainstem, and rapid chute cutoff (Constantine *et al.*, 2010a). Through bend extension, the chute adopts a more axial location (mid-bend, terminology after Lewis and Lewin, 1983), and there is a concomitant tendency for the chute-mainstem bifurcation angle and chute gradient advantage to increase, thereby reducing chute vulnerability to infill. This is discussed further in Chapter 3.

However, the effect of the bifurcation angle and gradient advantage are dependent on the suspended sediment load of the river; the Paraguay upstream of the Bermejo confluence, the Strickland (and Paraguay downstream of the Bermejo confluence), and the Beni (particularly within the foredeep) broadly illustrate an additional continuum with one extreme of low sediment load, extension rate, and chute initiation rate, and another of high sediment load, extension rate, and chute initiation rate, but high chute infill rate (Figure 2.10). The Strickland appears to have a combination of sediment load and bend migration style that most favours the formation of stable bifurcate bends, with highest frequency and rate of bend extension, a Qs/Q approaching 1 kg.m^{-3}, and a decadal-scale chute initiation to infill ratio ~1 (Figure 2.10). This suspended load continuum demonstrates the importance of suspended sediment in filling sloughs and suppressing chute formation, consistent with the experimental results of Braudrick *et al.* (2009), which (coupled with high vegetation cover on point bars) may explain why the Beni foredeep is not braided even though it plots within the range of highly braided channels in Figure 2.7.
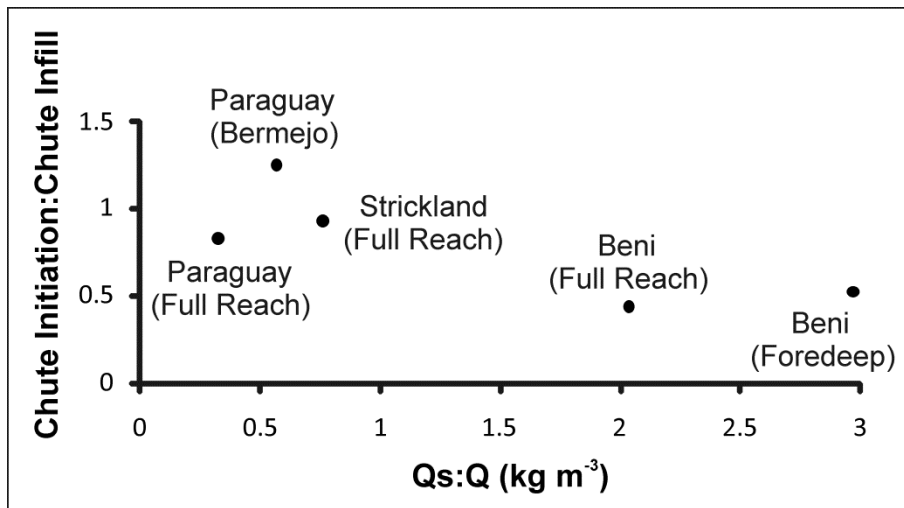
Figure 2.10: Decadal-scale interplay between chute initiation and chute infill on the Paraguay, Strickland and Beni defines a continuum mediated by sediment load (Qs/Q, annual average). The Paraguay occupies one extreme, with low sediment load, bend extension rate, and chute initiation rate, while the Beni occupies the other, with the extremely high sediment load reducing net chute presence through chute infill. The Strickland, where stable bifurcate bends are most common, has an intermediate sediment load (Qs/Q approaching 1 kg.m^{-3}), greatest frequency of bends subject to rapid extension, and a decadal-scale chute initiation to infill ratio ~1.

Exact conditions of bifurcate stability may only be understood through an analysis of the dynamics of flow and sediment division at chute-mainstem bifurcations (e.g. Slingerland and Smith, 1998; Bolla Pittaluga *et al.*, 2003; Kleinhans *et al.*, 2008), a subject developed further in Chapter 3. The nodal point relations describing sediment division at bifurcations proposed initially by Wang *et al.* (1995), and later refined by Bolla Pittaluga *et al.* (2003), Miori *et al.* (2006), and Kleinhans *et al.* (2008), provide a useful starting point for such investigation, although it is noted that these 1D relations are difficult to apply to channels with a high width-depth ratio (such as those studied here), as they do not account for bar dynamics in wide channels that play an important role in switching the dominant bifurcate (Kleinhans *et al.*, 2008). These relations also do not include the effect of bifurcation angle, which Constantine *et al.* (2010a) and the present study suggest should be important. Nevertheless, simulation studies that apply nodal point relations highlight a tendency for equilibrium

bifurcations with strongly asymmetrical configurations (see also, Edmonds and Slingerland, 2008), which at least in planform describe stable chute-mainstem bifurcations.

Third, field observations indicate that the island between chute and mainstem channels is rapidly colonised and stabilised by vegetation, either from the seed bank carried in suspended sediment that aggrades on bar surfaces, or by floating rafts of pioneer grasses (especially *Phragmites karka* in Papua New Guinea) that break away from bars upstream (Figure 2.11, t1 inset). In the tropics, vegetation encroachment toward the channel on point bars is rapid, and easily keeps pace with cutbank erosion at slowly migrating bends. Slough formation at rapidly extending bends thus represents a mechanism by which the continuity of vegetation encroachment may be broken – sloughs tend to remain permanently flooded following their formation, and remain poorly vegetated in comparison with adjacent ridges because the seeds of emergent macrophytes cannot germinate under water (Galatowitsch and van der Valk, 1998). Tal and Paola (2010) note that the effect of vegetation in bedload dominated (gravel-bed) rivers may be to stall the process of chute cutoff and allow bend elongation until a significant slope differential develops between the mainstem and a developing chute, such that the chute captures all flow. As indicated in Figure 2.8, the process of bend extension leads to bend elongation, an increase in bend sinuosity, and a reduction in mainstem slope, and increases the slope differential between the mainstem and potential chute path across the bend neck.

Thus, robust, flood-resistant grasses such as *Phragmites karka* and *Saccharum robustum* play a key role in stabilising the island separating chute and mainstem channels, and may play a role in chute formation by i) reducing the velocity of flood flow over the point bar (and enhancing scour of adjacent sloughs, also noted by Bridge *et al.*, 1986), ii) impeding island surface scour, iii) enhancing sediment accretion on the island surface, especially of fines that increase the cohesion and erosion resistance of the island, and iv) rapidly raising the island

surface elevation relative to the river water level, providing a suitable environment for the establishment of trees that further reduce flow velocity and further increase island surface erosion resistance (Figure 2.11). Colonisation of islands by *Phragmites* occurs on a timescale of weeks to months, and trees may become established over a period of years to decades (Figure 2.11, main photographs), highlighting the important role of vegetation in process-scale fluvial geomorphology in the tropics.

On the Sacramento, and smaller gravel-bed rivers, where chute cutoff is common, but 'partial cutoffs' (stable chute-mainstem bifurcations) do occur (see Micheli and Larsen, 2010), most chutes form within one channel width of a tangent connecting outer banks of meander bends (Lewis and Lewin, 1983; Constantine *et al.*, 2010b). Thus, particularly in the case of the Sacramento, the curvature of an upstream bend influences the location of chute formation at the downstream bend, as embayments form through scour at the locus of peak curvature that subsequently develop into chute channels (Constantine *et al.*, 2010b). In large, sand-bed meandering rivers, extension is generally associated with a reduction in bend curvature (Figure 2.8), but cause and effect in this relationship is difficult to ascribe, and it is likely that rapid extension is more broadly symptomatic of the morphodynamic effects of curvature on bend erosion rates, described most recently by Crosato (2009). In many cases, extension of one bend affects the planform of surrounding bends, and tracking bend extension rates may provide a surrogate predictive measure for chute formation in gravel-bed rivers as well.
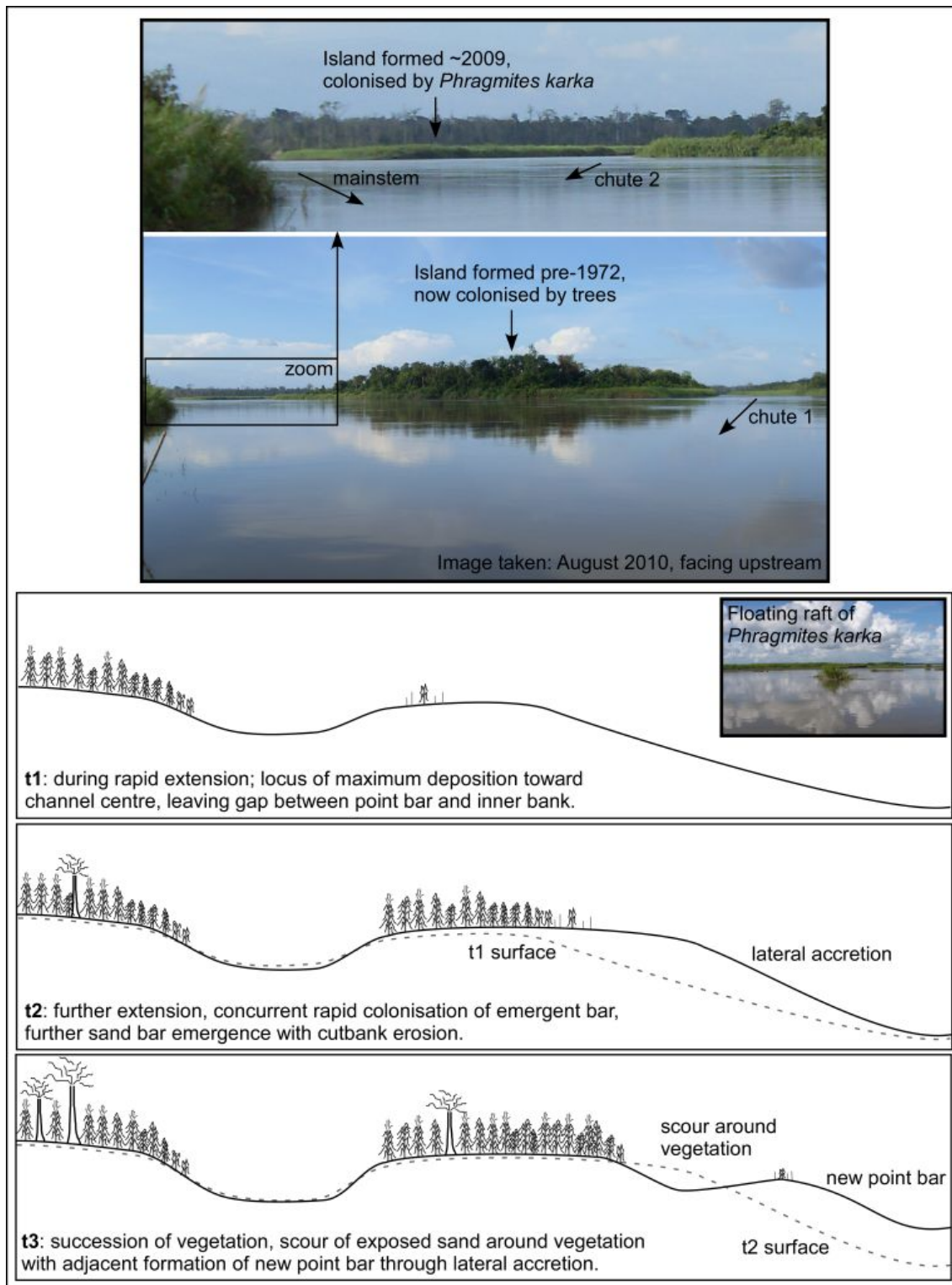
Figure 2.11: Photographs and conceptual model illustrating the key role of robust grasses in stabilising islands separating chute and mainstem channels in the tropics. Inset: Floating rafts of the robust, hydrophytic grass *Phragmites karka* (known locally as *pit-pit*) docked on a point bar in the lower Fly River.

2.7. Conclusion

In large sand-bed meandering rivers, chute formation is an inextricable component of scroll-slough development that occurs most frequently at rapidly extending bends. The analysis presented in this chapter provides some insight into the physical basis of this association. However, a fully-mechanistic understanding of processes leading to chute initiation in this setting may require more sophisticated synthesis of formulations that explain i) scroll-slough development, ii) breaks in the continuity of vegetation encroachment, iii) island colonisation and stabilisation by robust grasses, iv) the morphodynamics of flow and sediment division as sloughs develop, and v) the morphodynamic effects of channel widening on point bar development.

In planform terms, chute channels indicate a transition from single-thread meandering to braiding that is mediated by the relationship between stream power or shear stress and bed material calibre or bank resistance. It is apparent that no single mechanism can account for the development of chute channels in all meandering rivers. In some rivers, an increase in stream power or shear stress may lead to an increase in over-bar or over-bank incision, while in others the result may be an increase in embayment incision. In large, sand-bed meandering rivers, an increase in stream power has the potential to increase bend extension rates, leading to bend apex widening, a break in the continuity of point bar development and vegetation encroachment, and chute formation. While chute cutoff and chute infill maintain a single-thread planform, it is chute stability that mediates the transition from a single- to a multiple-thread channel planform, and in many large, sand-bed meandering rivers, the presence of stable chute channels that co-evolve with the mainstem for decades implies behaviour reminiscent of low-order multiple-thread channel environments.

CHAPTER 3

**Morphology and Stability of Bifurcate Meander Bends in the
Strickland River, Papua New Guinea**

3.1. Introduction

The persistence of a multiple-thread channel pattern requires that new channel branches form faster than old branches infill, or that new and old branches co-exist for a long period of time (decades). If old channel branches close off and infill with sediment soon after new branches form, the result will be a predominantly single-thread channel pattern. Thus, a focus of much recent research on channel planform dynamics, especially in braided and anabranching rivers, has been on understanding river bifurcation dynamics; the division of water and sediment at nodes of channel diffluence (see Kleinhans *et al.*, 2012, for a review). This chapter focuses on bifurcations formed by chute channels in large, sand-bed meandering rivers ('bifurcate meander bends'; Figure 3.1). The aim is to understand controls on chute stability in greater detail than was possible in the spatial statistical analysis presented in Chapter 2. It is imperative that we advance this understanding, because the division of flow and sediment at chute-mainstem bifurcations has implications for: i) the process of chute cutoff, which can occur only if a bend becomes hydraulically disconnected by sedimentation, and the chute captures all flow (Constantine *et al.*, 2010a), ii) channel-proximal sediment dispersal and sequestration overbank and in cutoff channel segments (Constantine *et al.*, 2010a; Chapter 4), and iii) the dynamics of transitional planform patterns that are common in nature but poorly understood (Ferguson, 1987; Kleinhans and van den Berg, 2011; Chapter 2).
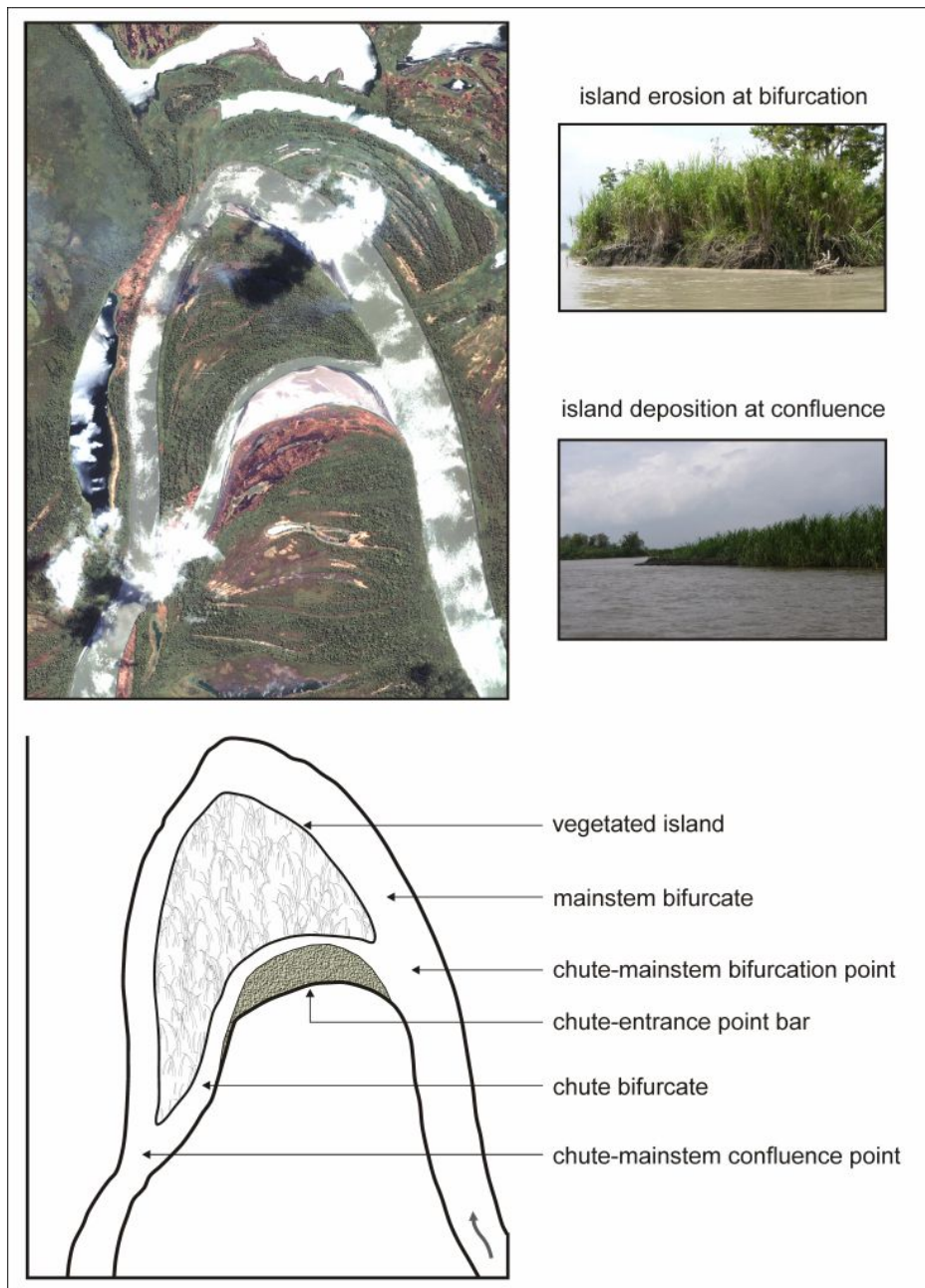
Figure 3.1: Morphology of a bifurcate meander bend. This example is from the Strickland River, Papua New Guinea. Image source: GeoEye, available through Google Earth Pro.

The dynamics of open channel bifurcations, and especially stability configurations, have been a focus of scientific interest for many years (e.g. Bulle, 1926). The problem of bifurcation stability has been tackled with renewed interest since the mid-1990's, initially due to increased recognition of the importance of these nodes of diffluence in the dynamics of braided river networks (Bristow and Best, 1993; Ferguson, 1993), and more recently in the dynamics of river avulsion (Kleinhans *et al*., 2008) and meander cutoff and

infilling (Constantine *et al.*, 2010a). Investigation has proceeded apace with rapid recent developments in physical laboratory (e.g. Federici and Paola, 2003; Bertoldi and Tubino, 2007) and physics-based numerical modelling (e.g. Bolla Pittaluga *et al.*, 2003, Edmonds and Slingerland, 2008; Kleinhans *et al.*, 2008), and advancements in field measurement and image analysis techniques (e.g. Mosselman *et al.*, 1995; Burge, 2006). Different approaches to understanding bifurcation stability focus on different spatial and temporal scales of channel dynamics, make different simplifying assumptions about channel geometry and bank mobility at and upstream of the node of bifurcation, and as a consequence offer different and in some cases conflicting insight into the problem. To provide a framework for the present study, a short review of general trends in the understanding of bifurcation stability follows, subdivided according to key relevant controls identified from the literature.

Shields Stress and Transverse Bed Slope Effects at the Nodal Point

Shields stress (τ_*) is a dimensionless parameter that expresses bed shear stress as a ratio of the hydraulic radius, slope, and median bed grain size in an alluvial channel:

$$\tau_* = \frac{\tau_o}{(\rho_s - \rho_w)gD_{50}} \qquad (3.1)$$

Where;

τ_o is the fluid shear stress per unit bed area (N m^{-2}):

$$\tau_o = \rho_w gRS \qquad (3.2)$$

ρ_s is sediment density (2650 kg m^{-3})

ρ_w is water density (1000 kg m^{-3})

g is acceleration due to gravity (9.81 m^2 s^{-1})

D$_{50}$ is the median bed grain size (m)

R is the channel hydraulic radius (m)

S is the channel slope (m m^{-1})

Dade and Friend (1998) identified modal values of Shields stress for three broad sediment transport regimes: i) suspended load rivers, in which material is transported primarily in the water column, ii) bedload rivers, in which material 'slides, rolls and hops' along the bed, and iii) mixed-load rivers, which are characterised by a mixture of both end member transport regimes. In the present study, a distinction is made between gravel-bed rivers, in which bedload transport is dominant, and sand-bed rivers, in which suspended load transport is dominant. The former tend to be subject to adjustments in hydraulic geometry that maintain a Shields stress close to a critical value for bed sediment transport (Parker, 1978; Dade and Friend, 1998), and have been defined as low Shields stress rivers (Edmonds and Slingerland, 2008). The latter tend to maintain a Shields stress of about 10 (Dade and Friend, 1998), a value that is typically substantially greater than the corresponding critical Shields stress, and have been defined as high Shields stress rivers (Edmonds and Slingerland, 2008).

In flume experiments of bifurcation by mid-channel bar development in low Shields stress channels, Federichi and Paola (2003) noted that stable bifurcations (both bifurcates open) formed when the Shields stress in the mainstem upstream was relatively high, and that at lower Shields stress one bifurcate would become abandoned. Similarly, using a quasi-2D numerical modelling approach for a low Shields stress channel, Bolla Pittaluga *et al*. (2003) found that a balanced (symmetrical) bifurcate discharge division (Qbf a = Qbf b = Qmainstem upstream / 2) requires a (relatively) high Shields stress in the mainstem upstream of the bifurcation. However, at low Shields stress, equilibrium solutions characterised by unbalanced (asymmetrical) bifurcate discharge divisions exist due to the development of an 'inlet step' (*sensu* Bertoldi and Tubino, 2007) or 'bed ramp' (*sensu* Edmonds and Slingerland, 2008); a rise in elevation from the single-thread upstream reach to the shallower of the two bifurcates. This morphology develops as one bifurcate begins to infill while the other begins to scour, and has the effect of deflecting the bedload vector on a transverse bed slope, which decreases sediment supply to the

infilling bifurcate and stabilises the bifurcation (Bolla Pittaluga *et al.*, 2003; Bertoldi and Tubino, 2007; Kleinhans *et al.*, 2008).

Edmonds and Slingerland (2008) also consider this transverse slope effect to be an explanation for the stability of asymmetrical bifurcations in high Shields stress channels, but identify an additional necessary condition for stability; non-uniform water surface elevation at the entrance to the bifurcate channels. They argue that this condition is an outcome of morphodynamic feedbacks between a co-evolving river bed and flow field. In contrast to predictions for low Shields stress channels (Bolla Pittaluga *et al.*, 2003; Miori *et al.*, 2006; Bertoldi and Tubino, 2007), Edmonds and Slingerland (2008) found that the bifurcate discharge division in high Shields stress channels becomes more asymmetrical as the upstream mainstem Shields stress increases; increasing the amplitude of the bed ramp results in lower discharge and bedload transport in one bifurcate, but also increased water surface slope in that bifurcate. The increased water surface slope increases the bedload transport rate, such that a stable equilibrium solution requires a higher bedload feed rate, which requires a higher upstream mainstem Shields stress (Edmonds and Slingerland, 2008).

Bifurcation Planform Geometry (Bifurcation Angle, Bifurcate Gradient Advantage)
Bulle's (1926) experiments showed that the bifurcation angle affects the location and size of a flow separation zone that forms downstream of the bifurcation in the off-taking channel, reducing the effective width of this bifurcate (Figure 3.2a). A bar forms in the separation zone that topographically enforces the reduction in width (Bridge, 1993). The role of the bifurcation angle in bifurcation stability has been considered from different perspectives, and consequently different definitions of 'bifurcation angle' have been applied (Figure 3.2b). Fortunately, all definitions are at least consistent in the sense that an increase in the 'deflection angle' according to Mosselman *et al.* (1995) would amount to an increase in the 'bifurcation angle' as defined by Burge (2006), and the 'diversion angle' as defined by Constantine *et al.* (2010a). It is noted that the latter definitions are essentially equivalent. Burge's (2006) definition of

bifurcation angle was also adopted by Kleinhans *et al.* (2011), and is the definition favoured in Chapter 2 of this thesis, and hereafter.
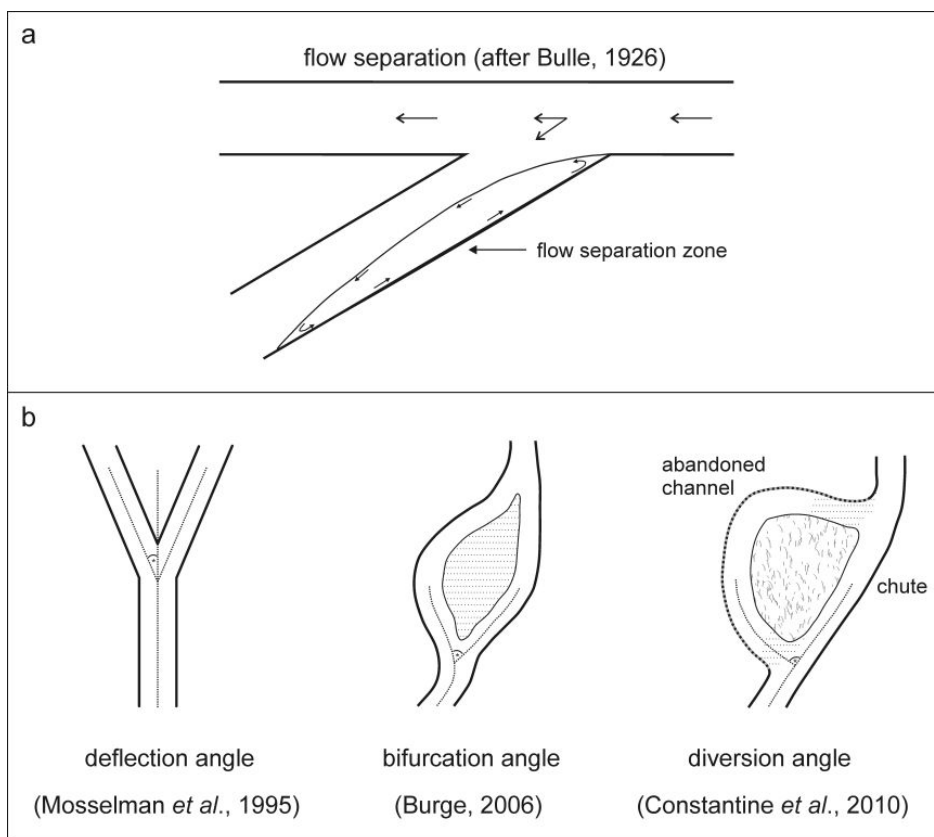
Figure 3.2: The flow separation zone identified in Bulle's (1926) experiments (a), and graphical representation of different definitions for the angle between two branch channels (bifurcates) in a bifurcation (b).

With the exception of results presented in Chapter 2, it has been observed that an increase in the bifurcation angle is associated with a decrease in bifurcation stability (Mosselman *et al.*, 1995; Burge, 2006; Constantine *et al.*, 2010a; Kleinhans *et al.*, 2011). Constantine *et al.* (2010a) accounted for this association mechanistically in the context of chute cutoff; an increase in the bifurcation angle between a chute channel and an abandoning meander bend leads to an increase in the width of the flow separation zone (a decrease in effective channel width in the abandoning bend). This is associated with extensive mouth bar development within, and rapid isolation of the bend. However, with the exception of Burge (2006) and Chapter 2, the above studies consider the role of the bifurcation angle in isolation of the effects of bifurcate gradient

advantages and changes in upstream flow alignment. Burge (2006) noted a weak positive relationship between bifurcate length ratio (gradient advantage) and bifurcation angle in wandering gravel-bed rivers, while Chapter 2 identified a tendency for the gradient advantage of chute channels in large, sand-bed meandering rivers to increase with active bend extension (elongation). This observation is advanced in the present study.

Alignment of Upstream Flow (e.g. Due to an Upstream Bend)

Burge (2006) noted that bifurcations that had been stable for several years could begin to rapidly destabilise following a change in the alignment of flow upstream of the bifurcation entrance, potentially due to meander migration, avulsion, or the addition of sediment by bank erosion (and associated effects on bar dynamics). Effects of migrating alternate bars on bifurcation stability are especially relevant in channels with large width-depth ratios (Kleinhans *et al.*, 2008), as this affects the character of bar dynamics (Struiksma *et al.*, 1985).

Changes in upstream flow alignment were also identified as a primary source of bifurcate 'switching' by Bridge *et al.* (1986), and Federichi and Paola (2003). Kleinhans *et al.* (2008) and Hardy *et al.* (2011) noted that redistributive effects of secondary circulation driven by an upstream meander bend can substantially modify the effects of local (nodal point) bifurcation characteristics, altering the dominant bifurcate and leading to highly asymmetrical divisions of water and sediment discharge. Kleinhans *et al.* (2008) discuss interplay between the effect of an upstream bend on flow alignment, and the gradient advantage of a bifurcate connected to the inner bend (as is the case with bifurcate meander bends). In their simulation series, if the inner bend bifurcate had a gradient advantage of more than 30 %, it would become dominant regardless of the curvature of the upstream bend, but for a gradient advantage of only 10 %, the inner bend bifurcate would be dominant if the bend upstream curved gently, but subordinate if the bend upstream curved sharply (such that the peak flow velocity core is guided toward the outer bank).

3.2. Morphology of Bifurcate Meander Bends

Illustrated in Figure 3.1, the basic structure of a bifurcate meander bend includes i) a chute-mainstem bifurcation point, defined here as the point of intersection of chute and mainstem centrelines, ii) a similarly defined chute-mainstem confluence point, and iii) a vegetated island separating chute and mainstem bifurcates (some bends have two to three chutes/islands). Sandy point bars that are exposed during periods of low flow are present at the entrance to chute channels (Figure 3.1). The outer bank of chute channels at the entrance (the island face at the bifurcation point) is typically vertical and displays signs of active erosion, while active bar growth and island accretion is often evident at the chute-mainstem confluence (Figure 3.1, inset photographs). The chute channels are typically fluted in plan, having a wide entrance at the bifurcation point, tapering to a narrower section, and in some cases flaring out again at the point of confluence with the mainstem (Figure 3.1). Many chute channels that have co-existed with the mainstem for several decades develop a sinuous planform, perhaps due to the interplay between point bar deposition and island face erosion at the chute entrance (e.g. Barkdoll, 2004).

3.3. GIS Analysis of Chute Stability

GIS analysis of the Strickland, Paraguay and Beni Rivers revealed that stable chute-mainstem bifurcations (where chute channels persist for two or more decades) have higher bifurcation angles, and greater chute gradient advantages than those subject to chute infill (Chapter 2). Further analysis for the Strickland River indicates that there is a statistically significant relationship between the chute-mainstem bifurcation angle, and the chute gradient advantage; higher bifurcation angles are associated with greater chute gradient advantages (Figure 3.3). This relationship is considered co-linear rather than causal, as Chapter 2 demonstrated a tendency for both the chute-mainstem bifurcation angle and chute gradient advantage to increase during the process of bend extension (elongation perpendicular to the valley-axis trend). This style of bend

migration is most common on the Strickland (relative to bend translation, rotation or expansion), and is considered the underlying driver of the bifurcation angle – gradient advantage relationship.
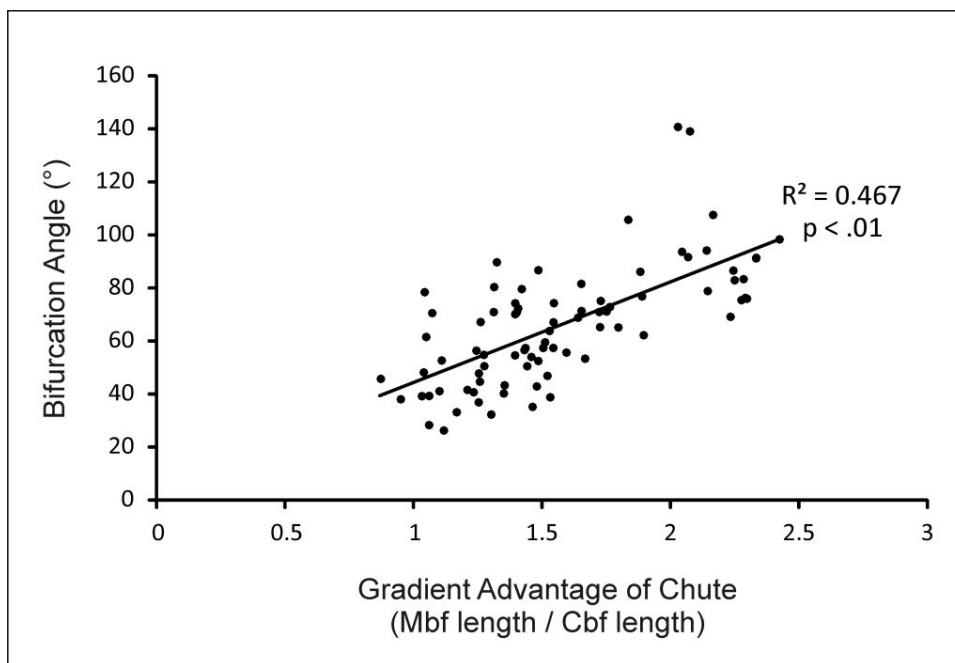
Figure 3.3: Linear relationship between chute-mainstem bifurcation angle and chute gradient advantage for the Strickland River. The dataset comprises measurements of angles and gradient advantages for chute-mainstem bifurcations for four image years; 1972, 1990/93, 2002, and 2007.

Chapter 2 noted that the majority of chute channels on the Strickland initiate during scroll-slough development, and are consequently initially located close to the inner-bend apex ('chord' location, cf. Lewis and Lewin, 1983). With ongoing bend extension, chutes adopt 'axial' locations (mid-bend, cf. Lewis and Lewin, 1983), such that the majority of chute channels are connected to the inner bend at the bifurcation point. As a consequence, the alignment of flow upstream of the bifurcation point typically favours the mainstem bifurcate (Figure 3.4a), and this may be more important to chute stability than the local bifurcation angle or gradient advantage (e.g. Kleinhans *et al.*, 2008; Hardy *et al.*, 2011). It is noteworthy that the only incident of complete chute cutoff recorded on the Strickland River during the period 1972-2007 occurred at the only bend at which the alignment of upstream flow favoured the chute (Figure 3.4b). In

this case, the chute occupies a 'tangential' location (connecting outer banks of alternate bends, cf. Lewis and Lewin, 1983). This is the most common location of chute formation on the Sacramento River, where complete chute cutoff is far more common than on the Strickland (Constantine *et al.*, 2010b).
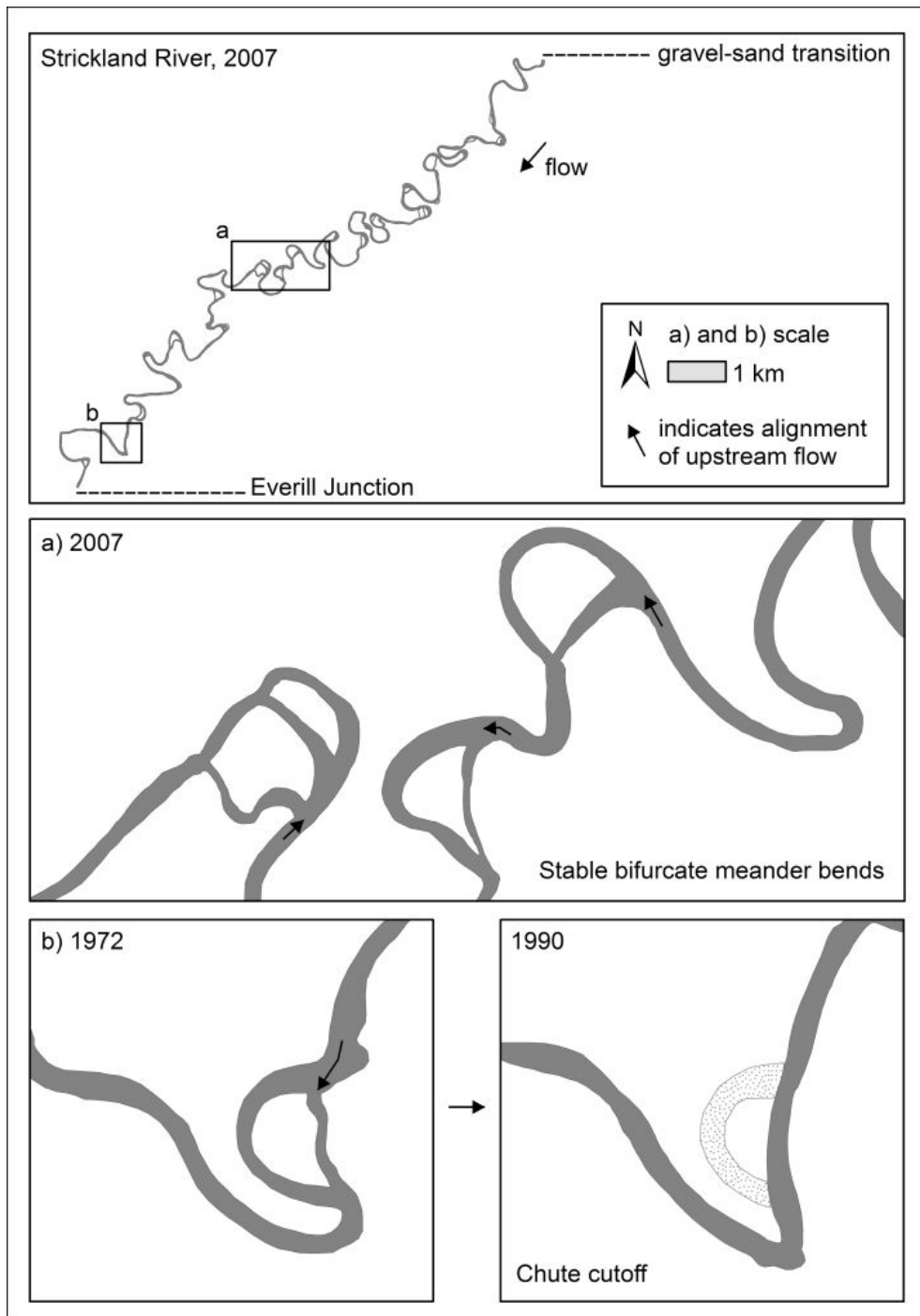
Figure 3.4: The role of upstream flow alignment in the stability of chute-mainstem bifurcations on the Strickland River, showing typical Strickland stable bifurcate meander bends (a), and the only observed incident of complete chute cutoff (b).

3.4. Channel Bathymetry and Bed Sediment Survey

A field campaign was conducted in August of 2010 to survey the bathymetry of several bifurcate meander bends on the Strickland River. The survey system comprised a Starfish 450F side scan sonar (CHIRP acoustic, 450 kHz, 60° vertical beamwidth at 3 dB), and a pair of SyQwest transducers linked to a SyQwest Bathy-2010 PC Precision Profiler (dual-frequency CHIRP acoustic, 3.5 kHz/31° vertical beamwidth at 3 dB, and 12 kHz/18° vertical beamwidth at 3 dB). The SyQwest pairing was designed for bathymetric and sub-bed survey, and optimised for shallow water operation. Only the bathymetric data were used in the present study. Survey data were spatially referenced through a link to a Trimble GPS with real-time differential correction (sub-meter accuracy in x, y, and z, discussed further below). All transducers were pole-mounted below the GPS antenna, and suspended from the side of a wood-fibreglass dinghy (Figure 3.5).
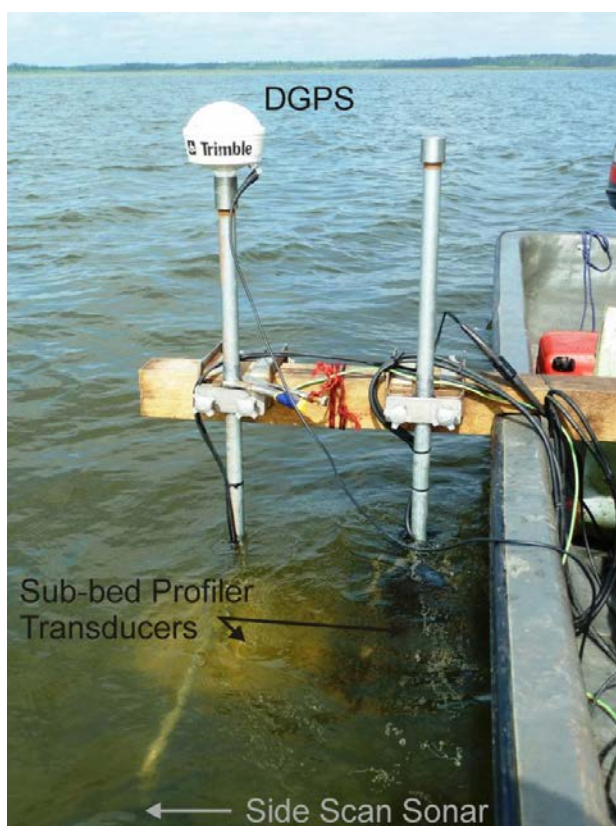
Figure 3.5: The survey system used to map channel bathymetry. Photograph by Anthony Aufdenkampe (August 2010).

Channel survey was undertaken by zigzagging from bank-to-bank across the river to cover as large an area of channel as possible with each pass. The mainstem upstream of a bifurcation was typically surveyed in a single pass, while each bifurcate was typically surveyed in at least two passes, with further survey passes undertaken over the chute-mainstem bifurcation point. Although a more systematic survey approach involving regularly-spaced cross-sections would have been preferable, this was not possible due to competing research-team requirements, time and battery-life constraints due to the remoteness of the location, and intermittent electronics failures due to alternate exposure to extreme heat and torrential rain. The minimum survey resolution comprised transverse passes across the channel spaced one to two channel widths apart to characterise general depths and bar morphology, with further longitudinal passes over the bifurcation point, to provide more detailed insight into the morphology of the bed ramp.

Data for four Strickland meander bends are presented in Figures 3.6 – 3.9. These data were interpolated to the numerical grid structure used in hydrodynamic simulations (discussed in Section 3.5), using the Delft3D grid and depth generation and manipulation software. The raw data set comprised depths below the water surface in an x, y, z point cloud. These needed to be corrected to bed elevations so that the slope of the bed was correctly represented in simulations, but since the GPS elevation data were not of sufficient accuracy to resolve the true slope of each surveyed reach, the best available knowledge of Strickland channel slope was used instead (0.0001 m m^{-1}; Lauer *et al.*, 2008): an initial DEM was developed using a linear interpolation of the vertical fall appropriate to each reach (elevation at inlet = 0, elevation at outlet = 0.0001 × grid centreline length). This DEM was added to a DEM developed by triangular interpolation of the raw depth data.
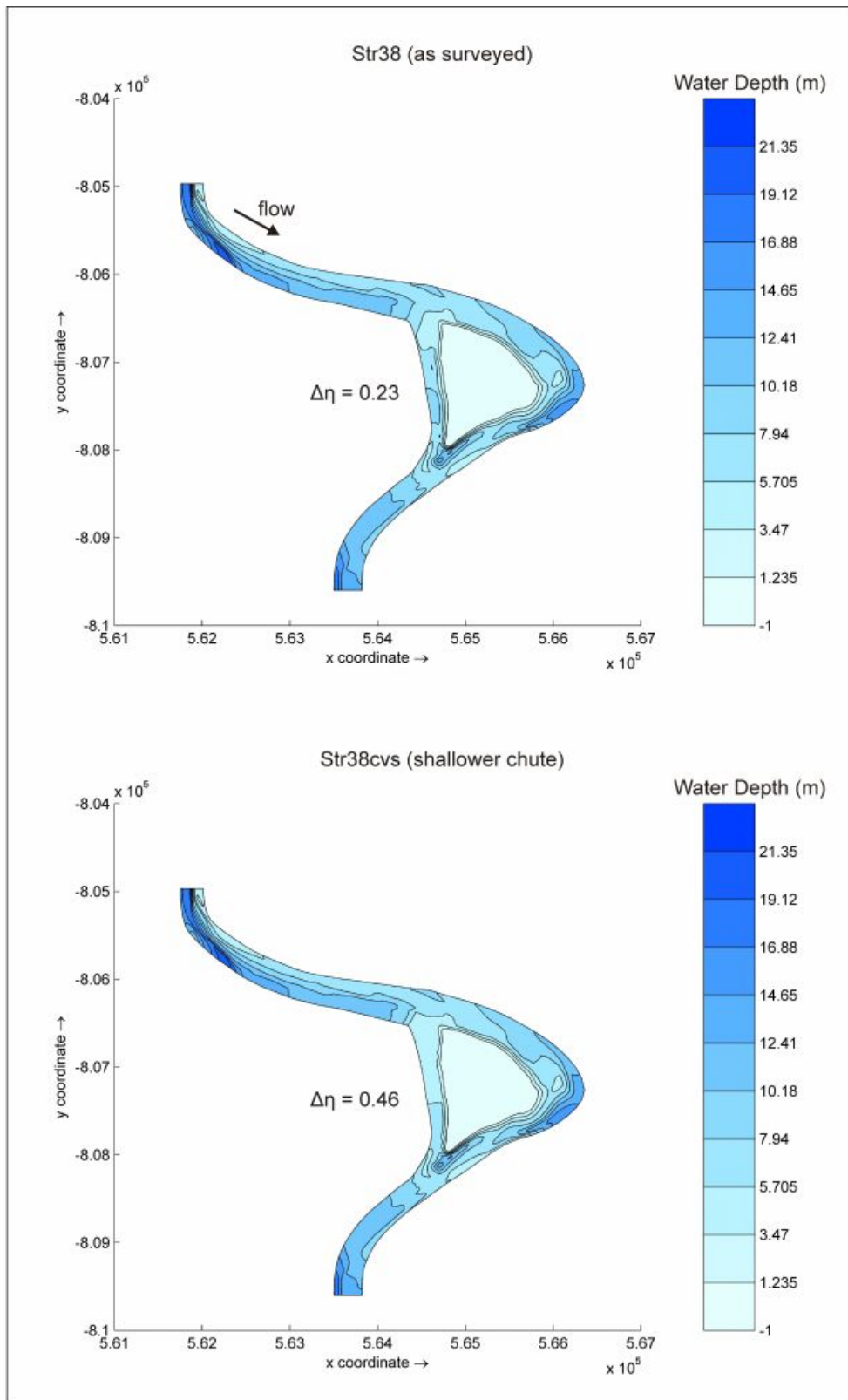
Figure 3.6: Triangular interpolation of bathymetric survey data to the numerical grid structure used in hydrodynamic modelling of meander bend Str38. This is the initial morphology run in morphodynamic simulations as well. A further set of hydrodynamic simulations was run on this geometric grid with a reduced chute depth (Str38cvs). $\Delta\eta$ denotes the bed ramp magnitude (see Section 3.5).
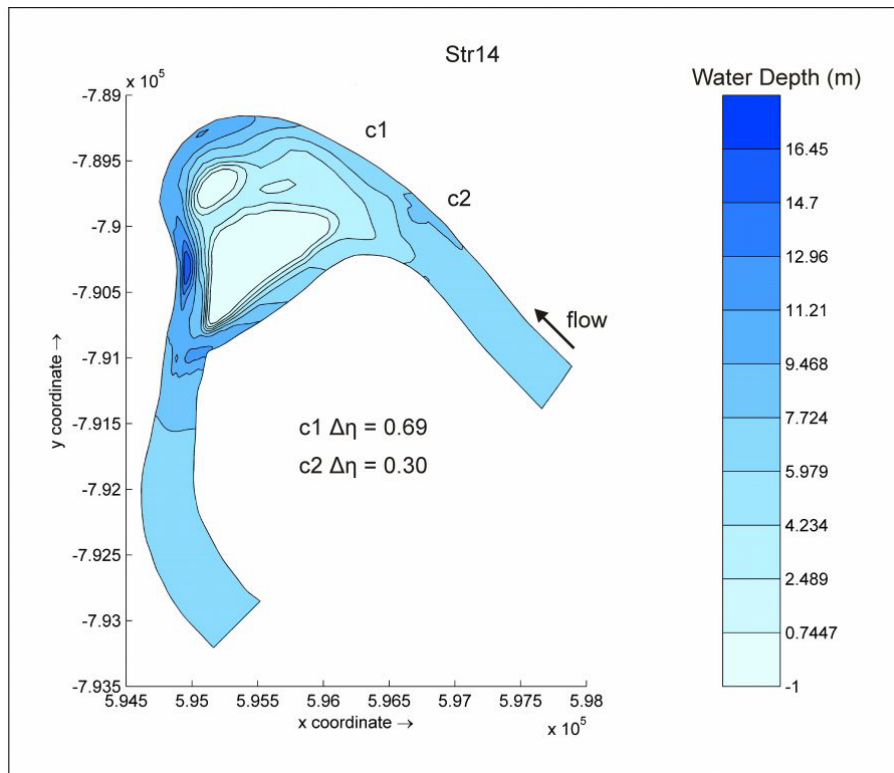
Figure 3.7: Triangular interpolation of bathymetric survey data to the numerical grid structure used in hydrodynamic modelling of meander bend Str14.
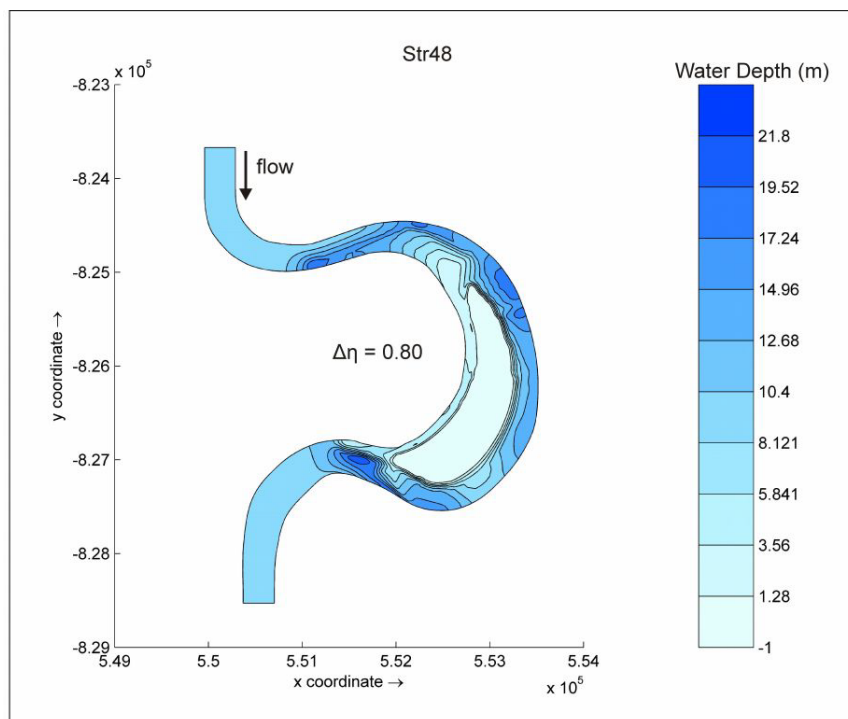
Figure 3.8: Triangular interpolation of bathymetric survey data to the numerical grid structure used in hydrodynamic modelling of meander bend Str48.
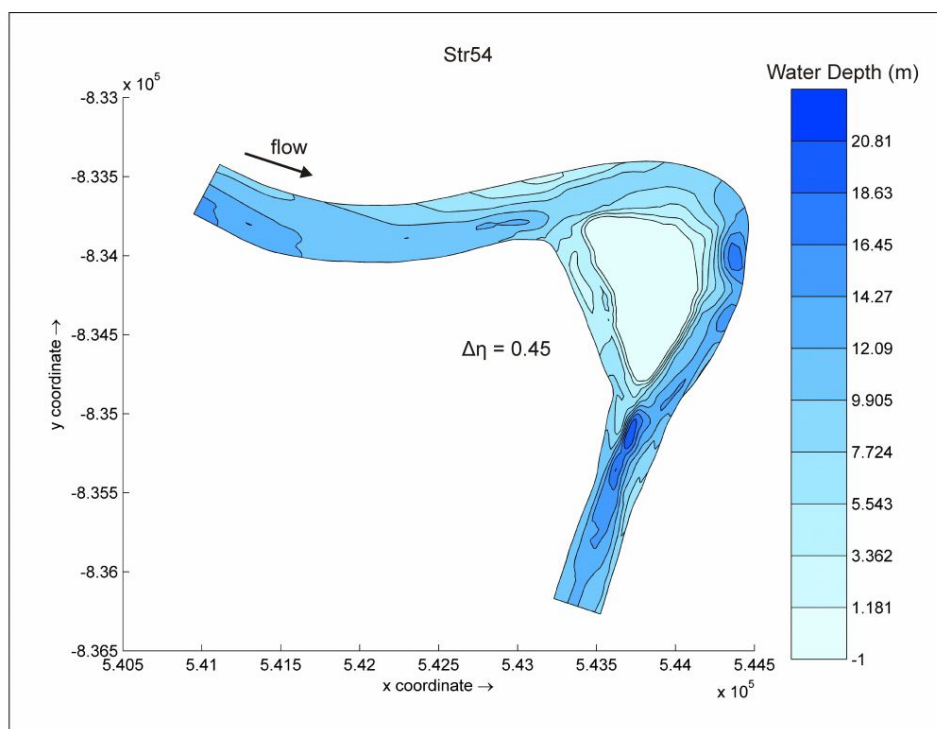
Figure 3.9: Triangular interpolation of bathymetric survey data to the numerical grid structure used in hydrodynamic modelling of meander bend Str54.

Two to three samples of bed sediment were taken within each of the chute and mainstem channels during the bathymetric survey, using a Petite Ponar Grab Sampler, to provide an indication of the bed sediment size. Sampling sites were located as close to the channel thalweg as possible. Samples were returned to Exeter, dried at 50 °C, gently ground to disperse clods, and passed through a vibrating stack of sieves with mesh sizes covering the full sand range (2000, 1000, 710, 500, 355, 250, 180, 125, 90, and 63 μm), to determine median grain size (D_{50}) and textural sorting (D_{84} / D_{16}; Soulsby, 1997). Median grain size (D_{50}) of the Strickland bed sediment samples (n = 20) ranged from 125 – 294 μm (fine-medium sand), and all samples were well-sorted (D_{84} / D_{16} < 2). A D_{50} of 250 μm was applied in simulations (Section 3.5, Table 3.1). Although it is intriguing to note that chute channels consistently yielded coarser bed sediment than their adjacent mainstem bifurcates, the sampling strategy was not of sufficient spatial resolution to determine whether this relationship is statistically significant.

3.5. Modelling Approach and Results

The two-dimensional depth-averaged version of Delft3D was used to model flow and sediment transport in the surveyed Strickland River meander bends, to provide insight into process dynamics at bifurcate meander bends. 2D computations were considered appropriate for this application because i) rivers are generally well-mixed (the fluid is vertically homogenous), ii) previous fluvial applications have found insignificant differences in morphological outcomes of the 2D and the full 3D modelling system (Lesser *et al*., 2004; Kleinhans *et al*., 2008; Edmonds and Slingerland, 2008), and iii) the 2D computations are substantially less computationally demanding. The 2D modelling system solves the two-dimensional depth-averaged form of the Navier-Stokes shallow water equations on a curvilinear finite-difference numerical grid, and has been validated for a range of hydrodynamic and morphodynamic applications (Lesser *et al*., 2004), including the modelling of river bifurcations (Kleinhans *et al*., 2008; Edmonds and Slingerland, 2008).

In this study, bed roughness is parameterised using a quadratic friction law, expressed in terms of a Chézy coefficient that is calculated using the White-Colebrook equation:

$$C_{2D} = 18 \,^{10}\!\log\left(\frac{12h}{k_s}\right) \qquad (3.3)$$

Where;

h is the water depth (m)

k_s is the Nikuradse roughness length (see equations 3.5 and 3.6)

Turbulence is modelled using a zero-order eddy viscosity model (see Uittenbogaard *et al*., 1992), with constant background horizontal eddy viscosity and eddy diffusivity coefficients used in the present study. When implemented in depth-averaged mode, Delft3D does not represent the effects of secondary circulation explicitly. Instead, these effects are parameterised using a secondary

circulation correction scheme, which quantifies the spiral flow intensity in each model grid cell as a function of streamline curvature. This can be accomplished using either the local flow curvature, or by solving a transport equation for spiral flow intensity in which the local streamline curvature provides the source term in the transport equation (this source term defines the equilibrium spiral flow intensity). The latter approach was used in the present study.

A range of sediment transport formulae are available for use in Delft3D. The Engelund and Hansen (1967; equation 3.4) sediment transport predictor was used in this study, following the work of Kleinhans *et al.* (2008):

$$Q_{st} = \frac{0.05 \alpha q^5}{\sqrt{g} C^3 \Delta^2 D_{50}} \qquad (3.4)$$

Where;

Q_{st} is the total sediment transport rate (bed load + suspended load)

α is a calibration coefficient (0(1))

q is the magnitude of flow velocity (m s^{-1})

C is the Chézy friction coefficient

Δ is the relative density ($\rho_s - \rho_w / \rho_w$)

The direction of sediment transport is adjusted to account for the effects of both secondary flow (see above) and the effects of gravity, which causes sediment to deviate from the near bed flow direction slightly and move in the direction of the local bed slope.

Model runs were conducted to examine a series of six separate inlet discharges for each Strickland River bend, from 1500 m^3 s^{-1}, increasing in 500 m^3 s^{-1} increments to 4000 m^3 s^{-1} (the mean annual discharge of the Strickland River is ~ 3100 m^3 s^{-1}). Mean discharge for the Strickland River at a gauging station upstream of the study site, for the month of August 2010, was 3296 m^3 s^{-1} (data provided by Porgera Mining). A short record of daily discharge (2004-2007) is available for a station within the study reach. The maximum recorded daily

flow for this station is 5285 m³ s⁻¹, and the minimum is 405 m³ s⁻¹. Flows of 2500 to 3500 m³ s⁻¹ occur for 43 % of this record, flows of 1500 to 2500 occur for 21 % of the record, while flows of less than 1500 or greater than 3500 m³ s⁻¹ each occur for ~ 18 % of the record. The flows selected for simulation thus cover a range characteristic of the available flow record. Increasing the inlet discharge is equivalent to increasing Shields stress in the mainstem upstream of the bifurcation. Parameter values used in these simulations are given in Table 3.1.

Hydraulic roughness of the bed (equivalent roughness of Nikuradse, k_s) was estimated using van Rijn (1984):

$$k_s = 3\,D_{90} + 1.1\,\Delta(1 - e^{-25\psi}) \qquad (3.5)$$

Where;
ψ is the bed-form steepness given by:

$$\psi = \Delta/\lambda \qquad (3.6)$$

Δ is the bed-form height (m)
λ is the bed-form length (m)

Dunes of 0.2 – 0.5 m in height and 7 – 10 m in length were identified during the bed survey, and appeared to be more numerous in chute channels. Large areas of the mainstem bed were devoid of bedforms altogether. A D_{90} of 300 µm was determined using the bed sediment sampling data. Based on the dune and D_{90} data, an appropriate value for k_s would lie in the range 0.15 to 0.3 m. Given the lack of bedforms in the mainstem, the lower limit was used in simulations. For reference, an average flow depth of 8 m (at the time of survey) would imply a constant Chézy roughness coefficient of 51 and 46 for k_s of 0.15 m and 0.3 m, respectively. Using the White-Colebrook formulation in Delft 3D results in hydraulic roughness (Chézy) varying dynamically with depth.

The transverse bed slope factor for bedload transport (α-bn) used in Delft3D is the inverse of the Talmon *et al.* (1995) formulation for lateral bed slope effects on sediment transport ($f(\tau_*)$), given by equation 3.7 (variables defined in equations 3.1 and 3.2). For an average flow depth of 8 m, α-bn for the Strickland River is ~ 2 (the Delft3D default value is 1.5). α-bn is applied to calculate the magnitude of the lateral bedload transport vector (aligned perpendicular to the main bedload transport vector) in each cell (after Ikeda, 1982 and van Rijn, 1993; equation 3.8).

$$f(\tau_*) = 9 \left(\frac{D_{50}}{h}\right)^{0.3} \sqrt{\tau_*} \qquad (3.7)$$

$$S_{b,n} = |S'_b| \alpha_{bn} \frac{u_{b,cr}}{|\vec{u}_b|} \frac{\partial z_b}{\partial n} \qquad (3.8)$$

Where;

$S_{b,n}$ is the additional bedload transport vector aligned perpendicular to the main transport vector in the down-slope direction

$|S'_b|$ is the magnitude of the main bedload transport vector

α_{bn} is a user-defined parameter, $1/f(\tau_*)$, equation 3.7

$u_{b,cr}$ is the critical near-bed fluid velocity

$|\vec{u}_b|$ is the near-bed fluid velocity

$\frac{\partial z_b}{\partial n}$ is the lateral bed slope

Table 3.1: Parameter values used in Delft3D hydrodynamic simulations for the Strickland River bifurcate meander bends studied in this chapter.

Parameter	Description	Value
Bed Roughness	White-Colebrook formulation, Nikuradse roughness length (k_s)	k_s = 0.15
Bed Grain Size	D_{50}	250 μm
Horizontal Eddy Viscosity and Diffusivity	Constant background values, parameterise sub-grid scale turbulence	Viscosity = 1, Diffusivity = 10 (Delft3D default values)
Alpha-bn (α-bn)	Determines magnitude of effect of transverse bed slopes on bedload transport	αbn = 2 (Delft3D default value = 1.5)

In summary, the model was parameterised as appropriately as possible using the available field data. From an experimental perspective, this set of parameters was applied consistently across all of the bends simulated. Simulations were run until hydrodynamic equilibrium was reached (i.e. until a steady flow solution was obtained) and model output data were then used to obtain two metrics that describe bifurcate flow and sediment partitioning (based on past studies of bifurcation dynamics, Section 3.1): i) the ratio of chute bifurcate to mainstem bifurcate discharge (Q-cbf/Q-mbf), and ii) the ratio of chute bifurcate to mainstem bifurcate sediment transport rate (Qst-cbf/Qst-mbf; total transport according to the Engelund and Hansen predictor). The magnitude of the bed ramp ($\Delta\eta$) into each chute was determined as the difference in bed elevation in chute and mainstem bifurcates, averaged over a distance of two bifurcate widths, normalised with the mainstem flow depth at the bifurcation. Bertoldi and Tubino (2007) tested this and two other methods of determining the bed ramp magnitude, and found that all methods gave very similar results. Bed ramp magnitudes are given in each bend bathymetric plot for visual comparison (Figures 3.6 – 3.9). Greater values of the bed ramp magnitude indicate shallower chute channels.

The model was implemented using orthogonal, curvilinear grids that were boundary-fitted to the planform of the Strickland River for surveyed reaches. Developing such grids poses several challenges due to the complexity of the channel planform. For example, iterative local refinement and de-refinement of the cell structure was needed to cater for large and abrupt changes in channel width, and sharp changes in channel curvature, while maintaining suitable cell aspect ratios and orthogonality (Figure 3.10). However, simulations using a high resolution regular grid produced flow instabilities for a range of sub-grid scale turbulence models, and were consequently abandoned in favour of simulations using a curvilinear grid. The standard simulation grid for each bend comprised 30 cells across the width (each cell ~ 10 – 30 m wide, varying with channel width), while the number of cells in the stream wise direction varied with grid length (each cell ~ 30 – 100 m long, varying with channel

curvature). Sensitivity to grid resolution was tested for Str38 using a grid with double the number of cells in across stream and stream wise directions (double the resolution). Chute-mainstem bifurcate discharge ratios differed by ~ 2 %, while sediment transport ratios differed by ~ 5 %.
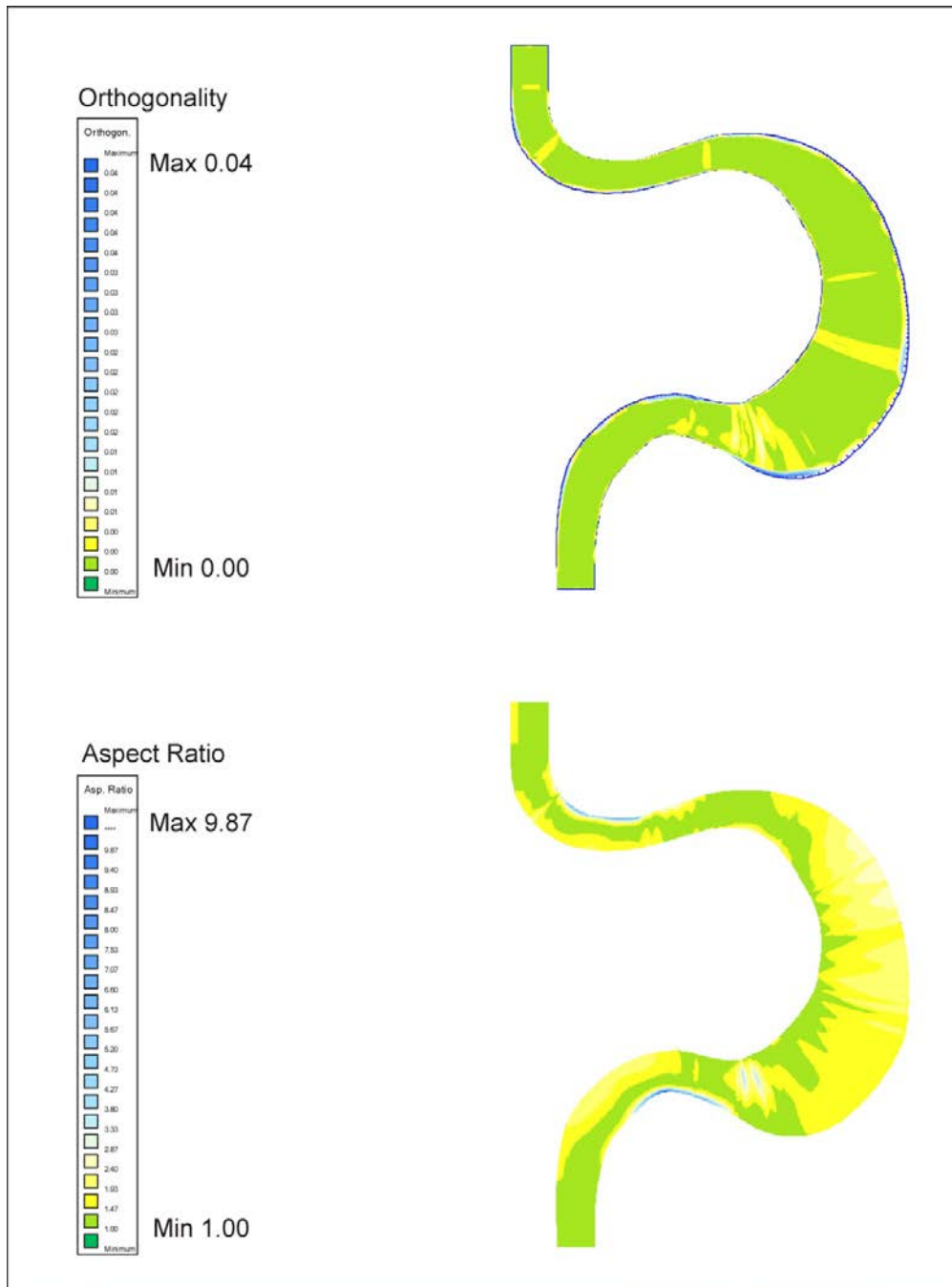
Figure 3.10: An example of variation in grid orthogonality and aspect ratio, for Str48. Aspect ratios up to 15 are acceptable in river simulations because there is a clear primary flow direction. The suggested upper limit for orthogonality is 0.06. Both these conditions are satisfied in the grid displayed.

Grids were refined to achieve orthogonality < 0.06 (the DELTARES Delft3D recommended limit), and cell aspect ratios < 10. Grids used by Edmonds and Slingerland (2008) had aspect ratios ~ 8, while those used by Kleinhans *et al.* (2008) had aspect ratios ~ 5, although neither of these studies employed grids fitted to realistic channel boundaries. For each simulation run, the flow field was examined for spurious oscillations, and the Delft3D diagnostics files were examined for warnings of numerical instability, to ensure that grids were numerically sound. Exemplar orthogonality and aspect ratio plots are shown in Figure 3.10.

Discharge and Sediment Transport Ratios at Hydrodynamic Equilibrium

This section discusses the ratios of water and sediment discharge between the mainstem and chute bifurcates obtained using the results of hydrodynamic model simulations and associated Delft3D sediment transport calculations. In all bifurcate meander bends surveyed in this study, the mainstem bifurcate is dominant (carries more flow), and the chute bifurcate is subordinate (Figure 3.11; a discharge ratio of 1 implies that the chute carries the same discharge as the mainstem bifurcate). Observation of bifurcate bend planform geometries and dynamics (Chapter 2) suggests that this is the case generally. The chutes initiate as sloughs in the lee of scroll bars, close to the inner bend apex, and the bifurcation that develops is asymmetrical in plan (and almost certainly in discharge division as well) from the outset. Thus, the probability of chute cutoff in this setting is very low. Despite this situation, the reasons why chute channels are able to coexist with the mainstem bifurcate for such a long period of time remain unclear (Chapter 2), particularly given the high sediment loads conveyed by rivers such as the Strickland (e.g. Dietrich *et al.*, 1999; Guyot, 1993).

In general, bifurcate bends with smaller bed ramps (deeper chute channels) are associated with larger discharge ratios, and larger sediment transport ratios (relatively more discharge and sediment transport in the chute; Figure 3.11). Discharge and sediment transport ratios varied little with increasing inlet discharge, and thus ratios presented in Figure 3.11 were averaged for the range

of inlet discharges used. The effect of increasing the bed ramp magnitude for the same bend plan geometry is illustrated in a comparison of Str38 and Str38cvs (identical in every respect to Str38, except that it has a shallower chute channel, developed using the Delft3D depth manipulation software). These results are broadly similar to those of Bertoldi and Tubino (2007; their Figure 8), and Kleinhans *et al*. (2008; their Figure 7), but the results are based on the effect of an imposed bed ramp on discharge and sediment transport ratios (rather than one that has developed in morphodynamic unison with the flow over time).

The bed ramp magnitude affects the division of discharge, and relative sediment transport rates within bifurcate meander bends, thus affecting the potential stability of these bifurcations. The chute channels Str14c2, Str38, and Str54 formed prior to 1972, and have coexisted with their respective mainstem bifurcates since. Chutes Str14c1 and Str48 formed between 1990 and 2002. GIS analysis suggests that chute channels with the characteristics of Str14c1 and Str48 are vulnerable to infill (Chapter 2), and one explanation for this in light of the results of the present analysis is that these chutes convey little water and have a low sediment transport capacity. Examples of depth averaged velocity plots for Str48 (large bed ramp) and Str54 (small bed ramp) are given in Figure 3.12.

Kleinhans *et al*. (2008) note for the parameterisation used in the present analysis that a reduction in depth results in an increase in relative roughness (k_s/h), and this affects total transport (proportional to $C^2h^{5/2}$; Engelund and Hansen, 1967). The large bed ramp present at chutes such as Str14c1 and Str48 may effectively deflect bedload transport toward the mainstem bifurcate during chute initiation, but a shallow chute morphology is vulnerable to drying and deposition at low flow, and to vegetation encroachment. Researchers on a recent field campaign on the Beni River in Bolivia, undertaken at a time of low flow, observed a proliferation of dry chute channels within which vegetation had begun to establish, which would increase the roughness of chute channels

and promote deposition at higher flow (Aalto, pers. comm.). Shallow chute channels are less resilient to the aggressive sediment-vegetation interactions that influence floodplain sedimentation in tropical environments. Similarly, Mosselman *et al.* (1995) noted that subordinate bifurcates in the sand-bed braided Brahmaputra-Jamuna River are abandoned by shallowing rather than narrowing, and explained that this was due to low secondary flow and lateral turbulent diffusion in these bifurcates, such that excess sediment entering a bifurcate is not distributed laterally, but settles on the bed (thus increasing the bed ramp magnitude).

To provide further insight into the development of the bed ramp at bifurcate meander bends, the bed ramp magnitude is plotted against the bifurcation angle and chute gradient advantage of surveyed bends (excluding Str38cvs, which has an artificially adjusted bed ramp, Figure 3.13). Illustrated in Figure 3.13, the relationship between the chute gradient advantage and bed ramp magnitude is substantially stronger than that between the bifurcation angle and bed ramp magnitude. Bolla Pittaluga *et al.* (2003) demonstrated that increasing the gradient advantage of the subordinate bifurcate leads to an increase in the discharge ratio, driven by a decrease in bed ramp magnitude. This is consistent with the results presented in Figures 3.11 and 3.13. Thus, although the bifurcation angle and chute gradient advantage of bifurcate meander bends on the Strickland River are related (illustrated in Figure 3.3, and discussed in Section 3.3), it is argued here that the gradient advantage of a chute channel exerts greater control on chute stability, by limiting chute infilling and thus ensuring relatively high discharge and sediment transport capacity in the chute. Incidentally, Papuans refer to the chute channels as 'barets', which translates directly as 'steeps', and shallow-draught vessels make use of these features to reduce travel times on the meandering Strickland River.

Notably, the shallowing induced by the bed ramp extends upstream further in bends with shallow, low gradient chute channels (Str14c1 and Str48; upstream influence ~ 2 mainstem widths), while in bends with deeper, higher gradient

chute channels (Str38 and Str54), the upstream influence of the bed ramp on mainstem morphology appears to be limited (Figures 3.6-3.9). The application of a nodal point relation requires some understanding of the upstream influence of a bifurcation, as this determines the length over which lateral exchange of sediment is modelled. Bolla Pittaluga *et al.* (2003) determined the upstream influence of bifurcations in braided rivers to be ~ 2-3 mainstem widths (also noted by Kleinhans *et al.*, 2008, and similar to the influence observed in Str14c1 and Str48). However, the variation in this upstream influence evident in the surveyed Strickland River bends suggests that generalising this effect in a nodal point relation may not be appropriate. Further data are needed to determine the planform geometric or morphodynamic controls on the upstream influence of bifurcations, which could be used to develop a function that predicts this upstream influence for the purpose of nodal point relations.
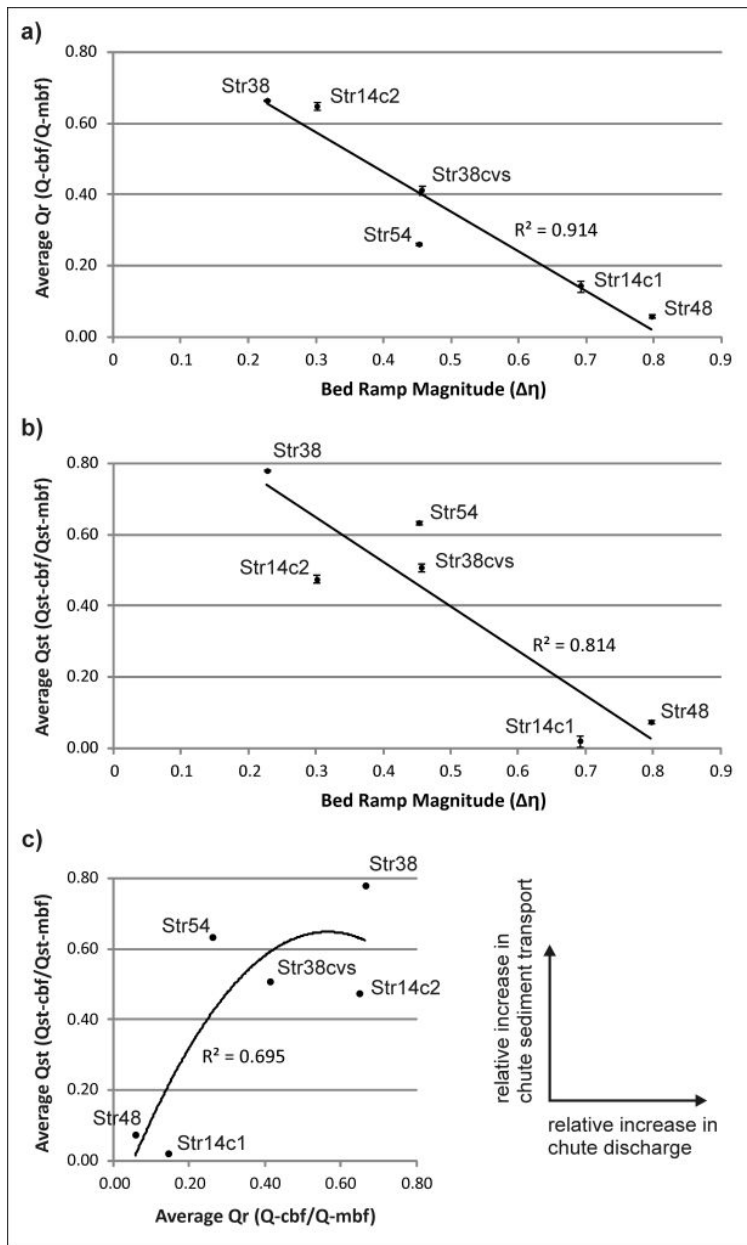
Figure 3.11: Discharge (Qr; a) and sediment transport (Qst; b) ratios as a function of bed ramp magnitude. Error bars indicate the range in Qr and Qst for different values of inlet discharge. Also shown is the relationship between Qr and Qst for the meander bends studied (c).
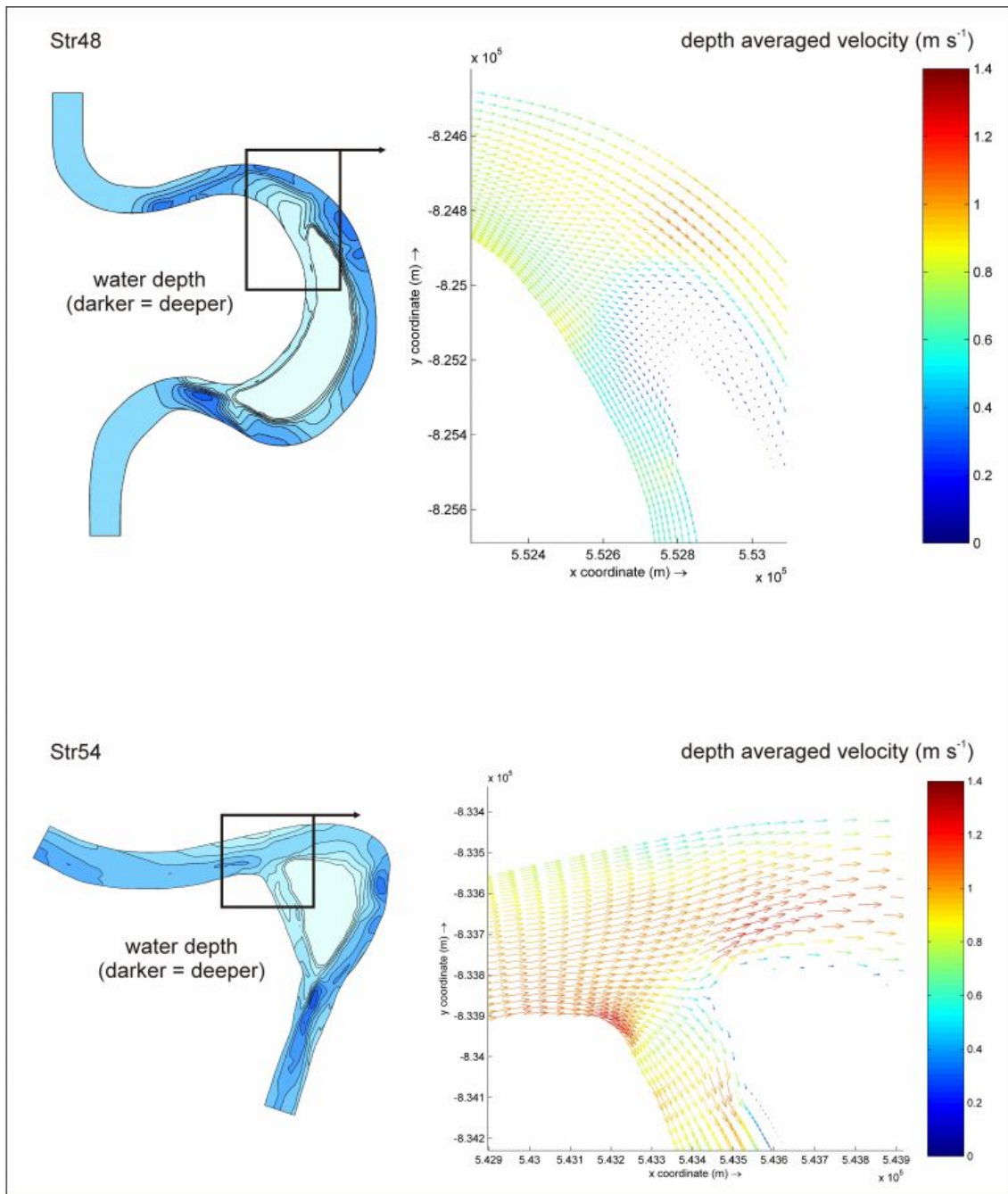
Figure 3.12: Depth averaged velocity plots for Str48 ($\Delta\eta$ = 0.8) and Str54 ($\Delta\eta$ = 0.45). Higher velocity flow is predicted in the larger gradient advantage, lower bed ramp magnitude chute channel of Str54.
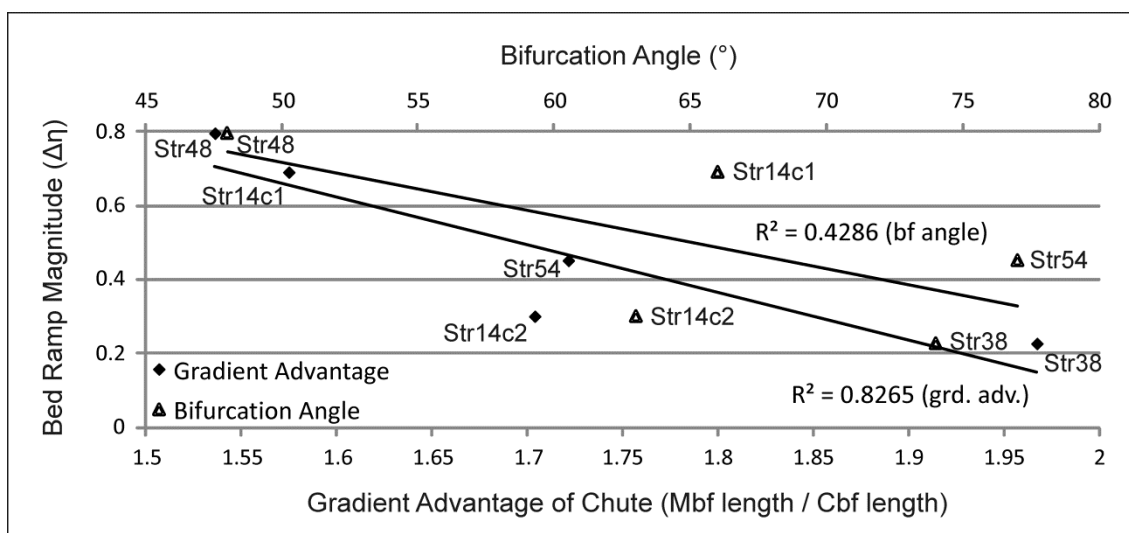
Figure 3.13: For the meander bends studied in this chapter, there is a stronger relationship between the gradient advantage of a chute and the bed ramp magnitude, than between the bifurcation angle and bed ramp magnitude.

Morphodynamic Sensitivity to Alpha-bn

A limited number of morphodynamic experiments were run for bend Str38, to test model sensitivity to α-bn, and to consider the heuristic value of such a simulation approach to understanding chute-mainstem bifurcation dynamics. Given the role of lateral slope effects induced by the bed ramp in the long-term development of bifurcation morphology and stability (Bolla Pittaluga *et al.*, 2003; Edmonds and Slingerland, 2008), it is important that the parameter controlling the magnitude of these effects (α-bn) is correctly calibrated for the particular simulation environment. This is a difficult task, because the effect will vary depending on grid resolution.

When morphological change is allowed for similar parameterisation (α-bn = 1.5 and α-bn = 3) to that used in the hydrodynamics experiments, a bar builds across the mouth of the chute channel (Figures 3.14 and 3.15), and the discharge ratio becomes highly asymmetrical (favouring the mainstem; Figure 3.19a). The hydrodynamic simulations suggest that the chute channel at Str38 at the time of survey conveyed a relatively large proportion of the reach-total discharge, and had a relatively high sediment transport rate (Figure 3.11). Moreover, image analysis suggests that this chute channel has coexisted with the mainstem for

several decades. Despite this, the chute begins to infill in morphodynamic simulations at low values of α-bn. However, the extent of chute infill is reduced if the value of α-bn is increased, but the relationship is complex; although doubling the default value of α-bn elicits little response in bifurcate morphology or Qr (Figures 3.14, 3.15, 3.19a and b), α-bn values of 4.5 (triple the default value) and 6 (four times the default value) elicit a step change in Qr (Figure 3.19a), and result in the development of a substantially more prominent (and stable) chute channel (Figures 3.16, 3.17, 3.19b). Increasing α-bn further has little effect (Figures 3.18 and 3.19). At the highest values of α-bn used in the sensitivity test, Qr approaches that observed in the hydrodynamics experiments for this bend. Thus, to maintain a stable morphology similar to that observed in the field, morphodynamic simulations for the grid, flow and sediment characteristics tested in the present study require a value of α-bn of at least 6.
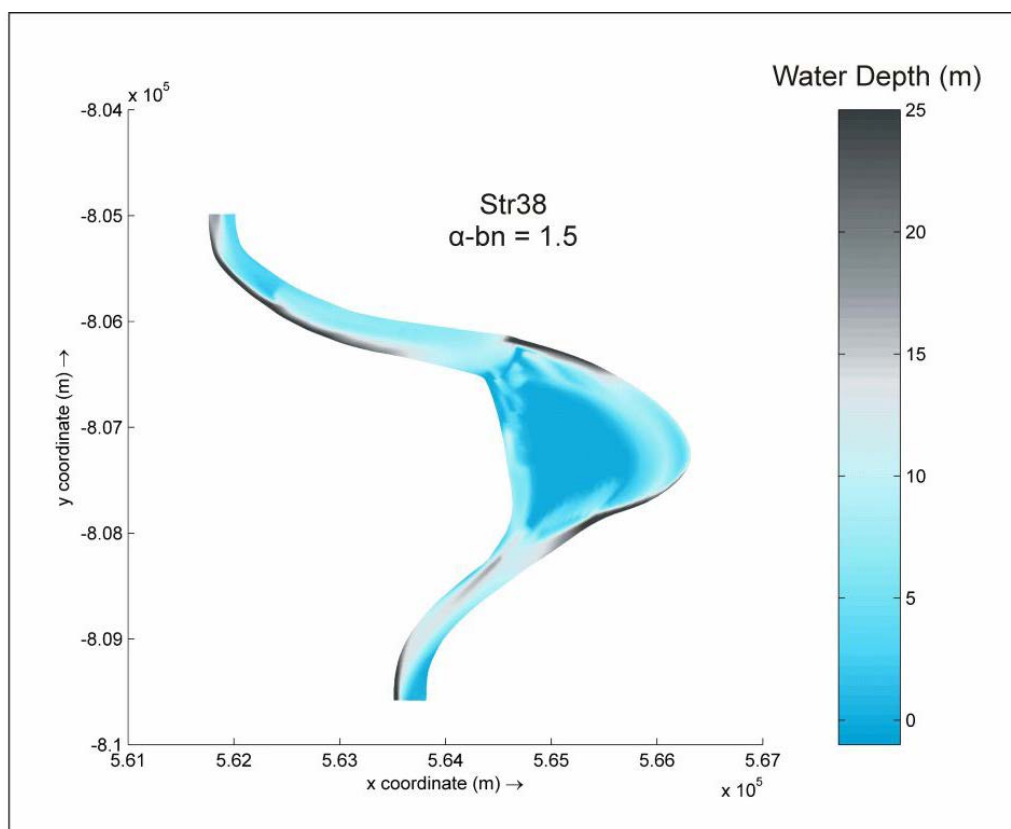
Figure 3.14: Bathymetry of Str38 after ~ 2 years of morphological development from an initial morphology based on field survey (see Figure 3.6), with α-bn = 1.5 (Delft3D default value). A constant inlet discharge of 2500 m³ s⁻¹ was used in all the morphodynamic simulations. There is little change in morphology with time after this point in simulations.
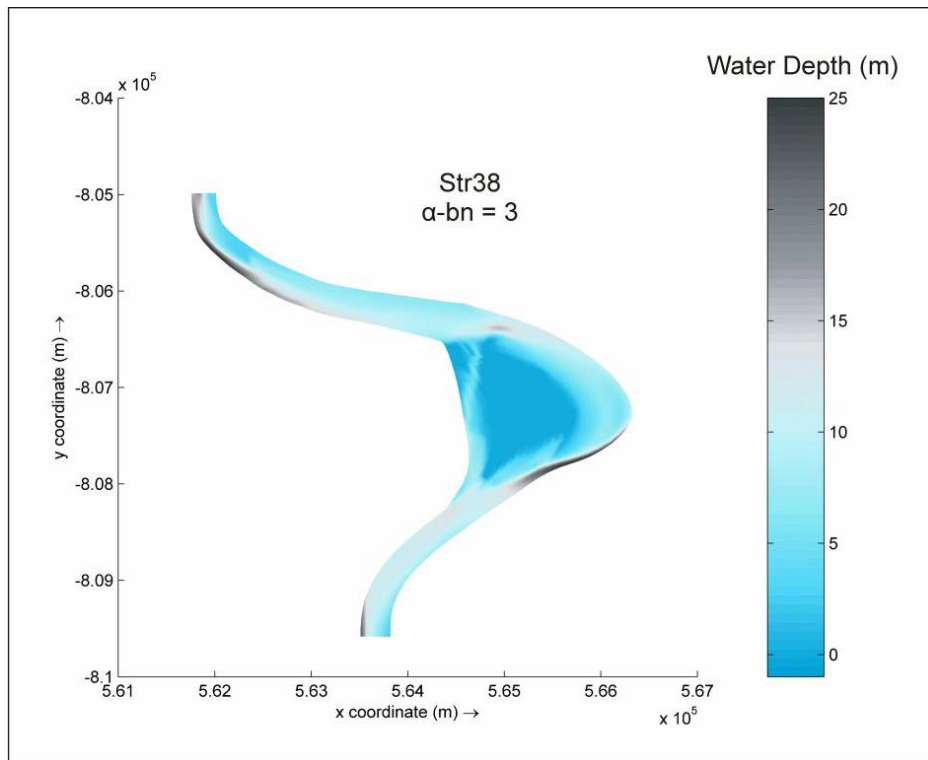
Figure 3.15: Bathymetry of Str38 after ~ 2 years of morphological development from an initial morphology based on field survey (see Figure 3.6), with α-bn = 3 (2 × Delft3D default value).
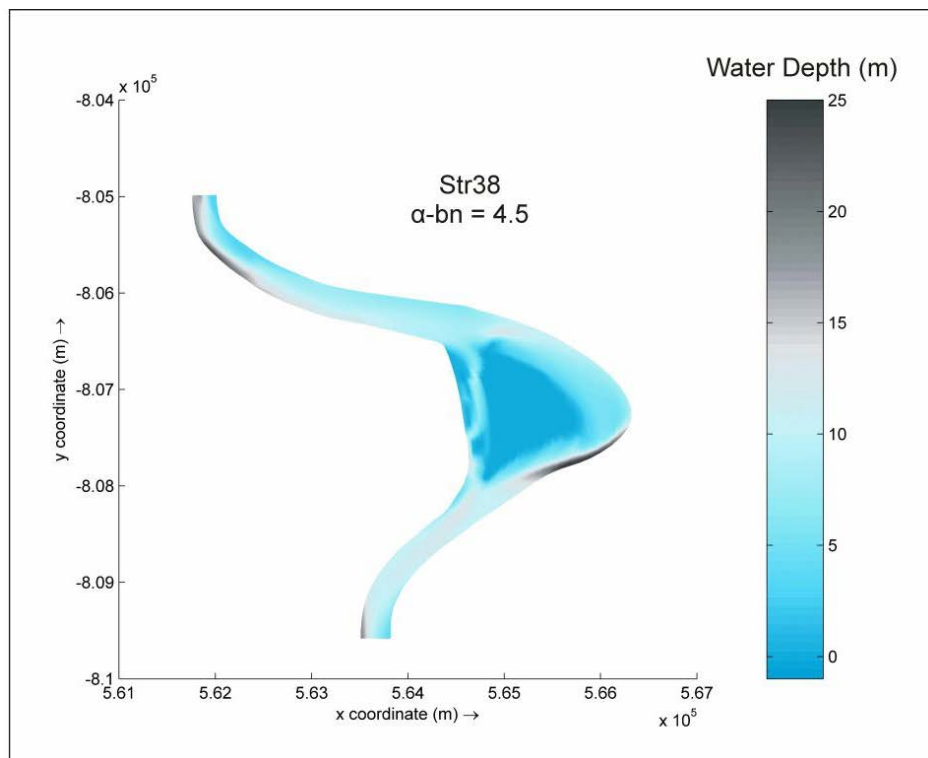
Figure 3.16: Bathymetry of Str38 after ~ 2 years of morphological development from an initial morphology based on field survey (see Figure 3.6), with α-bn = 4.5 (3 × Delft3D default value).
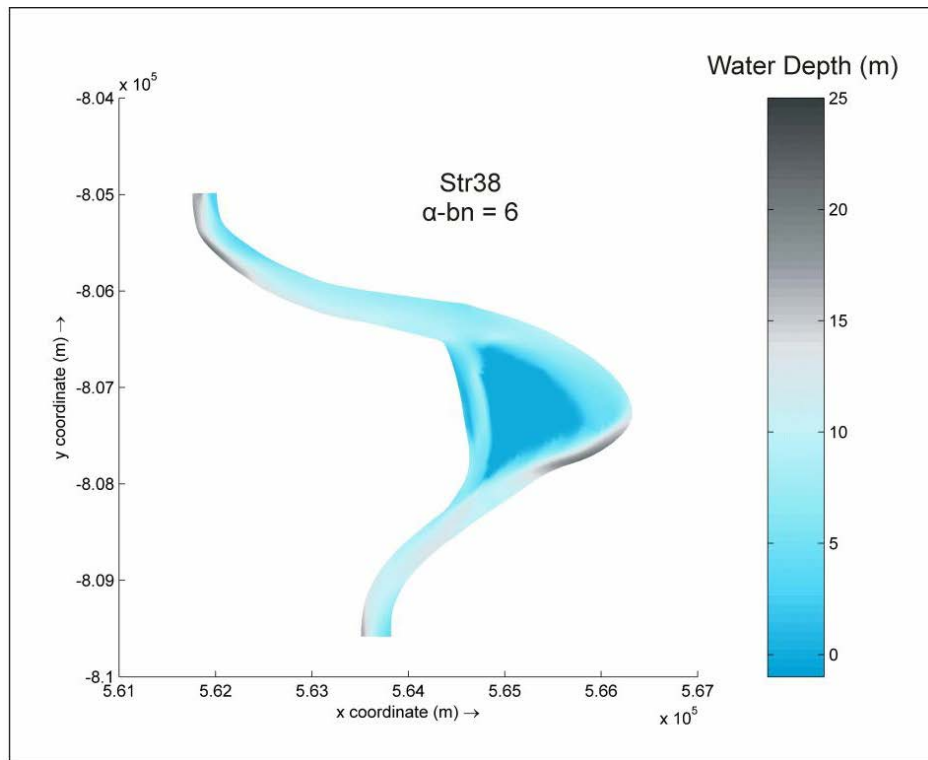
Figure 3.17: Bathymetry of Str38 after ~ 2 years of morphological development from an initial morphology based on field survey (see Figure 3.6), with α-bn = 6 (4 × Delft3D default value).
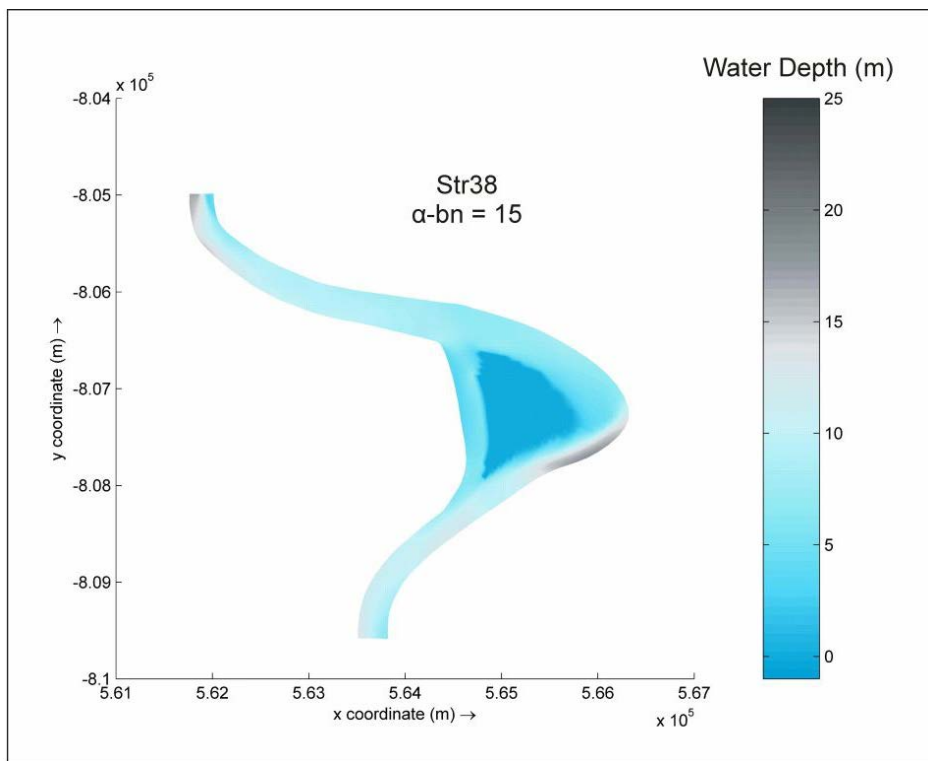
Figure 3.18: Bathymetry of Str38 after ~ 2 years of morphological development from an initial morphology based on field survey (see Figure 3.6), with α-bn = 15 (10 × Delft3D default value).
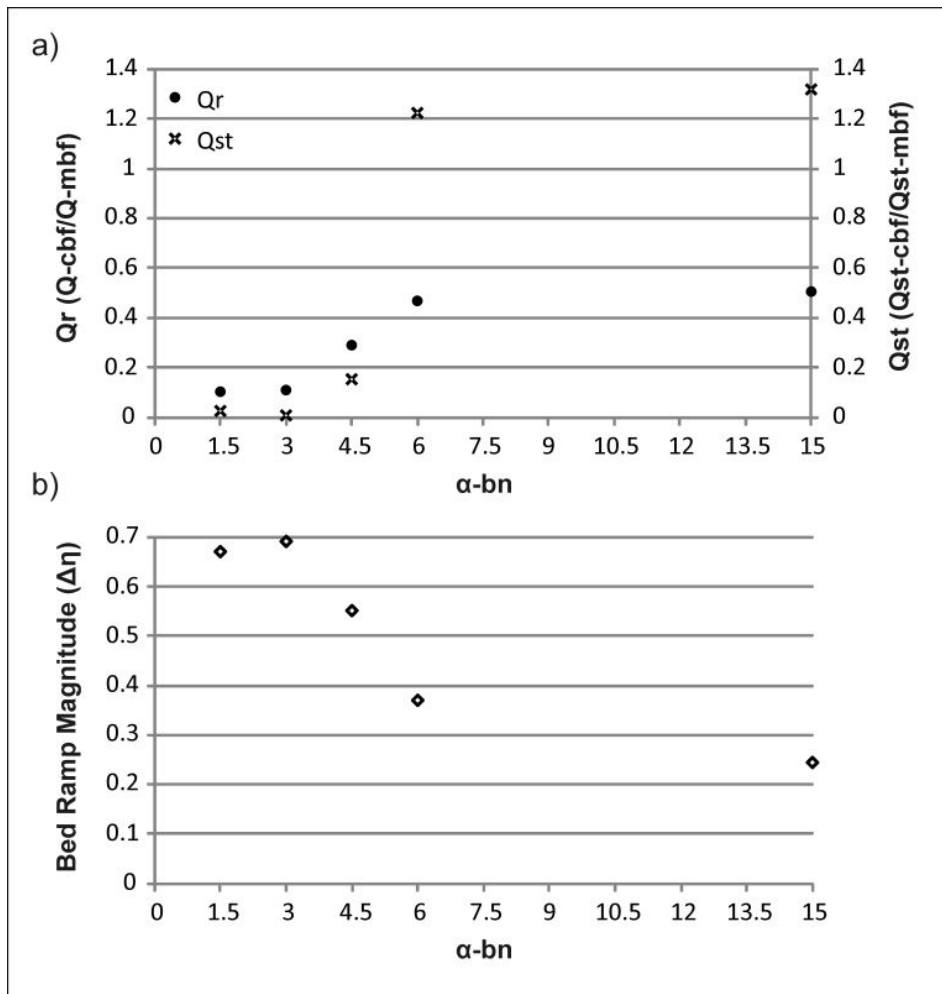
Figure 3.19: Qr and Qst (a), and bed ramp magnitude (b) after ~ 2 years of morphological development, as a function of α-bn.

The effect of changing the value of α-bn is evident over most of the grid; higher values reduce scour along sharply-curving parts of the outer bank, both directly because sediment is distributed laterally to fill zones of scour, and indirectly because lateral growth (across the mainstem bifurcate) of the bar that forms in the mouth of the chute channel, and steers flow toward the mainstem outer bank, is suppressed at higher values of α-bn (relatively more sediment is distributed laterally during bar development, dampening the vertical expression of the bar; Figures 3.14 to 3.18, and 3.19b). At low values of α-bn the bar in the mouth of the chute is periodically breached once flow is impeded in the mainstem bifurcate (once the bar grows across the mainstem), so that the chute does not close off entirely in any of the simulations. This breach results in

a slightly smaller bed ramp in the case of α-bn = 1.5 relative to the case of α-bn = 3 (Figure 3.19b).

Sediment transport ratios are more asymmetrical than discharge ratios, and at high α-bn the sediment transport rate in the chute is higher than that in the mainstem bifurcate (Figure 3.19a). At high α-bn, the mainstem bifurcate has aggraded relative to initial conditions, and the increase in relative roughness (k_s/h; Kleinhans *et al.*, 2008) in the mainstem (and decrease in relative roughness in the chute) is such that the chute conveys relatively more sediment. At low α-bn, the bed ramp into the chute is large (Figure 3.19b), and sediment transport in the chute is negligible despite the chute conveying a small proportion of the discharge, again due to the increase in relative roughness.

Overall, this sensitivity analysis suggests that stable bifurcate meander bends should exist where lateral slope effects on sediment transport are sufficient to reduce the vertical expression of chute entrance point bars, or where secondary flow is of a sufficient magnitude to sweep sediment toward the chute channel margin (and reduce deposition over the chute channel bed; Mosselman *et al.*, 1995). It is important to note that while an appropriate value of α-bn will vary with grid resolution, higher values of α-bn may be necessary to compensate for processes that are not represented by the model, such as bank erosion. Scour adjacent to the mainstem outer bank evident in simulations with low values of α-bn may be partly a consequence of a lack of sediment introduction by bank erosion, which would occur naturally in places where the channel bank is undermined by local scour. Increasing the value of α-bn may artificially compensate for a lack of sediment introduction by bank erosion.

3.6. Conclusion

The stability of bifurcations cannot be understood by focusing solely on dynamics at the nodal point; both upstream (e.g. flow alignment) and downstream (e.g. changes in bifurcate length) factors may influence bifurcation

stability (as noted by Federichi and Paola, 1993; and Kleinhans *et al.*, 2008). The apparent contradictory behaviour of Strickland River bifurcate meander bends, where higher bifurcation angles are associated with stable bifurcations, may be partly explained through 'quasi-balance by opposing factors' (Kleinhans *et al.*, 2008): high bifurcation angles which should lead to wide flow separation zones at the chute entrance, and chute closure, are balanced by large chute gradient advantages, and flow/sediment influx limitations induced by upstream flow alignment. Recent analyses of bifurcation dynamics in braided and anabranching rivers have neglected the role of the bifurcation angle. The present analysis suggests that one cannot consider the role of the bifurcation angle independently of other controls on bifurcation stability, and that its effect may be overshadowed by more fundamental controls on bifurcate morphological development (e.g. gradient advantage).

As is the case with bifurcations in braided rivers, the bed ramp plays an important role in the stability of chute channels in sand-bed meandering rivers, deflecting sediment toward the mainstem bifurcate in the early stages of chute initiation, but rendering chute channels vulnerable to infill if the geometry of meander bends does not change over time. Elongation of the mainstem bifurcate during bend extension increases the gradient advantage of a chute channel, a condition which is associated with lower bed ramps, and thus deeper chute channels that convey a greater proportion of the reach-total discharge, and transport relatively more sediment. However, the relative importance of lateral slope effects on sediment transport is paramount, since it affects the development of the chute entrance point bar (and bed ramp), and indeed the morphology of the entire bifurcation. Careful parameterisation of lateral slope effects in morphodynamic models is therefore necessary to adequately characterise the long-term morphodynamic stability of bifurcations.

CHAPTER 4

Effects of Meander Bend Bifurcation on Floodplain Sediment Dispersal: Strickland River, Papua New Guinea

4.1. Introduction

Chute channels are pervasive features of point bars in many meandering rivers, and where prolific, are indicative of channel planform patterning and dynamics that define a transition from single-thread meandering to braided river behaviour (Brice, 1975; Kleinhans and van den Berg, 2011; Chapter 2). Understanding bar dynamics and bar features such as chute channels is fundamental both to the mechanics of planform transitions (Lewin and Brewer, 2001; 2003), and the dynamics of floodplain development and sediment exchange fluxes (e.g. Lauer and Parker, 2008a; 2008b; 2008c). Significant recent progress has been made in understanding sediment division at nodes of channel diffluence in braided rivers (e.g. Bolla Pittaluga *et al.*, 2003; Federici and Paola, 2003), and in delta distributary networks, and meandering and anabranching rivers (e.g. Jerolmack and Mohrig, 2007; Edmunds and Slingerland, 2008; Kleinhans *et al.*, 2008). However, since the purpose of these studies has been to understand channel stability and pattern dynamics, or avulsion duration, the focus has been on flows up to bankfull. The broader implications of bar and bifurcation dynamics for floodplain development and channel-proximal sediment dispersal are not well known.

Overbank sediment dispersal affects floodplain geomorphological evolution, sequestration of sediment-associated (adsorbed) nutrients and contaminants, and catchment-scale sediment delivery (He and Walling, 1996; Walling *et al.*, 2003). Various apparatus and methods have been used alone or in combination to understand spatial and temporal variation in floodplain sedimentation, including sediment traps (e.g. wooden boards or Astroturf mats), floodplain

sediment cores with radionuclide or tracer geochronology, and modelling. This chapter revisits and extends a dataset of floodplain deposition rates for the Strickland River, Papua New Guinea, derived from Pb-210 alpha-geochronology of sediment cores collected in 2003 (Aalto *et al.*, 2008). Bend-scale floodplain sedimentation rates are assessed within the context of local channel planform geometry and dynamics, and floodplain topographic variation, to determine effects of chute channel formation on the dispersal of floodplain sediment (Figure 4.1). Further discussion centres on implications for large river floodplain sampling campaigns, and geomorphological aspects of floodplain development, vegetation dynamics, and sediment-associated nutrient and contaminant storage.
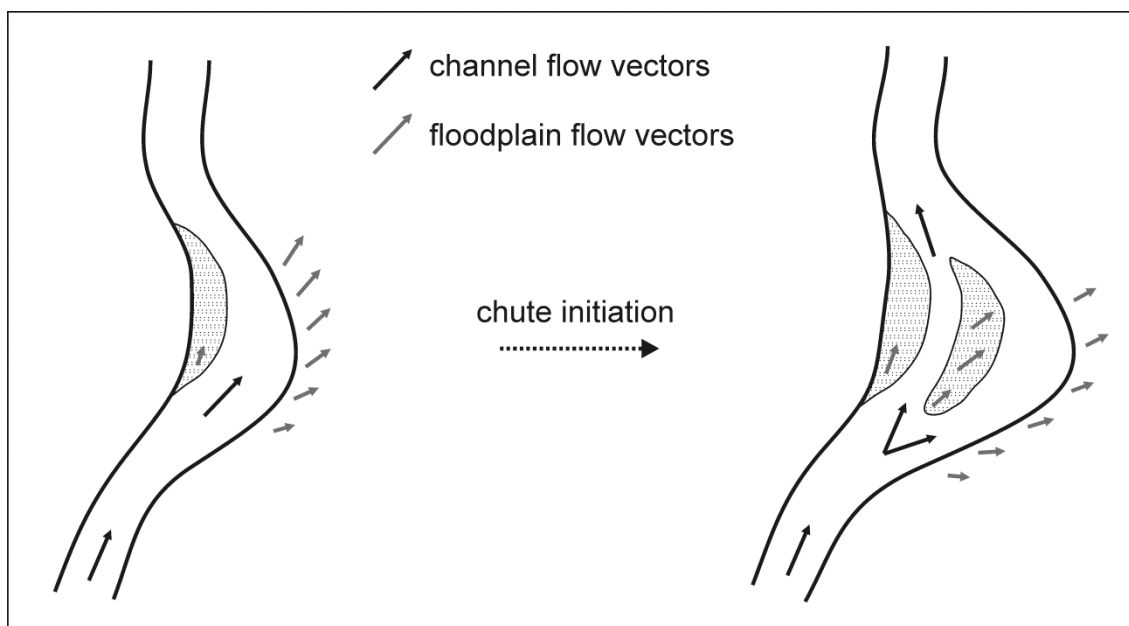
Figure 4.1: It is hypothesised that chute channels in large, sand-bed meandering rivers divert sufficient flow and suspended load from the mainstem to substantially reduce overbank sedimentation rates on adjacent mainstem cutbank floodplains.

4.2. Spatial Variation in Floodplain Sedimentation

Processes of meander migration, cutoff, avulsion, lateral and transverse accretion, and overbank sedimentation interact to populate meandering river floodplains with ridge-slough topography, levees, depressions, and abandoned

channels. The complex topography and roughness variation that result exert feedback effects on the spatial distribution of contemporary floodplain sedimentation (Lewin and Hughes, 1980; Nicholas and Walling, 1997), through their effect on overbank flow frequency, duration, magnitude and velocity (Lambert and Walling, 1987; Hobo *et al.*, 2010). Topographic variation may affect the mechanism of conveyance of overbank sediment, with diffusion dominant in areas of uniform relief (Pizzuto, 1987), and convection dominant in areas of irregular topography, where there are flow components perpendicular to the main channel (Gomez *et al.*, 1997; Nicholas and Walling, 1997; Middelkoop and Asselman, 1998).

Thus, while overbank sediment deposition rates, deposit thickness, and sediment particle size generally decline with distance from the main channel (e.g. Magilligan, 1992), interactions between flood hydraulics and floodplain topography produce considerable variation in this trend (e.g. Middelkoop and van der Perk, 1998). For example, proximal flood basins can channel floodplain flows, limiting basin-ward growth of levees (Filgueira-Rivera *et al.*, 2007), and interrupting the decline in sedimentation rates with increasing distance from the channel (Gretener and Strömqvist, 1987).

Well-developed levees may reduce proximal deposition by restricting the supply of water to the floodplain in their lee (Nicholas and Walling, 1997), or through turbulence-driven 'hydraulic shadow' effects associated with over-levee flow (Singer and Aalto, 2009). Levee width and proximal floodplain sedimentation are furthermore dependent on local channel curvature, affecting water surface superelevation and convective acceleration of channel flow, and on rates of channel migration that consumes newly-deposited levee sediment (Hudson and Heitmuller, 2003).

On meandering river floodplains, highest sedimentation rates typically occur in areas of lowest relative elevation and high channel sinuosity (Nicholas and Walling, 1997). Broad-scale sedimentation patterns are controlled by both

channel-proximal and -distal floodplain topography, which determine the suspended sediment supply point and hydraulic conditions on the floodplain (Nicholas and Walling, 1997; Middelkoop and van der Perk, 1998). Where floodplain flow lines diverge, velocities decrease and deposition is enhanced, whereas at convergent floodplain flow lines, velocities and the potential for scour and entrainment of floodplain sediment increase (Middelkoop and van der Perk, 1998).

Additional complexities in sedimentation pattern are encountered in many large river floodplain systems. For example, in some parts of the Ganges-Brahmaputra system, high local rainfall remobilises floodplain sediment and increases accumulation rates in distal flood basins to a level comparable with deposition proximal to the active channel (Goodbred and Kuehl, 1998). In other large floodplains, pre-flood inundation affects the flood hydraulic head and therefore the extent to which, and the mechanisms by which, sediment is conveyed to the distal floodplain (Aalto *et al.*, 2003). Documenting these complexities is a critical prerequisite to understanding the role of large river floodplains as intermediaries in source-to-sink sediment transfer (Aalto *et al.*, 2003; Aalto *et al.*, 2008), and their associated role in global biogeochemical cycles (Aufdenkampe *et al.*, 2011).

4.3. Methods

2003 Field Campaign
Floodplain sediment cores were extracted in conjunction with floodplain topographic surveys, along transects oriented perpendicular to the Strickland River channel. Coring transects were located at both straight and curved reaches of channel, and extended up to ~ 700 m from the channel bank, with core locations spaced 25-50 m apart. Cores were extracted using a 25 mm diameter cylindrical push-corer encasing clear pvc inserts that were immediately capped at both ends to ensure sample preservation prior to laboratory analysis. Transect locations covered a wide range of channel and

floodplain environments, allowing the present comparison of floodplain sedimentation rates at straight, curved bifurcate, and curved single-thread channel reaches. Core locations are illustrated in Figure 4.2.
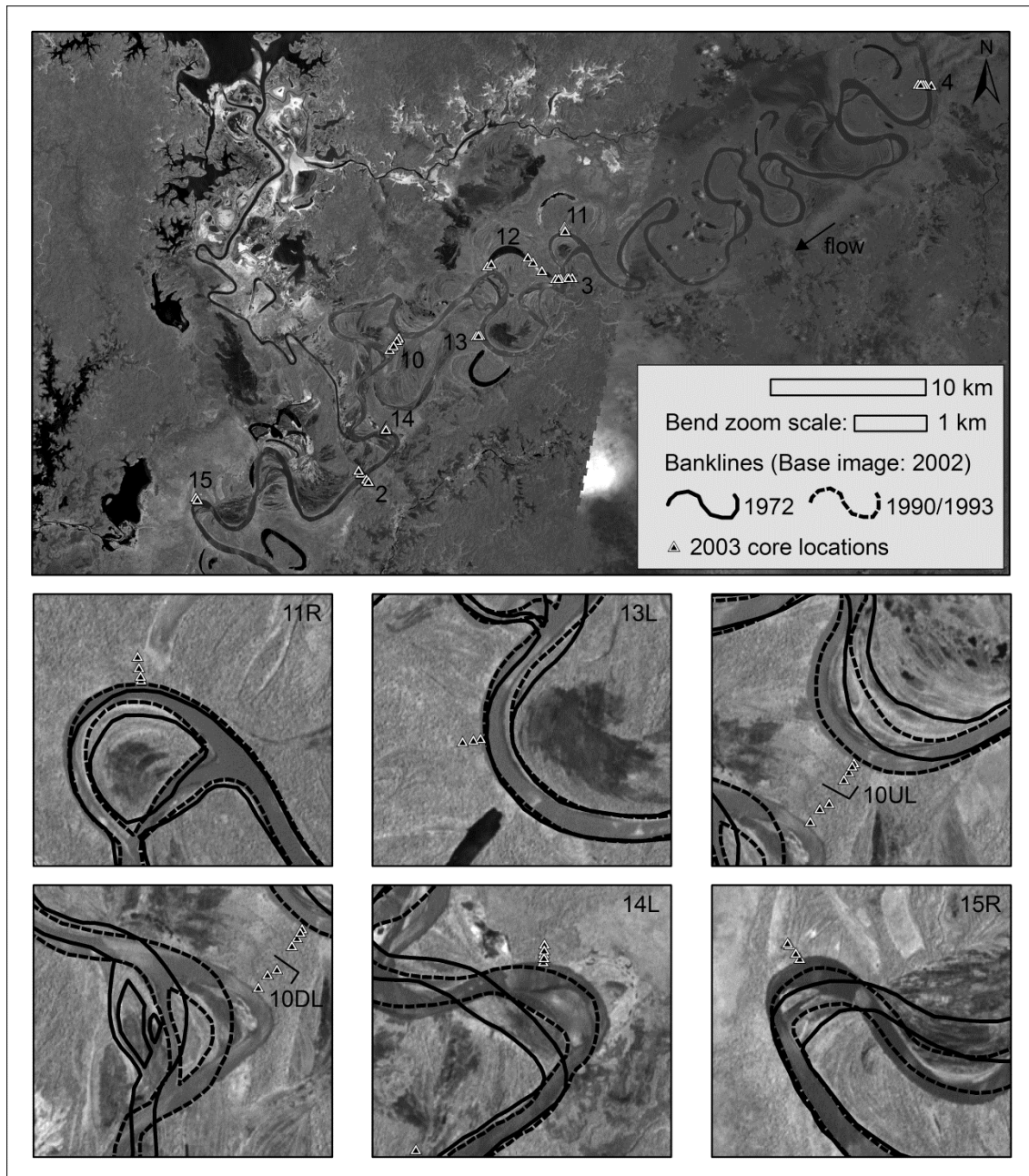
Figure 4.2: Strickland River floodplain transect locations from the 2003 field campaign (main map). The series of inset maps shows core locations for bends studied intensively in this chapter, as well as bend geometry and dynamics preceding the 2003 survey. Transect 12 covered the levee of an oxbow lake, and is not discussed in the present analysis (cores on Transect 12 were located 400 – 2000 m from the active channel, and showed sedimentation rates < 20 mm a^{-1}, with 0 mm a^{-1} typical).

Pb-210 Alpha-Geochronology

The laboratory procedure for Pb-210 alpha-geochronology is explained in detail in Aalto *et al.* (2008), and is summarised hereafter. Cores were sub-sampled at 20 mm intervals for analysis. Sub-samples were dried, crushed and homogenised, and split for particle size analysis (~ 3 g) and Pb-210 geochemistry (1-5 g). Micromeritics Sedigraphs were used for particle size analysis, providing accurate mass distributions by X-ray opacity of the fine fraction (clay), with which the majority of Pb-210 activity is associated (Goodbred and Kuehl, 1998).

In Pb-210 alpha-geochronology, the activity of Pb-210 is determined by counting the alpha activity of the Po-210 daughter. An acid extraction was used to leach mobile, exogenic Po-210 from sediment grain surfaces. This Po-210 was then autoplated onto silver planchettes suspended in a solution of the leachate and dilute HCl (Nittrouer and Sternberg, 1981). Alpha-emission from the planchettes was then counted for 48-72 hours in Ortec alpha-spectrometers. The majority of core data (46 cores) used in the present study were processed at the University of Washington, USA, with data from an additional 11 cores processed at the University of Exeter, UK (using equivalent laboratory protocols), to increase spatial coverage of the floodplain.

Core activity profiles were plotted following calculation of Pb-210 excess activity (normalised to account for clay variability). Supported background activity was determined using a system-wide relationship for clay concentration versus all Pb-210 concentration data for subsamples from deeper zones of uniform activity (Aalto *et al.*, 2008, their Figure 3c). The meteoric rainout rate of Pb-210 was determined using profile data from cores extracted atop raised pre-Holocene terrace remnants abutting the Strickland River (Figure 4.3).
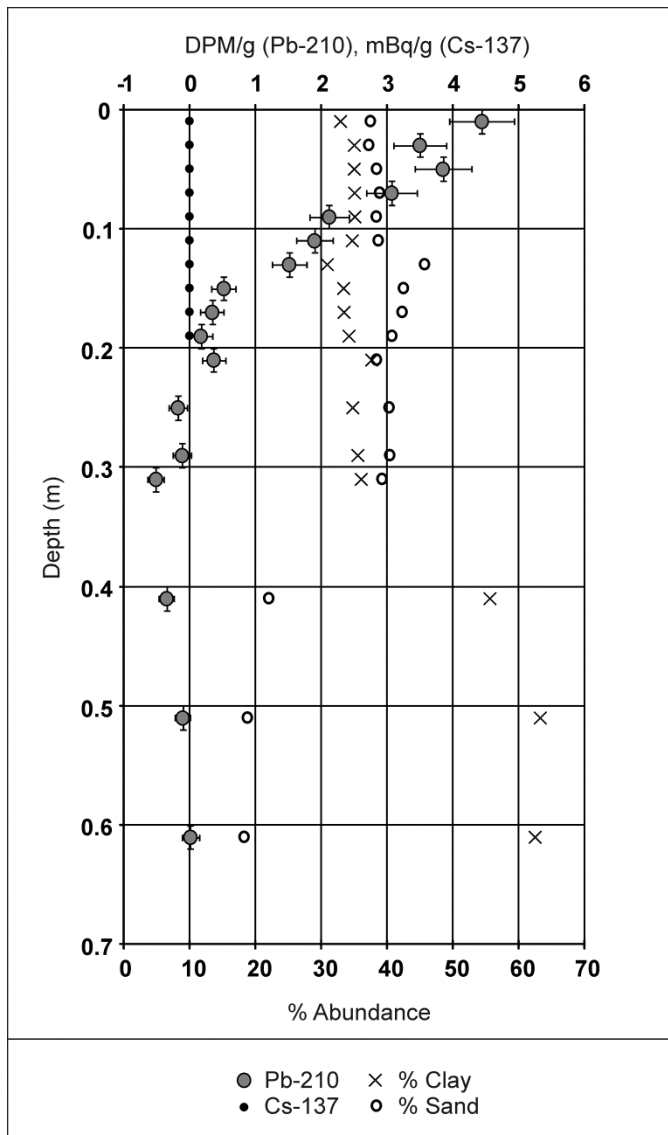
Figure 4.3: Stable-surface core, taken on a pre-Holocene terrace remnant elevated well above the modern floodplain. Meteoric rainout of Pb-210 supports a 'meteoric cap' excess activity of 16.85 DPM cm^{-2}, within the range of 16-17 DPM cm^{-2} found in other terrace cores. Excess activity is adsorbed mostly in the top 0.1 m. Cs-137 fallout was undetectable within this or either of the two other terrace cores processed for gamma spectrometry at Exeter.
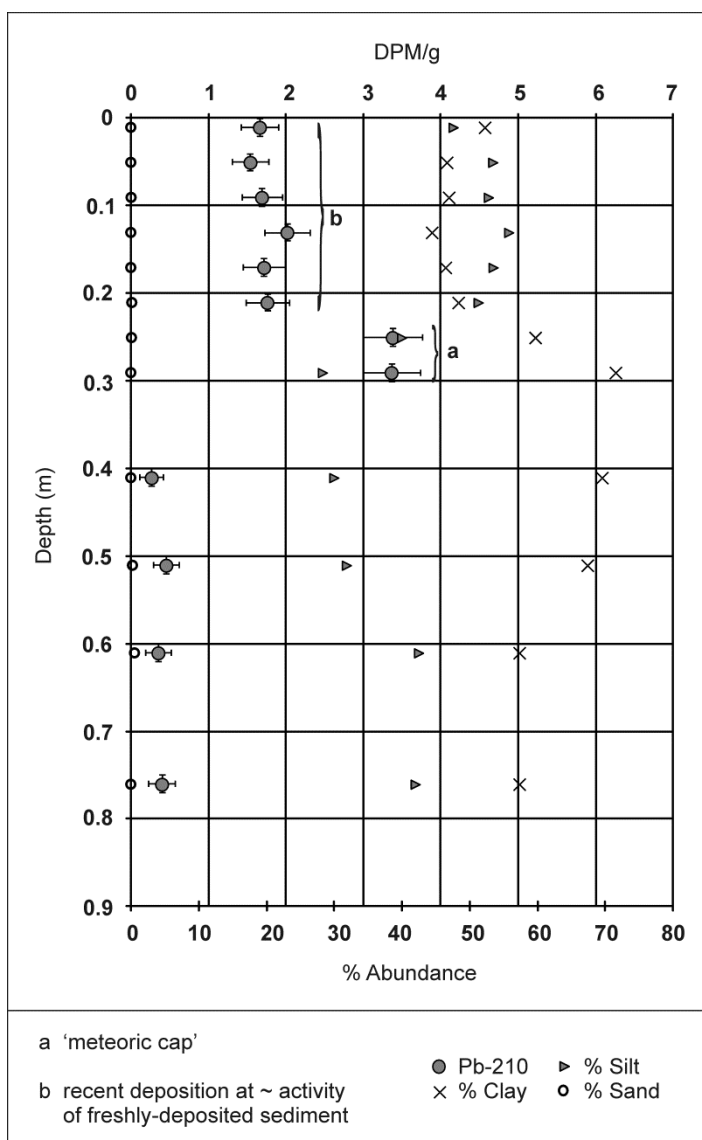
Figure 4.4: Floodplain core located ~ 50 m from the active channel on Transect 14. A recent deposit of silty-clay 0.21-0.25 m thick overlies a predominantly clay fining-upward sequence with a meteoric cap excess activity of ~ 17 DPM cm^{-2} (equivalent to the cap activity of terrace cores, i.e. old sediment).

The excess activity of fresh river sediment recently transported onto the floodplain provided an initial Pb-210 concentration. Dating by radionuclide decay then took either of two forms: i) where a buried 'meteoric cap' was evident in core profile data (*a* in Figure 4.4), dating was based on the difference between buried cap excess activity and the excess activity of the fully-developed meteoric cap of terrace cores, and ii) where a zone of uniform excess activity was evident (e.g. indicating a deposition event such as *b* in Figure 4.4), dating was based on the difference between a documented initial Pb-210

concentration (the activity of freshly-deposited sediment for that part of the floodplain) and the mean activity of the zone of deposition. This dating approach has been tailored to large river floodplains characterised by an event-based sedimentation record, and is described in greater detail by Aalto and Nittrouer (2012).

Subsamples from the upper ~ 0.3 m of three terrace cores processed at Exeter were additionally counted in Ortec gamma-spectrometers to detect Cs-137 fallout. Since no Cs-137 was detected (e.g. Figure 4.3), no floodplain cores were subjected to gamma spectrometry, but sedimentation rates derived by Pb-210 alpha-geochronology were found to be in good agreement with rates derived from a mine-tracer study undertaken using a duplicate core set (Swanson *et al.*, 2008).

4.4. Results

Synthesis of Overbank Sedimentation Rates

Focusing initially on cores located within 100 m of the active channel, floodplains of straight reaches and bifurcate bends show similar sedimentation rates overall, while those of single-thread bends show substantially higher rates (Table 4.1). Differences are more pronounced when only recent sedimentation rates are considered. Recent rates are derived by the thickness of freshly-deposited sediment at each site (constrained by dating resolution to encompass sediment deposited within a 5 year period prior to 2003, see Aalto *et al.* 2008). For multi-decadal rates (determined by averaging all individual event rates within a core), sedimentation on floodplains of single-thread bends is about double that on floodplains of bifurcate bends, while recent rates are higher by a factor of 3. However, variability in sedimentation rates is high (Table 4.1, σ-values), given that sedimentation rates decline rapidly with distance from the active channel (Aalto *et al.* 2008), and cores used to determine average rates in Table 4.1 cover a 100 m swath of channel-proximal floodplain. It is therefore

necessary to scrutinise sedimentation rates in relation to local floodplain topography and bend development history.

Table 4.1: Summary of sedimentation rates for cores located within 100 m of the active Strickland River channel.

Channel Planform	Sedimentation Rates (mm a^{-1})				
	n (cores)	Mean	σ	Mean (recent)	σ (recent)
Straight reaches	11	38.3	42.3	39.4	46.5
Single-thread bends	7	58.7	60.9	68.7	59.4
Bifurcate bends	5	34.3	36.7	20.0	36.4
Note: 'recent' indicates rate for freshly-deposited sediment					

Local Floodplain Sedimentation, Topography, and Channel Planform Dynamics

Figures 4.5 – 4.7 show surveyed floodplain surface profiles for transects illustrated in Figure 4.2, as well as core locations and sedimentation rates. Profiles are grouped in these figures such that transects from a straight reach, a single-thread bend and a bifurcate bend located in similar parts of the floodplain may be compared (10UL and 10DL are the exception, having no accompanying straight reach in close proximity). Floodplains of single-thread bends consistently show higher sedimentation rates than those of nearby straight reaches and bifurcate bends (Figures 4.5 – 4.7). The analysis will now focus separately on each profile group.

Starting upstream, Figure 4.5 shows high sedimentation rates on Transect 13L (single-thread), even at locations >100 m from the active channel. In contrast, sedimentation rates on Transect 11R (bifurcate) are low, and decline to zero >200 m from the active channel. Topographic variation of the single-thread and bifurcate bend profiles is qualitatively similar, each profile comprising a gently-undulating surface sloping gradually away from the channel. However, comparison of channel-proximal cores, where the effect of topographic

variation is limited, shows higher multi-decadal and recent floodplain sedimentation rates for the single-thread bend. The floodplain of the bifurcate bend is ~1 m higher than that of the single-thread bend, which may affect inundation frequency of small floods. Unfortunately, flow data for this set of profiles are not available to correct for variation in stage. Otherwise, local channel curvature (R:w) and bend migration rate (m a^{-1}) prior to the survey period are similar at both profile locations (Figure 4.2, Table 4.2). The bend of 11R has been partitioned by a prominent chute channel since at least 1972, while the bend of 13L has remained single-thread throughout the same period (Figure 4.2).
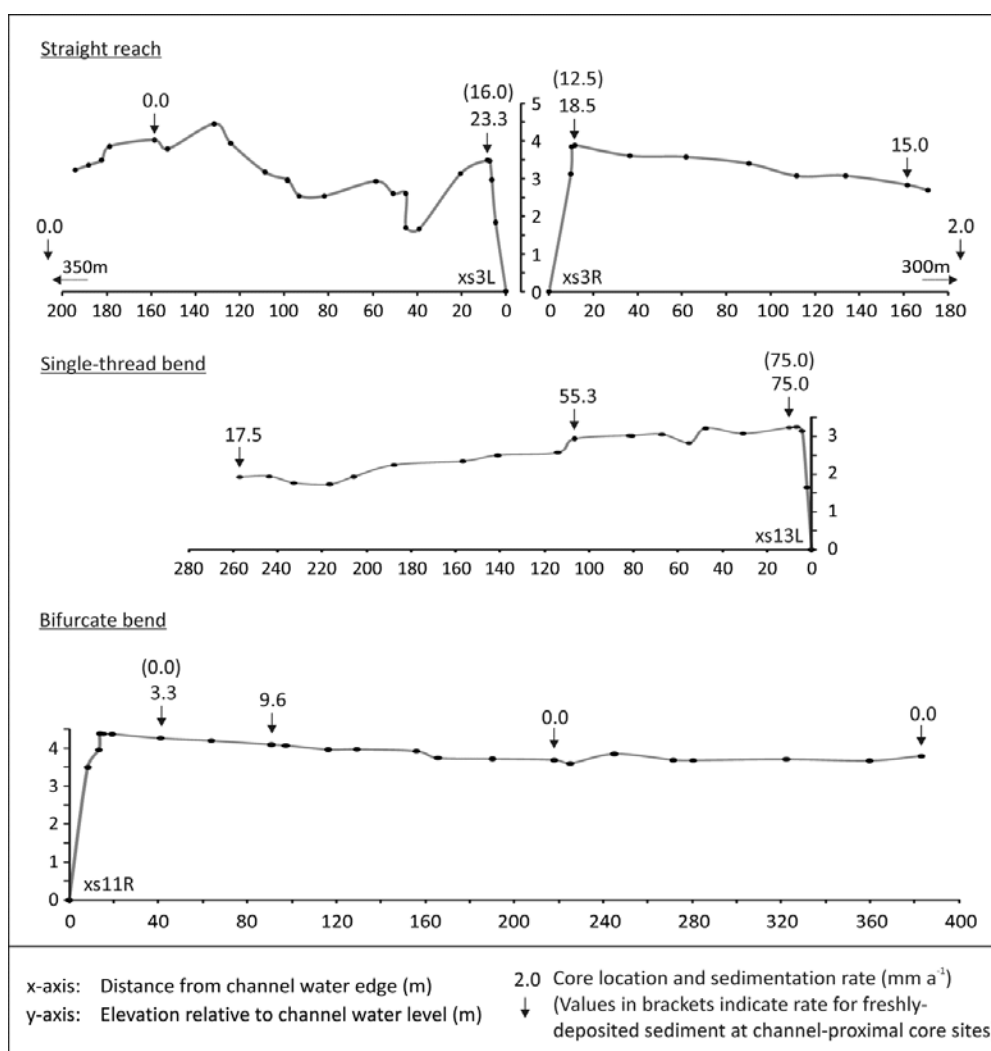
Figure 4.5: Surveyed floodplain surface profiles for transects 3 (straight reach), 13L (single-thread bend) and 11R (bifurcate bend). Profiles are presented at the same vertical and horizontal scale.

Table 4.2: Local curvature at transect locations, and bend average migration rates prior to the survey. The first migration rate given is an average of the migration rate between 1972 and 1990/93, and that between 1990/93 and 2002, the second represents the migration rate between 1990/93 and 2002, roughly corresponding with the period of recent deposition.

Bend	Curvature (local R:w ratio)	Bend Migration Rate 1972-2002 (m a^{-1})	Bend Migration Rate 1990/93-2002 (m a^{-1})
11R	4.2	7.0	10.1
13L	3.7	6.3	9.8
10UL	3.1	12.8	17.0
10DL	3.5	21.9	17.0
14L	3.4	14.0	15.8
15R	2.0	9.3	11.2

Figure 4.6 shows high sedimentation rates on Transect 10UL (single-thread), even at locations >200 m from the active channel. In contrast, sedimentation rates on Transect 10DL (bifurcate) are low. Again, topographic variation of the single-thread and bifurcate bend profiles is qualitatively similar, and comparison of equivalent channel-proximal cores shows higher multi-decadal and substantially-higher recent floodplain sedimentation rates for the single-thread bend. In this case, the floodplain of the single-thread bend is ~0.5 m higher than that of the bifurcate bend, and these profiles were surveyed on the same day at the same flow stage. Local channel curvature and recent migration rates are similar at both profile locations (Figure 4.2, Table 4.2). The bend of 10DL has been partitioned by a prominent chute channel since at least 1972, while the bend of 10UL has remained single-thread throughout the same period (Figure 4.2).
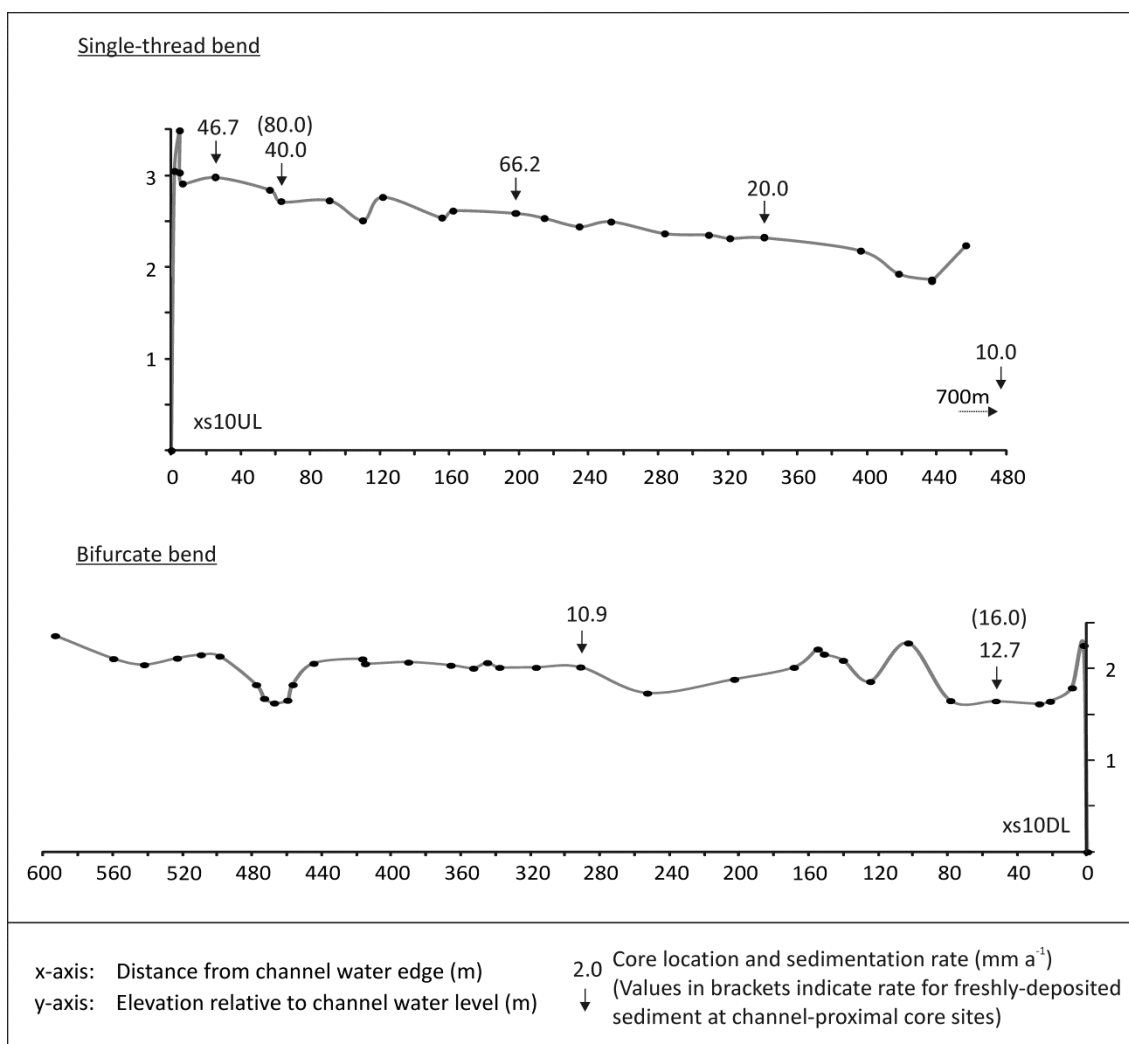
Figure 4.6: Surveyed floodplain surface profiles for transects 10UL (single-thread bend) and 10DL (bifurcate bend). Profiles are presented at the same vertical and horizontal scale.

Figure 4.7 shows very high sedimentation rates within 100 m of the active channel on Transect 14L (single-thread). Channel-proximal sedimentation rates on Transect 15R are lower than those of Transect 14L, but still relatively high in comparison with other bifurcate bends. The bifurcate bend has a lower curvature in the vicinity of the transect, and a slightly lower migration rate prior to the survey period (Figure 4.2, Table 4.2). In addition, Transect 15R is located in close proximity to a tie-channel (channel connecting mainstem and off-river water bodies; Rowland *et al*. (2005), Figure 4.8), which should improve sediment conveyance to the distal floodplain (see Day *et al*., 2008; 'dispersal web' sedimentation). Another key feature of Transect 15R is that the chute channel at this bend formed shortly before the survey (Figure 4.2, Figure 4.7).

Topographic variation and overall floodplain elevation of the single-thread and bifurcate bend profiles are qualitatively similar, and available flow data suggest that discharge varied by ~ 250 m³ s⁻¹ between surveys. For a channel with an average width of 300 m, an average depth of 8 m, and an average flow velocity of 1 to 2 m s⁻¹ (Chapter 3), this change in discharge would amount to a change in stage of < 1 m. The bend of 14L has remained single-thread throughout the period 1972-2002 (Figure 4.2).
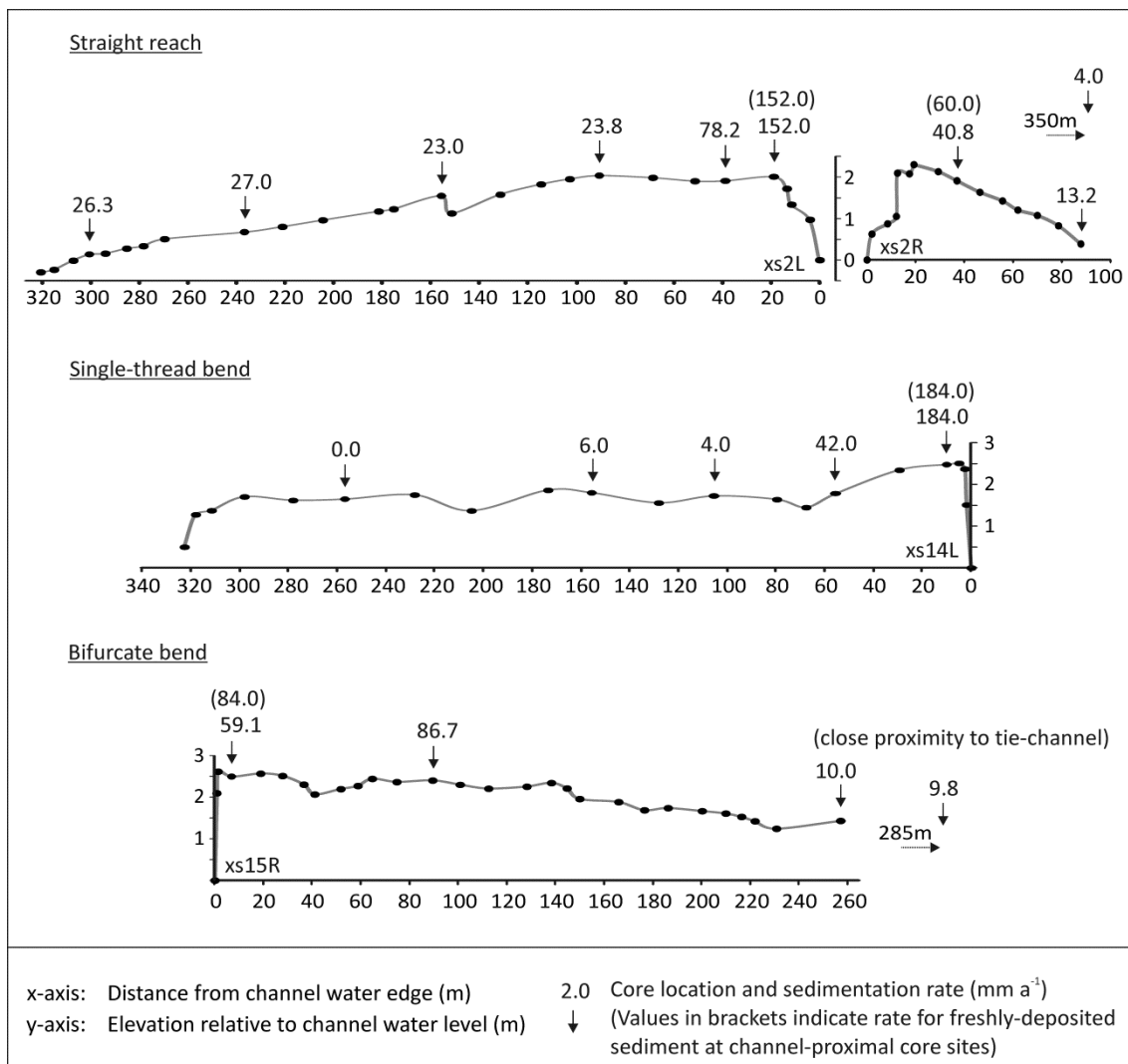
Figure 4.7: Surveyed floodplain surface profiles for transects 2 (straight reach), 14L (single-thread bend) and 15R (bifurcate bend). Profiles are presented at the same vertical and horizontal scale.
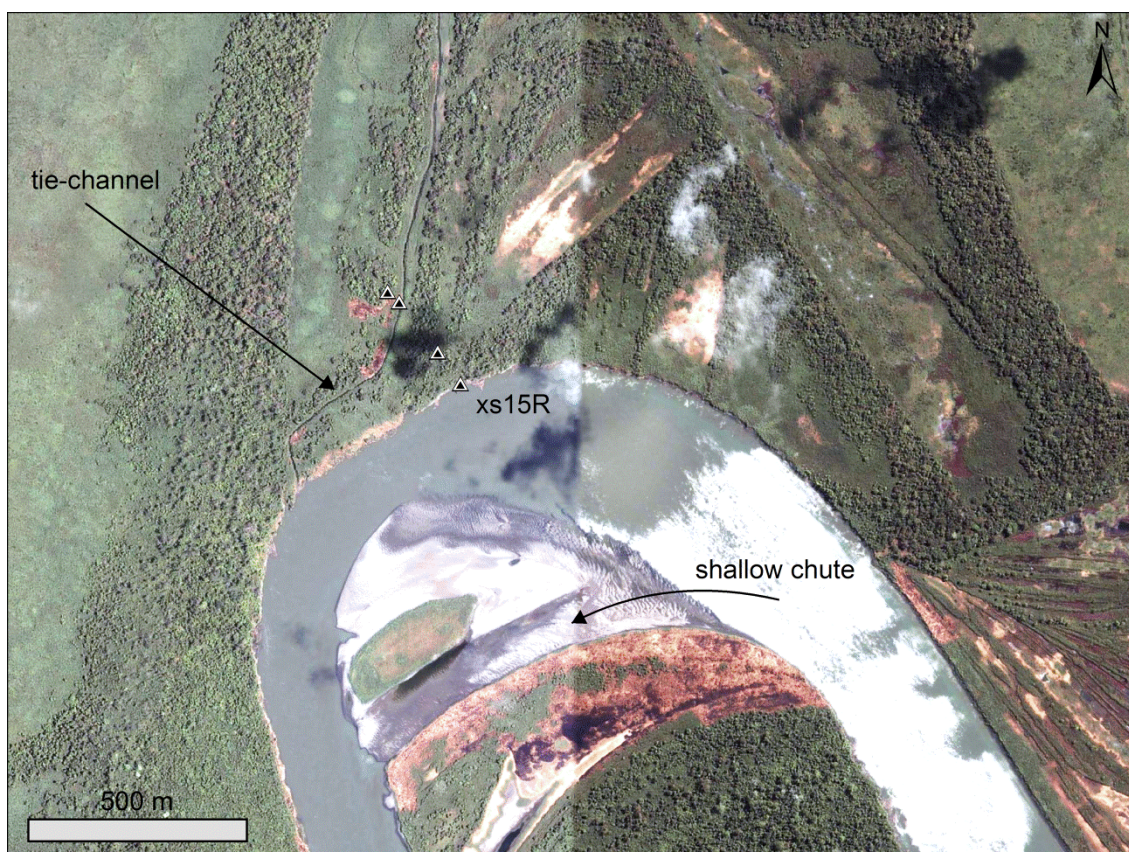
Figure 4.8: Zoom view of the bend at Transect 15R, showing the close proximity of cores to an infilled oxbow lake tie-channel. Combined field and GIS observations (see Chapter 2) suggest that the chute channel pictured would have initiated within 5 years of the image date (20 September 2002): The island separating chute and mainstem channels is only sparsely vegetated by robust grasses (most likely *Phragmites karka*), an early stage in vegetation succession typically followed by the establishment of trees within 5 years. Image source: GeoEye, available through Google Earth Pro.

4.5. Discussion

Topographic variation of the single-thread and bifurcate bend profiles is qualitatively similar in all profile groups, and comparison of proximal (levee) core sites, where topographic variation is limited, highlights differences in sedimentation rates between single-thread and bifurcate bends. In the case of the most-upstream profile group (13L, 11R), it might be argued that the relatively higher floodplain of the bifurcate bend (11R) has contributed to the lower sedimentation rate observed there. However, examination of the Strickland River discharge record indicates that the most significant floods,

defined by magnitude and rate of rise in stage, occurred in 1994, 1998, 1999, 2002 and 2003 (4 of which fall in the 'recent' deposition window, Aalto *et al.*, 2008). However, the variation in floodplain elevation observed in the profiles is unlikely to have been a limiting factor in floodplain inundation and sedimentation, considering the recent flood and sedimentation records, but there is uncertainty in estimates of stage variation during the survey that is difficult to quantify (in some cases due to a lack of data).

In the case of the most-downstream profile group, it might be considered surprising that proximal sedimentation rates at the bifurcate bend (15R) are lower than those of the single-thread bend (14L), given the presence of a tie-channel, the lower curvature of the bifurcate bend, and the greater migration rate of the single-thread bend. Hudson and Heitmuller (2003) found a negative correlation for bend curvature and levee width, and explained this in terms of the effect of curvature on superelevation of the water surface at the cutbank (and concomitant efficiency of local overbank flow and sediment conveyance). In addition, slower migration preceding core sampling would effectively increase the time period for which a proximal core has been located in close proximity to the channel (Hudson and Heitmuller, 2003), and it might therefore be expected that the slower migrating bifurcate bend would have higher proximal sedimentation rates than the single-thread bend, but this is not the case. This aside, given the difference in migration rates presented in Table 4.2 (about 5 m a^{-1}), the proximal cores of Transects 14L and 15R illustrated in Figure 4.6 would only have been separated by about 25 m (relative to their respective local cutbank) 5 years prior to core sampling (within the 'recent' deposition window).

The strength of this core-based analysis of sedimentation rates may be questioned on the grounds that it is difficult to determine the extent to which single core locations and linear (1D) transects are representative of sedimentation patterns over a wider floodplain area. In isolation, the data presented suggest that the difference in sedimentation rates between bifurcate

and single-thread bends is largely a consequence of bifurcation: differences are most pronounced where chute channels are most prominent and have coexisted with the mainstem for several decades (Figures 4.2, 4.5 – 4.7). The interpretation offered here is that chute channels offer a low-roughness diversion from the mainstem, across the neck of a bend, and divert sufficient flow (and suspended load) to substantially reduce sedimentation rates on the floodplain of the mainstem cutbank. The results certainly motivate further study, perhaps in the form of a two dimensional flood modelling exercise, to determine whether the effect of bifurcation is significant beyond the uncertainties associated with variation in stage and floodplain topography.

Bathymetric survey data for four Strickland River bifurcate meander bends (see Chapter 3) suggest that the average cross-sectional area of the Strickland mainstem in single-thread reaches upstream and downstream of bifurcate meander bends is 1.3 to 2 times smaller than the collective average cross-sectional area of chute and mainstem channels in bifurcate bends. This increase in channel capacity through bifurcate bends may be sufficient to reduce flooding, and thus reduce sedimentation rates on the mainstem bifurcate cutbank floodplain. A further effect worth investigating using modelling would be the effect of bifurcation on flow structures at bifurcate bends, as this can effect sediment concentrations in the mainstem bifurcate, and thus reduce suspended sediment supply to the mainstem bifurcate cutbank floodplain.

4.6 Further Implications

Field survey of large river floodplains, especially those located in remote regions such as Bolivia or Papua New Guinea, is fraught with logistical challenges. Due to the vast area of ground to be covered, it is necessary to stratify sampling effort such that the array of hydrogeomorphic environments present is relatively equally represented in subsequent analyses. Results of the present study suggest that floodplain dispersal patterns are likely to vary with channel pattern, and future coring campaigns aimed at quantifying floodplain

sedimentation rates for large meandering rivers should strive to cover a variety of straight reaches, single-thread bends and bifurcate bends to account for the expected variation. Similarly, field studies investigating impacts of sediment-associated contaminant dispersal on floodplain biota should be cautious of extrapolating and generalising results from small areas of large floodplains.

More broadly, the results raise questions about patterns and processes of sediment dispersal and sequestration in multiple-thread rivers. It is known that avulsion can both liberate and sequester large volumes of sediment in anabranching channel networks (e.g. Jerolmack and Paola, 2007), and links between avulsion frequency and aggradation rate are well-documented (e.g. Törnqvist and Bridge, 2002; Jerolmack and Mohrig, 2007). Further coupled field/geochronology studies quantifying both channel and floodplain-surface sediment exchange fluxes are needed in large, multiple-thread channel systems, to complement the work that has been undertaken in large meandering river floodplains. These studies should be complemented by modelling, to account for uncertainty in core-based estimates of sedimentation rates.

There has been considerable recent interest in the interplay between geomorphological aspects of floodplain development, and floodplain vegetation dynamics (e.g. Perucca *et al.*, 2007; Tal and Paola, 2007; 2010; Crosato and Saleh, 2011). Changes in the floodplain dispersal path due to point bar dynamics and bifurcation may affect floodplain ecology (plant species assemblages, disturbance regimes etc.; Perucca *et al.*, 2006; Camporeale and Ridolfi, 2010), and may have played a significant role in the coupled evolution of fluvial style and floodplain floristic diversity (Gibling and Davies, 2012). Point bars are key features of transitions in fluvial style, as they are in essence transitional sedimentary features; they initiate as channel-margin deposits, and are successively incorporated into the floodplain as the channel migrates, and they become capped by overbank sediment, and vegetated. Indeed, it is the presence and topographic complexity of point bars that distinguishes 'laterally immobile channels with no bars', 'meandering channels with scrolls', and

'moderately braided and meandering channels with scrolls and chutes' (Kleinhans and van den Berg, 2011). Understanding linkages between channel pattern and floodplain sediment dispersal may provide a fundamental template for research at the interface of floodplain geomorphology and ecology.

CHAPTER 5

Mediative Adjustment of River Dynamics:
Interplay between Sediment Supply, Channel Migration, and
Chute Formation in Large, Sand-Bed Meandering Rivers

5.1. Introduction

Process Sedimentology in Large River Systems

Large rivers are associated with fluxes of water, sediment and solutes of an order that is significant to global biogeochemical cycles (Sinha and Friend, 2007; Aufdenkamp *et al.*, 2011). These rivers flow great distances from their source areas to intra-continental or oceanic sinks, in the process linking a vast mosaic of physiographic settings (Gupta, 2002; 2007). One of the key challenges for large rivers research is to understand the nature of these physiographic links; the manner in which signals of spatial and temporal physiographic variation are transmitted through large rivers, and in particular, whether signals are amplified or damped during transmission (e.g. Gupta, 2002; Blum, 2007; Guyot and Walling, 2009). To fully understand river sensitivity to climate or other environmental change, or the effects of such change on river behaviour, it is necessary to be able to distinguish between processes of self-adjustment (Nanson and Huang, 2008), and responses to external forcing, or at least to understand how autogenic adjustments interact to mediate, moderate or amplify the effects of external forcing.

From the sedimentologist's perspective, such understanding is crucial in deciphering the response of sedimentary sinks to source perturbations driven by environmental change, tectonics, or drainage rearrangement. This is a complex, and perhaps impossible task, because the fluvial response to external forcing is typically non-linear and discontinuous even if the forcing itself is

applied in a continuous manner (Singh *et al.*, 2009; Jerolmack and Paola, 2010). Indeed, it has been argued that processes of sediment transport in fluvial systems tend to disrupt signals of environmental change, as process-form feedbacks mediate the distribution of energy, and cloud interpretations of the sedimentary response (Jerolmack and Paola, 2010). This chapter illustrates how channel pattern dynamics can play a similar role in mediating fluvial energy distributions and process sedimentology in large, sand-bed meandering river floodplains.

Where the course of a large river is not set by structural lineations, or confined within an incised rock-walled valley, channel-floodplain sediment exchanges may play a significant intermediary role in source-to-sink sediment transfer (Guyot, 1993; Walling *et al.*, 1996; Gomez *et al.*, 1999; Aalto *et al.*, 2002; 2008). Channel planform change (e.g. transitions from meandering to braiding) in these environments is typically indecipherable from the floodplain sedimentary record, where analysis of morphostratigraphic units (e.g. bar platform, chute channel, ridge, or remnant floodplain) provides more reliable insight into mechanisms of floodplain development (Brierley, 1989; 1991; Brierley and Hickin, 1991). Even if planform transitions were decipherable in floodplain sedimentary archives, rates of lateral channel migration in some settings are such that a full floodplain width may be reworked in one or two millennia (Mertes *et al.*, 1996; Aalto *et al.*, 2008), offering relatively short-term insight into the nature of past change.

The work presented herein is motivated by a broader interest in understanding how changes in water or sediment supply may influence patterning processes (Kleinhans 2010; Kleinhans and van den Berg, 2011), and fluxes of sediment-associated contaminants and biogeochemically-reactive elements (Aalto *et al.*, 2008; Swanson *et al.*, 2008), as these interactions of process, pattern, and flux are fundamental to ecosystem integrity and ecosystem service provision in fluvial systems (MEA, 2005; Brierley, 2008). Process sedimentologists have a lot to offer this field of enquiry (see, for example, Lewin and Brewer, 2001; 2003).

Planform Dynamics of Meandering Rivers

Meandering rivers are characterised by an interplay between processes that operate to increase channel length (the development and elongation of meander bends), and processes of bend cutoff (Stølum, 1996; Camporeale *et al.*, 2005; 2008; Constantine and Dunne, 2008; Frascati and Lanzoni, 2009). Most studies of long-term meandering dynamics have considered only the role of neck cutoff, which is to: i) reduce planform geometrical complexity driven by fluid dynamic processes; and ii) generate an intermittent noise that may influence the spatiotemporal dynamics of long river reaches (Camporeale *et al.*, 2008; Frascati and Lanzoni, 2009). A consequence of (i) is that meandering river sinuosity tends to stabilise within relatively narrow limits of an average value reflecting the nature of interplay between reach elongation and bend cutoff (Stølum, 1996; Camporeale *et al.*, 2005; Constantine and Dunne 2008). The role of chute initiation and chute cutoff in meandering dynamics is less clear (see Hooke, 2007). Chute cutoff is considered to limit channel sinuosity (Howard, 1996), but since chute cutoff less efficiently reduces channel length than neck cutoff, rivers dominated by chute cutoff must be subject to a high cutoff rate for the average value of sinuosity to be maintained (Constantine and Dunne, 2008).

Common to many analyses of the role of bend cutoff in meandering rivers is the use of sinuosity as a single metric describing the dynamical state of the system. Sinuosity is certainly a useful metric, as it relates directly to channel slope and stream power. However, the focus on sinuosity is severely restrictive in that it ignores other mechanisms by which energy may be mediated in alluvial channel environments, such as bar formation and dissection (Huang and Nanson, 2007; Phillips, 2010), or changes in channel width (Harmar and Clifford, 2006). Coupled with neglect of the process of chute cutoff (except in the case of Constantine and Dunne, 2008), a focus on sinuosity essentially restricts the relevance of these analyses to a single class of planform pattern (this is acknowledged by Stølum, 1998); low energy meandering rivers that migrate slowly and are dominated by neck cutoff (see Kleinhans and van den Berg, 2011).

Many rivers display a planform pattern that is transitional between single-thread meandering and braided, driven primarily by chute channel dynamics (Ferguson, 1987; Kleinhans and van den Berg, 2011; Chapter 2; Figure 5.1). Such transitional rivers are the focus of this chapter. The chapter revisits and extends an analysis of chute initiation and stability in large, sand-bed meandering rivers (Chapter 2), to consider controls and morphodynamic implications of chute channel dynamics in terms of river energy transfer, and mass-energy interactions (Nanson and Huang, 2008; Phillips, 2010; Jerolmack and Paola, 2010). The analysis is used to provide a theoretical context for an assessment of the planform response of the lower Ok Tedi River in Papua New Guinea to direct addition of mine tailings.

Figure 5.1: A sand-bed reach of the Strickland River in Papua New Guinea. Rapid bend extension here leads to wide scroll-slough spacing and associated initiation of chute channels, resulting in a planform dynamic and pattern that is transitional between single-thread meandering and braided (see Chapter 2).

5.2. Chute Channel Dynamics and Channel Planform Transitions

Spatial Statistical Analysis of Chute Channel Dynamics

Using automated and reproducible ArcInfo GIS applications, planform attributes were quantified for 213 meander bends on sand-bed reaches of three large meandering rivers; the Strickland in Papua New Guinea, the lower

Paraguay on the Paraguay/Argentina border, and the Beni in Bolivia (Chapter 2). The history of chute initiation and infilling was tracked at each bend over a ~40 year image record, and binary logistic regression analysis was used to determine whether chute channel initiation was statistically more probable at bends with particular planform characteristics (e.g. curvature or sinuosity) or dynamics (e.g. rate of migration in the direction of the valley axis trend, defined as translation, versus rate of migration perpendicular to the valley axis trend, defined as extension, Figure 5.2). The only statistically significant predictor of chute initiation at a bend was the average rate of bend extension, accounting for 30-60 % of the variation in the data for each river ($p < .01$). An increase in the rate of bend extension significantly increased the probability of chute initiation at a bend.
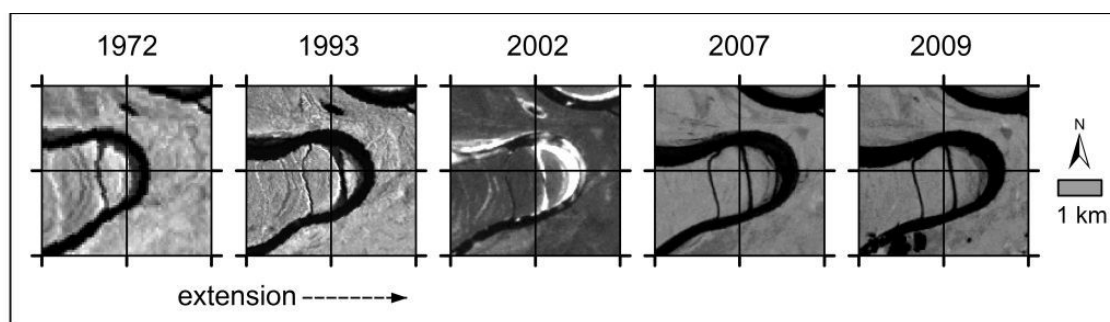
Figure 5.2: Meander bend migration by extension, with associated chute initiation; an example from the Strickland River, Papua New Guinea.

Chapter 2 considered several reasons why the rate of bend extension was important to chute initiation. First, rapid extension is associated with bend apex widening, where cutbank erosion outpaces point bar deposition (Brice, 1975). This leads to wide scroll bar spacing (Hickin and Nanson, 1975), and alignment of intervening sloughs that favours flow across a developing point bar. Second, the formation of prominent sloughs breaks the continuity of vegetation encroachment on point bars, which easily keeps pace with and even promotes point bar deposition where migration is slow. In addition, the island that forms between chute and mainstem bifurcates is rapidly colonised and stabilised by robust grasses (e.g. *Phragmites karka* in Papua New Guinea), and this focuses

scour in the adjacent chute. Third, through ongoing extension following chute formation, the chute adopts an axial location within the bend (mid-bend, cf. Lewis and Lewin, 1983) such that the alignment of upstream flow favours the mainstem bifurcate. In addition, ongoing extension increases the chute-mainstem bifurcation angle and chute gradient advantage, such that chutes at extending bends are kept open through 'quasi-balance' by factors that interact to limit bedload influx and increase chute competence (Kleinhans *et al.*, 2008; Chapter 3).

Spatial Variation in Chute Initiation

The analysis presented in Chapter 2 is advanced here by considering inter-reach and sub-reach scale variation in chute channel initiation in greater detail. The binary logistic regression analysis revealed that the probability of chute initiation increases as the bend extension rate increases. In plots of bend extension rate with down-channel distance (Figure 5.3), it is evident that chute initiation becomes increasingly probable as the extension rate exceeds the reach or sub-reach scale mean (this is discussed further with reference to Figure 5.6). Average migration rates vary with specific stream power, which is greatest within the Beni foredeep sub-reach, and lowest in the Paraguay sub-reach located upstream of the Bermejo confluence (Chapter 2; Figure 5.3). There is an increase in bend extension rates and chute initiation downstream of the Bermejo confluence, where discharge and slope increase slightly, leading to an increase in stream power (also see Brewer and Lewin, 1998, for an example of how increased discharge can drive a transition from meandering to braiding).
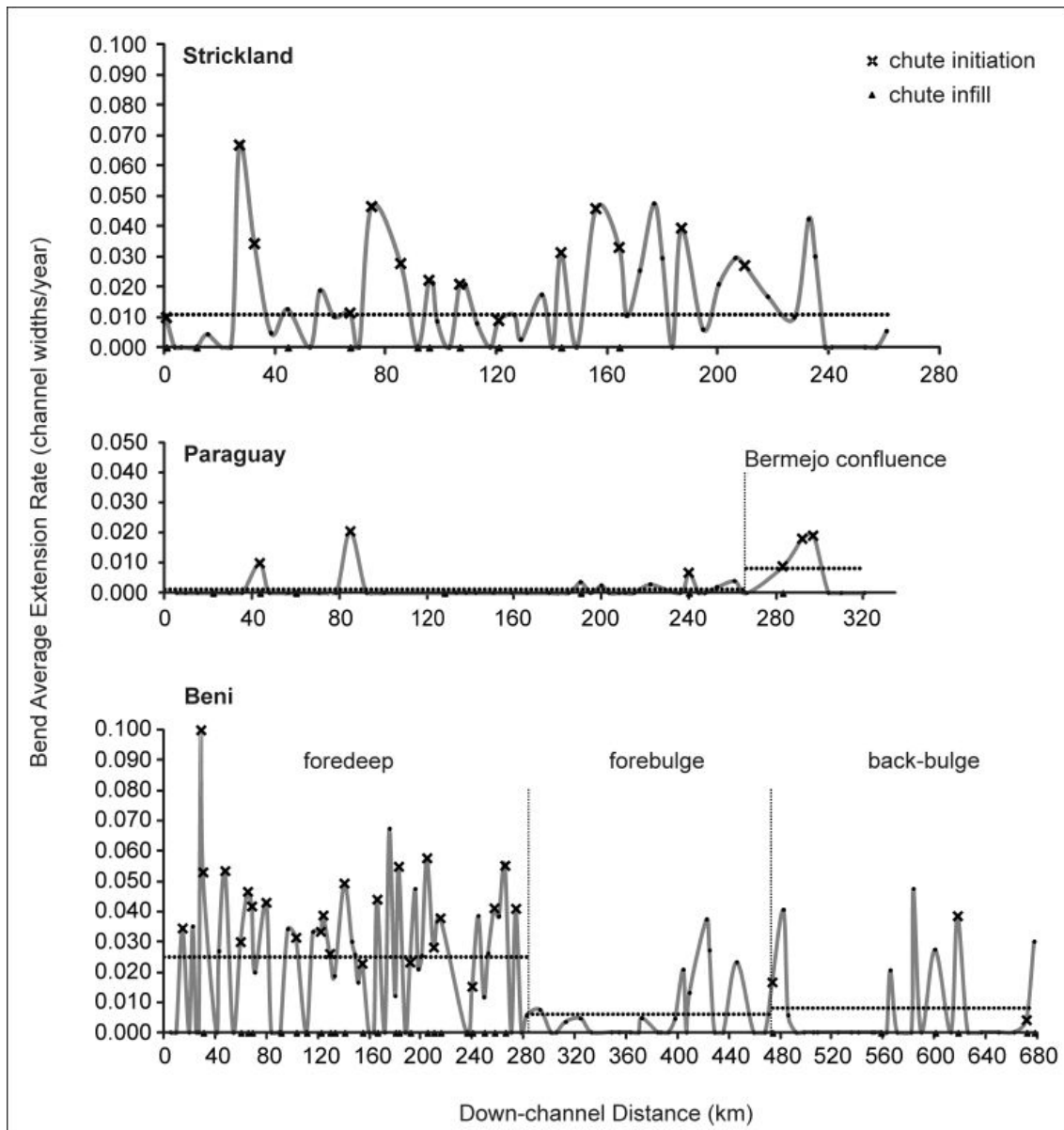
Figure 5.3: Spatial variation in chute initiation as a function of bend average extension rates in the Strickland, Paraguay and Beni Rivers. Dashed lines indicate mean sub-reach spatial extension rates.

Temporal Variation in Chute Initiation: Insights from the Ok Tedi, Papua New Guinea

Open-cast copper and gold mining at Mount Fubilan in the headwaters of the Ok Tedi has embroiled scholars of environmental justice (e.g. Low and Gleeson, 1998), engineering geology (e.g. Griffiths *et al.*, 2004), ecology (e.g. Storey *et al.*, 2009), and geomorphology (e.g. Pickup and Marshall, 2009) in engaging debate that might easily be mistaken for the script of the film *Avatar*! The mine is located at ~1500 m elevation in an area of weak and highly deformed lithology

(see Davies, 2009 for a full account of the geology of Papua New Guinea). The surrounding terrain is steep and highly dissected, and an annual total rainfall of over 10 m is regularly recorded at the mine site (Pickup and Marshall, 2009). This physiographic setting combined with tectonic instability results in frequent debris flows and landslides despite a dense cover of rain forest (Pickup and Marshall, 2009), and the overall environment poses a significant challenge to the establishment and operation of an open-cast mine.

Griffiths *et al*. (2004) provide a detailed account of the history of mine development and tailings disposal: production was due to commence by mid 1984, and mine tailings were to be stored in a dam on the Ok Ma, a tributary of the Ok Tedi. The tailings dam was destroyed by landslides in late 1983/early 1984, but mining was allowed to commence as scheduled with an interim coarse tailings storage dam at the mine site. Mill tailings were discharged directly into the Ok Tedi headwaters from the outset of mining, with coarse tailings added from 1989, when the interim coarse tailings storage dam had filled. As a result, the Ok Tedi sediment load increased from 3-5 Mt a^{-1} to 35-45 Mt a^{-1} (Pickup and Marshall, 2009). Extensive alluvial fans developed in the immediate vicinity of the mine, and prominent braid plains developed over long reaches of the upper Ok Tedi close to the mine site (near the town of Tabubil, Pickup and Marshall, 2009).

For comparison with the sand-bed reaches of the Strickland, Paraguay and Beni Rivers studied previously, planform changes of the sand-bed lower Ok Tedi were studied in detail in the present work (Figure 5.4). Reach-average as well as individual bend average migration rates were calculated using the channel centreline overlay methods described in Chapter 2 (and associated georeferencing and error checking methods), and chute initiation at each meander bend was tracked over an image record spanning ~50 years. Royal Australian Survey Corps topographic maps provided a view of the channel in 1966 (compiled using aerial photography). Islands are mapped and described in map legends, indicating that some care was taken in delineating channel

pattern in this map series. Ok Tedi channel bank lines were digitised from these maps, and from Landsat false-colour composites for 1972, 1988, 2001, 2004, and 2010, and collapsed to channel centrelines using a generalisation utility in ArcInfo.
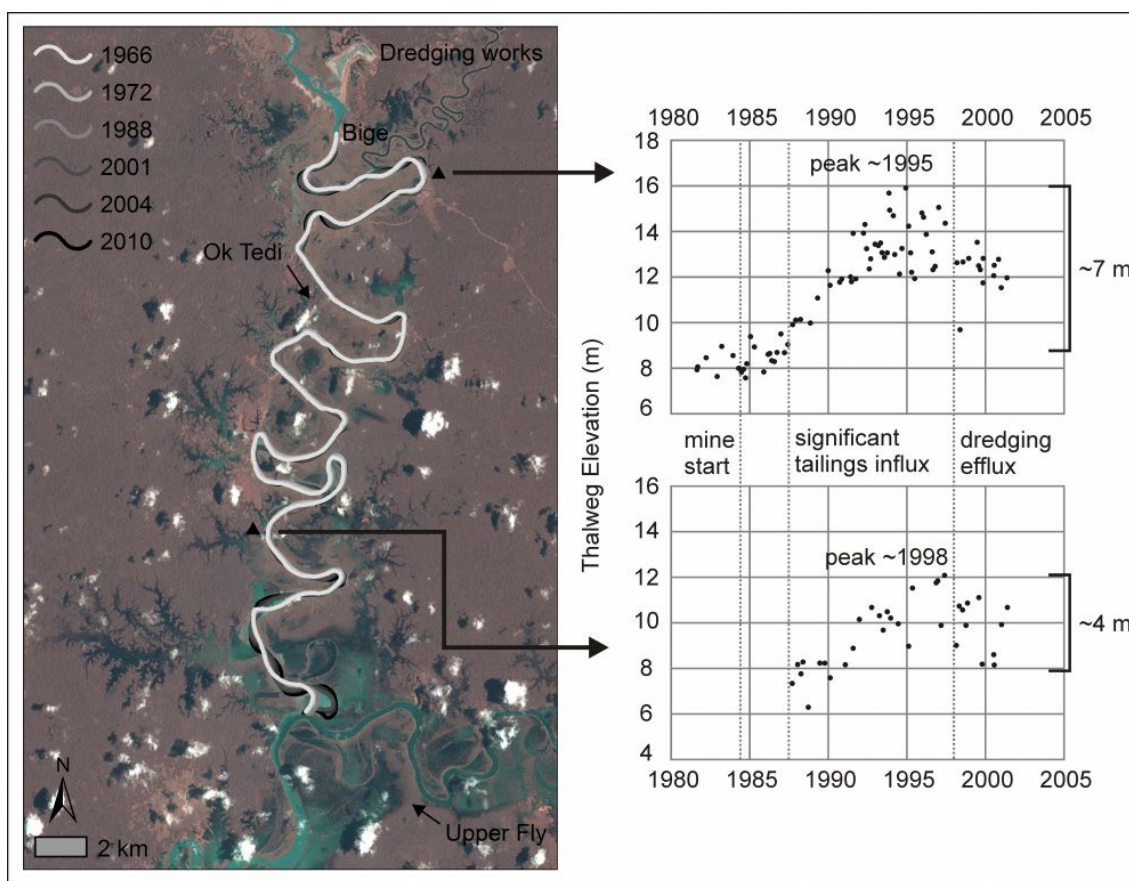
Figure 5.4: 2010 Landsat 5 TM false-colour composite of the lower Ok Tedi in Papua New Guinea, with overlain channel centrelines for the period 1966-2010 derived using ArcInfo GIS utilities described in Chapter 2. Bed level monitoring locations are displayed on the image, with accompanying bed level data shown in the adjacent graphs (bed level data are from Pickup and Marshall, 2009). The centreline overlay shows limited channel migration until the period between 1988 and 2001, during which tailings were discharged directly into the river, and bed aggradation was most rapid.

The lower Ok Tedi has been subject to substantial bed aggradation since the tailings influx (Pickup and Marshall, 2009; Figure 5.4). Much of the river is confined within pre-Holocene terrace material, but where the channel is free to migrate, a number of chute channels have initiated at rapidly extending bends

(Figures 5.5 and 5.6). Migration rates have increased over time in association with the passage of a sediment slug (cf. Nicholas *et al.*, 1995) – bed aggradation in the upper part of the reach peaked higher and earlier than aggradation in the lower part of the reach (Figure 5.4), creating a steepened front that has increased stream power (this steepened front is evident also in simulation studies of the tailings problem, e.g. Cui and Parker, 1999, and is a well-established consequence of the direct disposal of mining debris in rivers, e.g. Gilbert, 1917). The increase in slope and stream power is manifest in increasing bend extension rates and chute initiation over time (Figures 5.5 and 5.6). Thus, the sub-reach and inter-reach spatial sequence of chute initiation on the Strickland, Paraguay and Beni Rivers is mirrored in the temporal sequence of chute initiation on the Ok Tedi, where an increase in stream power is associated with increasing chute activity.
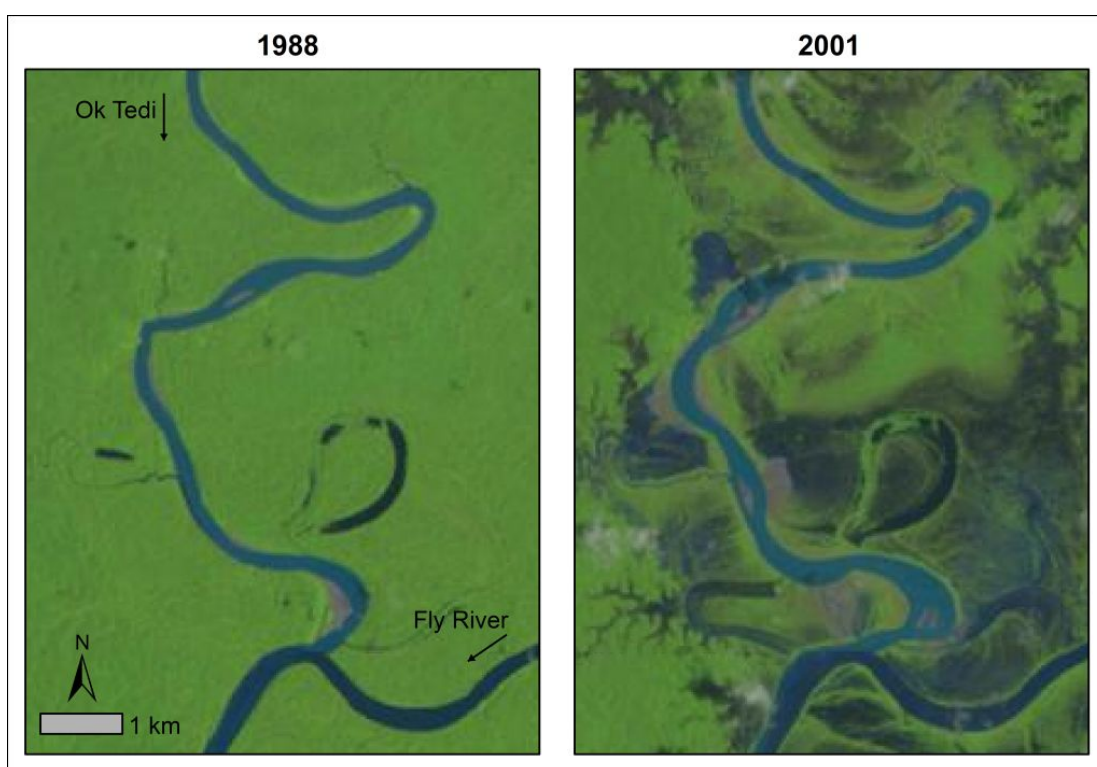
Figure 5.5: Meander bend development and bifurcation in a relatively unconfined reach of the lower Ok Tedi, immediately upstream of the confluence with the upper-middle Fly River, during the 1988-2001 period of dramatic tailings influx and channel change ('Lansatlook' false-colour composites; 1988 Landsat 5 TM, 2001 Landsat 7 ETM+, sourced through the USGS Global Visualisation Viewer).
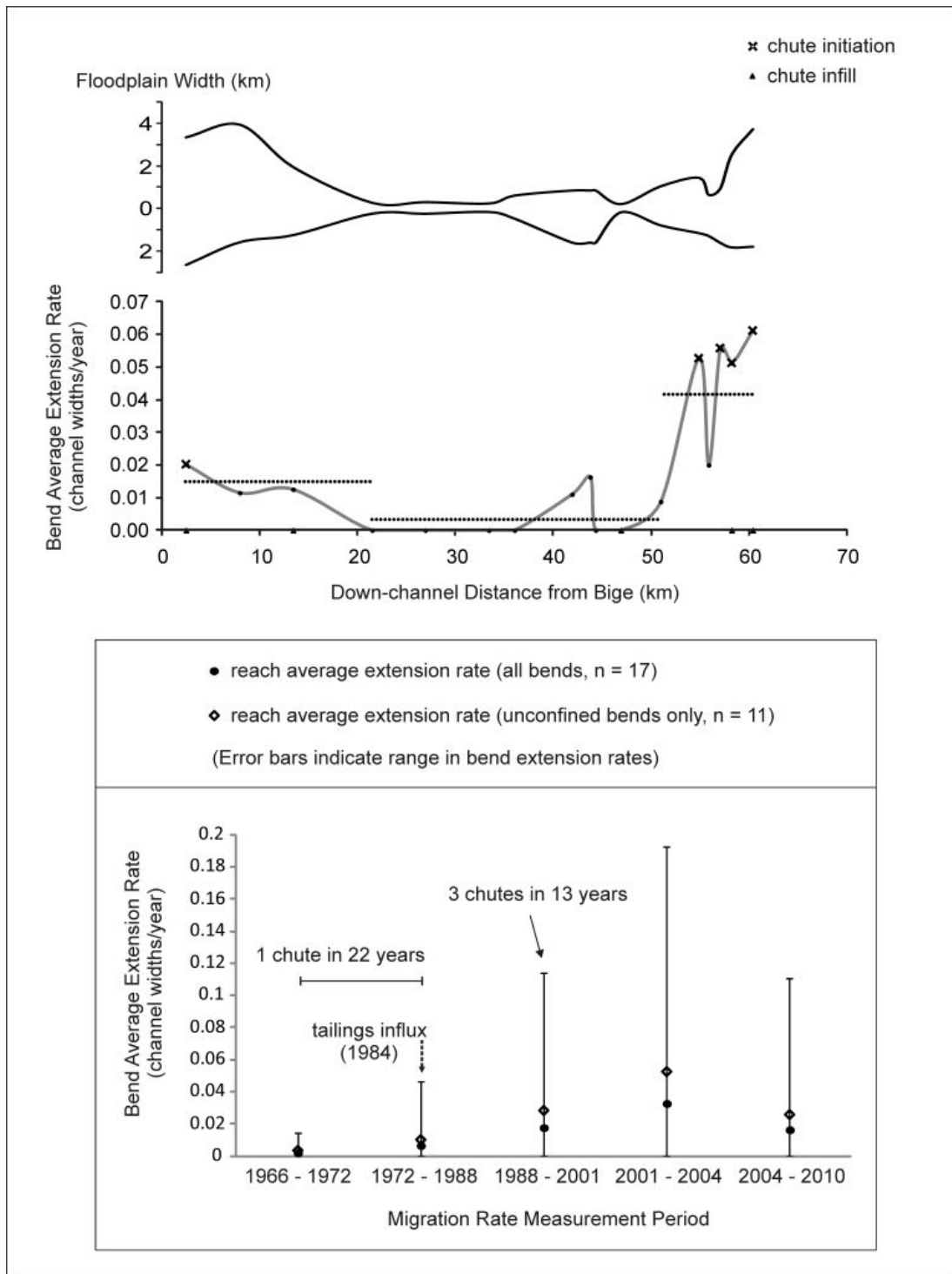
Figure 5.6: Spatial and temporal variation in chute initiation as a function of bend average extension rate on the lower Ok Tedi. Note the effect of valley confinement on spatial variation in extension rates and chute initiation, and the increase in extension rates and chute initiation following the tailings influx. Dashed lines indicate mean sub-reach spatial extension rates.

Rate-Frequency Distributions as a Function of River Energy

The reaches and sub-reaches of the Strickland, Paraguay and Beni Rivers studied in Chapter 2 plot in order of increasing chute activity on the empirical planform discriminant functions of Kleinhans and van den Berg (2011), and cover the full continuum of transitional planform patterns: i) the Paraguay upstream of the Bermejo confluence plots within the range of 'meandering channels with scrolls', ii) the Paraguay downstream of the Bermejo confluence plots at the transition from 'meandering channels with scrolls' to 'moderately braided and meandering channels with scrolls and chutes', iii) the Strickland and the full Beni reach plot at the transition from 'moderately braided and meandering channels with scrolls and chutes' to 'highly braided channels', and iv) the Beni foredeep plots within the range of highly braided channels, but braiding is suppressed by an extremely high suspended sediment load (Chapter 2).

In the case of the lower Ok Tedi, the increase in extension rates and chute activity over time where the river is not confined may be partly explained by the increase in slope associated with the tailings influx (Figure 5.4), which is estimated to be 15-25 % (based on Royal Australian Survey Corps topographic maps, compiled using aerial photography flown in 1966, and radar imagery flown in 1970, and the bed survey data from Pickup and Marshall, 2009; Figure 5.4; slope ~0.00085 m m^{-1} before the tailings influx, slope ~0.001 m m^{-1} after the tailings influx). This increase in slope (and corresponding increase in stream power) would be sufficient to shift the Ok Tedi higher up the energy continuum defined by Kleinhans and van den Berg (2011), and is manifest in an increase in transitional planform dynamics where the channel is not confined.

Bends at which chute channels initiate undergo more rapid extension on the Beni and Ok Tedi than on the Paraguay and Strickland ('chute-forming bends'; Figure 5.6, horizontal bars). The extension rate – chute initiation frequency plots for all rivers (Figure 5.7) show that chute initiation is rare at bends undergoing extension at a rate less than the reach-scale mean (this is illustrated qualitatively

in Figures 5.3 and 5.6). Furthermore, the rate-frequency plots of the Beni and Ok Tedi peak in the range of one standard deviation greater than the mean extension rate, whereas the plots of the Paraguay and Strickland peak between one and two standard deviations greater than the mean. Thus, in rivers with very high bend extension rates, most chute channels form at bends that are extending at a rate just greater than the reach-scale mean, whereas in rivers with lower bend extension rates, most chute channels form at bends that are extending at a rate that is substantially greater than the reach-scale mean.
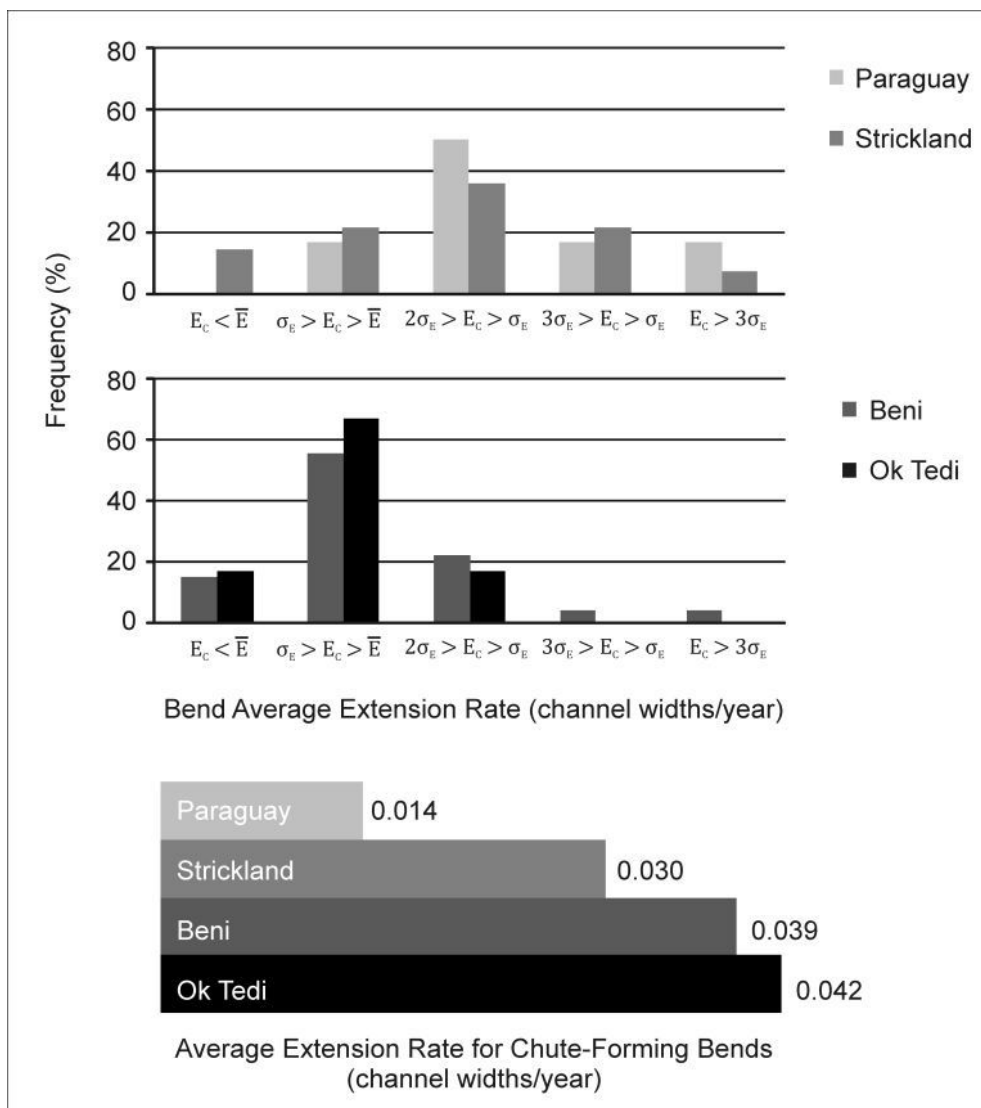
Figure 5.7: Frequency of chute initiation as a function of bend extension rates relative to the mean extension rate, for chute-forming bends on the Strickland, Paraguay, Beni and Ok Tedi. E_C is the extension rate where chutes form, $\overline{E}$ is the mean extension rate, and σ_E is the standard deviation of the extension rate.

In other words, the frequency of chute activity is rate-dependent; meander bends of rivers with lower extension rates must be subject to very high extension rates before a chute channel will form, whereas meander bends of rivers with very high extension rates need only be subject to an extension rate that is marginally higher than the mean for a chute channel to form. An explanation for this may lie in the dynamics of bend extension already described; chute initiation is typically suppressed at bends subject to slow extension because point bar morphology and vegetation cover is allowed to develop in a way that prohibits bar dissection (Braudrick *et al.*, 2009; Tal and Paola, 2010; Chapter 2). Thus, extension must be rapid to overcome these resisting forces.

Another allied interpretation of the pattern illustrated in Figure 5.7 is that there is an absolute threshold extension rate for chute initiation that varies little between the rivers studied. Where the reach-scale mean bend extension rate is much lower than this threshold, it follows that the individual bend migration rate must be several times the mean rate for the threshold to be exceeded. This interpretation parallels with theory on river avulsion that expresses avulsion likelihood in terms of a cross-valley to down-valley slope ratio (Törnqvist and Bridge, 2002; 2006). The threshold value of this ratio varies with the absolute down-valley slope, and is much higher on systems with low down-valley slopes (e.g. Aslan *et al.*, 2005). In the case of chute initiation, the threshold extension rate may also vary with down-valley slope (and stream power), and should be higher in low-slope settings with slower bend extension rates (also see Micheli and Larsen, 2010, for a discussion of down-valley slope control of planform geometry thresholds for chute cutoff).

There is a further possibility that the addition of sediment in the Ok Tedi is in itself a driver of bend development and chute initiation, through mid-channel bar formation. This mechanism of chute formation was described by Bridge *et al.* (1986), but was observed to be a substantially less-common mechanism of chute initiation in the Strickland, Paraguay, and Beni Rivers, where most chutes

form during scroll-slough development at established bends (Chapter 2). Mid-channel bar formation features prominently in the reach of the lower Ok Tedi illustrated in Figure 5.5. Bifurcations formed by mid-channel bars in high Shields stress rivers (i.e. sand-bed rivers) are inherently unstable, and rapidly develop an asymmetrical morphology and discharge division (Edmunds and Slingerland, 2008). Topographic steering of flow by the bar (Smith and Maclean, 1984; Nelson and Smith, 1989) accelerates cutbank erosion in the dominant bifurcate, and leads to bend development (Bridge *et al.*, 1986; Barkdoll, 2004), promoted by the energy excess. In addition, a large supply of bed sediment would increase the likelihood of shoaling of bedload sheets and unit bars, which promotes chute formation by forcing flow over point bars (Carson, 1986; Ashmore, 1991; Peakall *et al.*, 2007). Mass-energy interaction is therefore important in this setting, and it is difficult to disentangle the effects of hydraulic and sedimentary drivers of channel dynamics.

Interactions between channel sediment supply and slope are well documented in the literature, and case studies of catchment disturbance and mining impact have yielded valuable insight into the dynamics of channel change. Dollar and Rowntree (1995) and Rowntree and Dollar (1996; 1998) quantified the interplay between riparian vegetation, and increased channel sediment supply and slope due to catchment disturbance. Channel steepening led to bank erosion and braiding except where channel banks had been stabilised by trees. In the reach subject to bank stabilisation, increased overbank flow led to chute formation and bend cutoff (see Thompson, 2003, for a related example), indicating that chute formation may be a consequence of an energy excess even where lateral migration is impeded, albeit through a different mechanism to that observed in large, sand-bed rivers.

Accounts of the impact of historic metals mining in Wales on channel dynamics show that the source of increased sediment can arise from increased channel activity alone (Lewin and Macklin, 1987), rather than from a direct addition of tailings (as in the case of the Ok Tedi). In Wales, the addition of toxic metals is

considered to have caused widespread death of riparian vegetation, leading to bank erosion, concomitant aggradation and channel steepening, and a transition from meandering to braiding (Lewin *et al.*, 1977; 1983; Lewin and Macklin, 2010). The mechanism of braid formation reported for the Welsh rivers studied involves aggradation, channel crevassing and splay formation, suggesting direct control by sediment rather than indirect forcing of channel migration and chute initiation by a change in channel slope (Lewin *et al.*, 1983). However, a transition from braiding to wandering following the cessation of mining indicates ongoing lateral activity in the altered high energy, high load environment (Lewin *et al.*, 1983). This temporal trend is mirrored in the downstream trend in planform pattern from braiding to wandering to meandering that is common of many river systems (e.g. Brierley, 1989; 1991; Brierley and Hickin, 1991), and is evident in the Ok Tedi as well (Figure 5.8).
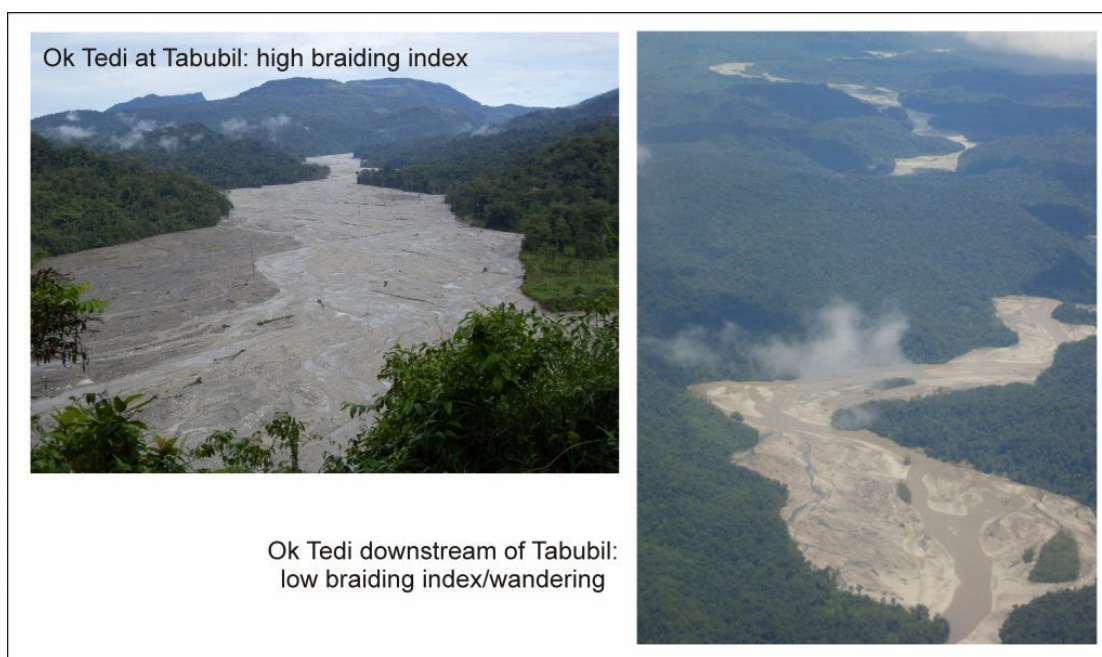
Figure 5.8: Downstream trend in planform pattern (braiding to wandering) along the Ok Tedi. The wandering pattern gives way to meandering downstream in the reach studied in this chapter.

Lewin and Macklin (1987) note that contaminants may be incorporated into lateral accretion deposits within floodplains, and subsequently reworked by

lateral migration. This can lead to dilution of contaminants with 'clean' floodplain sediment, but also results in extending the timescale of contaminant delivery to the aquatic environment downstream (Lewin and Macklin, 1987). Thus, channel-floodplain exchange processes mediate the delivery of sediment and associated contaminants from source-to-sink, potentially reducing the magnitude and intensity of impact, but prolonging the duration of impact. The characteristic floodplain reworking time, or time required to cycle one floodplain width was calculated for the Strickland River by Aalto *et al*. (2008) to be ~ 920 years (1500 km² floodplain area divided by areal reworking rate due to meander migration of 318 km channel length times the average migration rate of 5.1 ± 0.8 m a^{-1}).

Using this approach, and assuming that calculated reach-average migration rates are approximately representative of a long-term norm, the characteristic floodplain reworking time for the lower Paraguay upstream of the Bermejo confluence is ~ 2700 years; downstream of the Bermejo confluence it is ~ 1200 years; for the Beni River within the Foredeep it is ~ 780 years; and for the lower Ok Tedi (unconfined) it is ~ 420 years (but likely to be longer once the sediment wave passes and migration rates decline). For comparison, the characteristic floodplain reworking time for the modern floodplain of the Brazilian Amazon is estimated to be < 5 ka (Mertes *et al*., 1996). Thus, channel-floodplain exchange mediates sediment delivery over timescales that may be considered long in geomorphological process, ecological, or environmental health terms, but relatively short in geological terms.

5.3. Mediative Adjustment of River Dynamics

It is hypothesised that the effect of bend extension on river energy is twofold; i) extension increases sinuosity and thereby reduces slope, an important component of Shields stress and stream power, and ii) rapid extension leads to chute initiation which diverts flow from the mainstem, thereby reducing Shields stress in the mainstem bifurcate (at the eroding cutbank face).

Quantifying the feedback effect of chute formation on bend extension rates in a GIS analysis is difficult due to the temporally-stuttered nature of the available image record, and the existence of other controls on bend extension rates such as channel curvature and interactions with alluvial inhomogeneities (e.g. clay plugs; Fisk, 1947), which are numerous in many large, sand-bed meandering river floodplains. Instead, the feedback effect of chute formation (and flow diversion) on energy within the mainstem bifurcate is tested herein using a two-dimensional depth-averaged hydrodynamic model (Delft3D applied in depth-averaged mode), implemented using field data from the Strickland River.

A detailed account of fieldwork and the general modelling approach is given in Chapter 3, and summarised hereafter. A field campaign was conducted in August of 2010 to survey the bathymetry of several bifurcate meander bends on the Strickland River, using sidescan sonar. Bathymetric data were georeferenced in real-time using DGPS (sub-meter accuracy in x, y, and z). Bathymetric data were interpolated onto a curvilinear grid structure for use in hydrodynamic simulations. This was achieved using the Delft3D grid and depth generation and manipulation software. The raw survey data set comprised depths below the water surface in an x, y, z point cloud. Correction of water depth measurements to yield bed elevation data is problematic in large sand-bed rivers with very low water surface slopes. Because the GPS elevation data were not of sufficient accuracy to resolve the true water surface slope, bed elevations were determined from depth measurements using the best available estimate of the mean bed gradient for the Strickland (0.0001 m m^{-1}; Lauer $et\ al.$, 2008).

The specific aim of the modelling presented herein was to test the effect of increasing chute flow diversion on bed shear stress in the mainstem bifurcate, for an inlet discharge of 3000 m^3 s^{-1} (~ Strickland River mean annual Q). Changing the magnitude of chute flow diversion was achieved by constructing a second DEM in which the depth of the chute channel was reduced to 50% of that for the surveyed channel topography. Thus, model runs compared the

bifurcate meander bend configured using the field survey data (B in Figure 5.9), and an exactly equivalent planform configuration, but for a chute that was 50 % shallower (A in Figure 5.9).

The 2D Delft3D modelling system solves the two-dimensional depth-averaged form of the Navier-Stokes shallow water equations on a curvilinear finite-difference numerical grid, and has been validated for a range of hydrodynamic and morphodynamic applications (Lesser *et al.*, 2004), including the modelling of river bifurcations (Kleinhans *et al.*, 2008; Edmonds and Slingerland, 2008). In this study, bed roughness was parameterised using a quadratic friction law, expressed in terms of a Chézy coefficient that is calculated using the White-Colebrook equation. Samples of bed sediment were taken within the chute and mainstem bifurcates during the bathymetric survey, using a Petite Ponar Grab Sampler, to provide an indication of the bed sediment size. Dunes of 0.2 – 0.5 m in height and 7 – 10 m in length were identified during the bed survey, and appeared to be more numerous in chute channels. Large areas of the mainstem bed were devoid of bedforms altogether. A D_{90} of 300 µm was determined using the bed sediment sampling data. Based on the dune and D_{90} data, an appropriate value for k_s would lie in the range 0.15 to 0.3 m. Given the lack of bedforms in the mainstem, the lower limit was used in simulations. For reference, an average flow depth of 8 m (at the time of survey) would imply a constant Chézy roughness coefficient of 51 and 46 for k_s of 0.15 m and 0.3 m, respectively. Using the White-Colebrook formulation in Delft3D results in hydraulic roughness (Chézy) varying spatially with depth.

Turbulence is modelled using a zero-order eddy viscosity model (see Uittenbogaard *et al.*, 1992), with constant background horizontal eddy viscosity and eddy diffusivity coefficients used in the present study. When implemented in depth-averaged mode, Delft3D does not represent the effects of secondary circulation explicitly. Instead, these effects are parameterised using a secondary circulation correction scheme, which quantifies the spiral flow intensity in each model grid cell as a function of streamline curvature. This can be accomplished

using either the local flow curvature, or by solving a transport equation for spiral flow intensity in which the local streamline curvature provides the source term in the transport equation (this source term defines the equilibrium spiral flow intensity). The latter approach was used in the present study.

The modelling approach and parameter set described above was applied consistently across both depth configurations. Simulations were run until hydrodynamic equilibrium was reached (i.e. until a steady flow solution was obtained), and output data for bed shear stress at hydrodynamic equilibrium were compared. Bed shear stress was quantified both over the full area of each mainstem bifurcate, and at the locus of peak bed shear stress at each mainstem cutbank (a region ~ 60 m wide or 20 % of the width of the mainstem adjacent to the cutbank, in the region of peak shear stress; Figure 5.9). Simulations were conducted using two grid resolutions to assess the significance of this parameter; a low resolution grid with 30 cells across the channel width (300 to 1500 m), and ~ 250 cells down the channel length (~ 9000 m), and a grid with double the number of cells in across-stream and down-stream directions. Results for the different grid resolutions differ by less than 10 % in the case of mainstem bifurcate average shear stress, and by less than 5 % at the locus of peak shear stress (results are reported for the higher resolution grid).

The average bed shear stress in the mainstem bifurcate in (A) is 3.35 N m^{-2}, while in (B) it is 2.45 N m^{-2}. The relative difference in bed shear stress at the locus of peak stress in (A) and (B) is of an equivalent magnitude to the difference in average bed shear stress, and is reported in Figure 5.9. The discharge ratio (Q-chute / Q-mainstem bifurcate) in the case of (A) is 0.41, while in the case of (B) it is 0.66. Thus, the deeper chute channel (B) diverts ~ 60 % more flow, which is associated with a ~ 40 % reduction in bed shear stress in the mainstem bifurcate. Since bank erosion (and channel migration) is a function of excess bed shear stress at the cutbank, a reduction in bed shear stress due to flow diversion by a chute channel can exert negative feedback on bend migration.
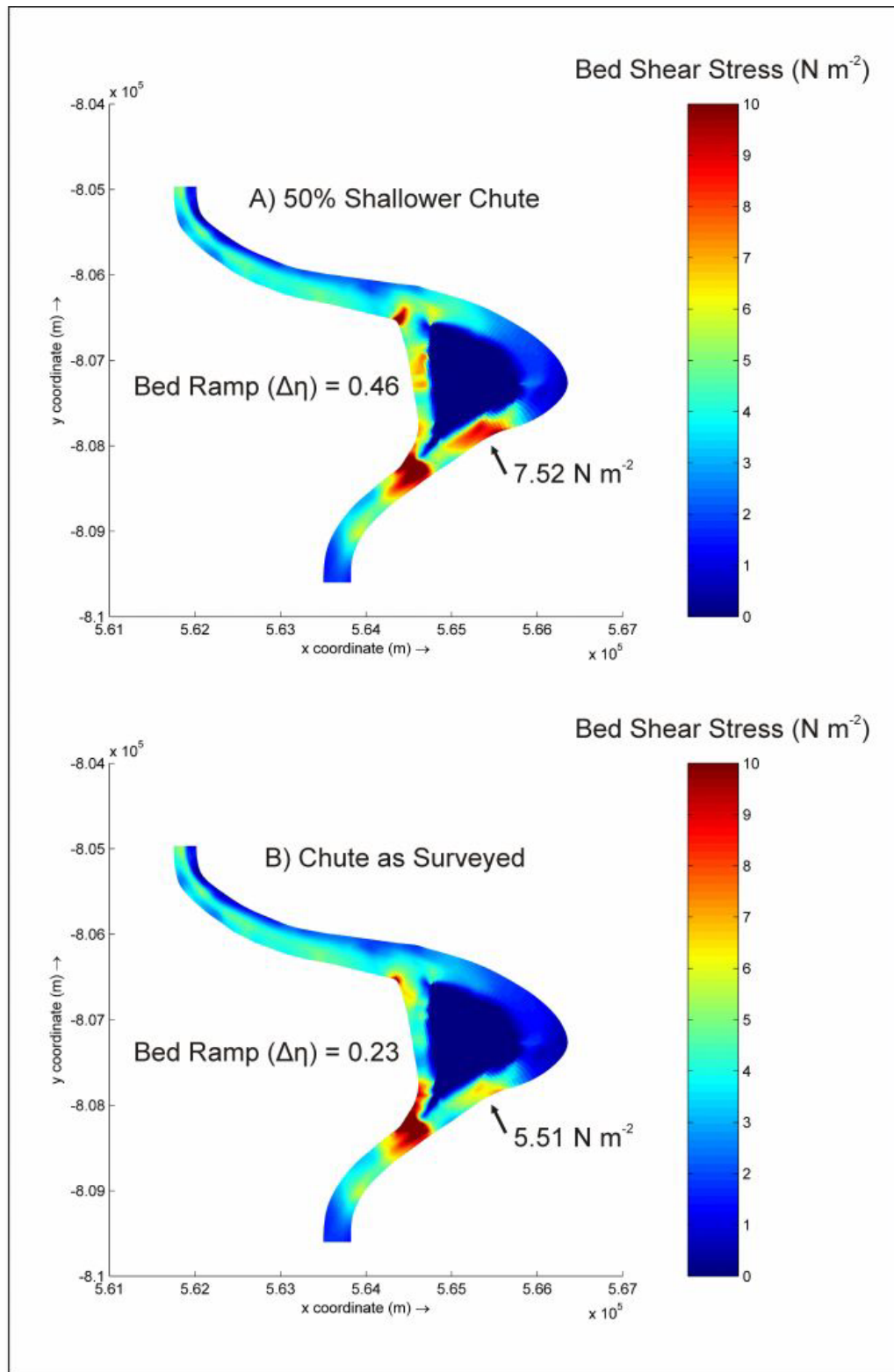
Figure 5.9: Bed shear stress distributions predicted by Delft3D in a bifurcate meander bend of the Strickland River. The planform geometry, grid, and depth configurations of A) and B) are identical, except that the chute in A) is half the depth of the chute in B). This results in a ~ 60 % greater discharge ratio (Q-chute / Q-mainstem bifurcate) in B), with an attendant ~40 % lower bed shear stress (N m^{-2}) within the mainstem bifurcate as a whole, and at the locus of peak shear stress at the mainstem cutbank.

5.4. Implications

A key observation here is the rate-dependency of the processes of bend extension, chute formation and flow diversion – a greater extension rate will elicit a more rapid response both in increasing local sinuosity (and reducing local slope) and in increasing the probability of chute initiation with associated diversion of flow and feedback effects. Bend extension has broader implications for bifurcate meander bend geometry and dynamics; elongation of the mainstem bifurcate increases the gradient advantage of the chute, thereby enhancing flow diversion (Chapter 2; Chapter 3). Nanson and Huang (2008) proposed that many alluvial rivers could be regarded as 'directional iterative systems', where change (erosion, transport, or deposition) in a particular direction is more probable than changes in other directions. The rivers considered in this study exhibit such behaviour; the probability of chute initiation increases as bend extension rates increase. This behaviour in the large, sand-bed meandering rivers studied is activated iteratively in space and time in response to changes in river energy. It is both rate-dependent, and rate-limiting, selectively (subject to probability) affecting sites of greatest energy excess, and thereby mediating river energy (e.g. Brooks and Brierley, 2002). Thus, this behaviour may be described as mediative adjustment.

Chute formation is a stochastic process (Camporeale *et al.*, 2005; 2008), and may best be modelled probabilistically (e.g. Howard, 1996), but understanding the overall role of chute formation in meandering river dynamics is perhaps less daunting. If only sinuosity is considered, then both neck cutoff and complete chute cutoff do reduce planform geometrical complexity (Camporeale *et al.*, 2008). In addition, due to the feedback effect of chute formation on meander bend shear stress, chute formation and persistence alone (rather than complete chute cutoff) may be sufficient to limit the width of the meander belt (e.g. Howard, 1996). However, in many large, sand-bed meandering rivers, chute initiation and the formation of stable bifurcate bends has the effect of increasing planform geometrical complexity in terms of the bar structure. Many bifurcate

bends persist until they are ultimately excised by neck cutoff, and become complex abandoned channel sedimentary features of these large floodplains (Chapter 2; Figure 5.10).
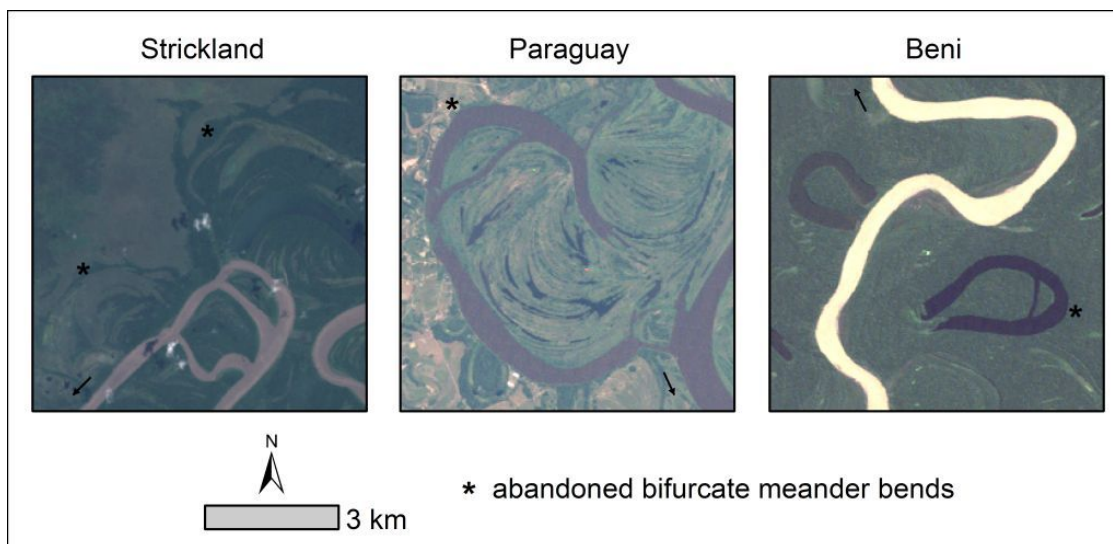
Figure 5.10: Abandoned bifurcate meander bends on floodplains of the Strickland, Paraguay and Beni Rivers. Chute channels that form in these rivers rarely progress to full cutoff, and are in many cases preserved in abandoned channels ultimately excised by neck cutoff.

Meander migration simultaneously creates floodplain sediment at point bars, and consumes it at cutbanks, and some intriguing observations have been made on the balance of these opposing processes (e.g. Lauer and Parker, 2008a; 2008b; 2008c; Aalto *et al.*, 2008). Meander bend cutoff is an important component of this balance that has been little explored, but can result in a significant and rapid increase in local sediment efflux (Fuller *et al.*, 2003; Zinger *et al.*, 2011). It is suggested that the style of sediment release by cutoff in the range of meandering rivers considered in this chapter is influenced by the river energy regime, and further research is needed to fully elucidate the interplay between meandering river energy, cutoff processes, and floodplain sediment fluxes.

Most intriguing in this respect is the observation that different mechanisms of chute formation are characteristic of different floodplain environments (Camporeale *et al.*, 2008). Steeper gravel-bed rivers exhibit a higher frequency of

complete chute cutoff than sand-bed rivers, and are associated with mechanisms of chute formation that involve scour and dissection of the floodplain surface, with a great proportion of chute channels initiating mid-bend or connecting outer banks of alternate bends (Lewis and Lewin, 1983; Constantine *et al.*, 2010; Micheli and Larsen, 2010). In contrast, chute channels in sand-bed rivers typically form during scroll-slough development, close to the inner bank apex of meander bends, or initiate with mid-channel bar development. The feedback effect of chute channels differs according to the floodplain environment; chute formation typically leads to cutoff in steep, gravel-bed meandering rivers, thereby maintaining a steep slope and exerting positive feedback on river energy, while chute formation in sand-bed rivers is more commonly followed by chute infill, or leads to bend bifurcation, which maintain a gentle slope and exert negative feedback on river energy.

CHAPTER 6

Conclusion

6.1. Project Summary

This research combined GIS and spatial statistical analyses, field survey, Delft3D hydrodynamic and morphodynamic modelling, and Pb-210 alpha-geochronology, to investigate the role of chute channels in the planform dynamics of large, sand-bed meandering rivers. The thesis addressed controls on chute channel initiation and stability, and effects of chute channels on channel planform dynamics and floodplain sedimentation patterns.

Reach- and bend-scale controls on chute channel initiation were examined through binary logistic regression analysis of channel planform data derived through image analysis in a GIS. Regression models developed for the Strickland River, Papua New Guinea, the lower Paraguay River on the Paraguay/Argentina border, and the Beni River, Bolivia, revealed that the probability of chute initiation at a meander bend is a function of the bend extension rate (the rate at which a bend elongates in a direction perpendicular to the valley axis trend). It was discovered that the Paraguay, Strickland and Beni Rivers plot in order of increasing chute activity on an empirical meandering-braided pattern continuum defined by potential specific stream power and bedload calibre. Increasing stream power was considered to result in higher bend extension rates, with implications for chute initiation. Rates of chute infill were shown to increase with river sediment load (Qs/Q), which is highest for the Beni River. The high sediment load of the Beni may suppress braiding within the Andean foredeep, by filling chute channels as they form.

Rapid bend extension was considered important to chute formation because it is associated with bend apex widening, where cutbank erosion outpaces point

bar deposition. This leads to wide scroll bar spacing, and alignment of intervening sloughs that favours flow across a developing point bar. The formation of prominent sloughs breaks the continuity of vegetation encroachment on point bars, but the island that forms between chute and mainstem bifurcates is rapidly colonised and stabilised by robust grasses (e.g. *Phragmites karka* in Papua New Guinea), thereby focusing scour in the adjacent chute. Field-based bathymetric surveys of several Strickland River meander bends formed a basis for Delft3D simulations of discharge and sediment transport ratios at chute-mainstem bifurcations. The field data and simulation results suggested that the chute gradient advantage exerts fundamental control on morphology, and discharge and sediment division within bifurcate meander bends, thus affecting the stability of bifurcate meander bends. Bifurcate bends with low chute gradient advantages are associated with large bed ramps (shallow chute channels), low discharge ratios (Q-chute bifurcate / Q-mainstem bifurcate), and low sediment transport rates, making these chutes vulnerable to infill. The process of bend extension increases the chute-mainstem bifurcation angle and chute gradient advantage, such that chutes at extending bends are kept open through 'quasi-balance' by factors that interact to limit bedload influx and increase chute competence: high bifurcation angles which should lead to wide flow separation zones at the chute entrance, and chute closure, are balanced by changes in the alignment of flow at the bend entrance, and increases in the chute gradient advantage, associated with ongoing extension.

Further GIS analysis of the response of the Ok Tedi in Papua New Guinea to direct addition of mine tailings elucidated interplay between channel steepening due to the propagation of a tailings sediment slug, and mid-channel bar formation induced by the increased sediment load, with associated topographic forcing of bend and chute development. A temporal pattern of increased chute initiation frequency on the Ok Tedi, in response to the addition of mine tailings, mirrors the inter- and intra-reach spatial pattern of chute initiation frequency on the Paraguay, Strickland and Beni Rivers, where increased stream power is associated with increased bend extension and chute

initiation rates. The process of chute formation was shown to be rate-dependent, and the threshold value of bend extension for chute initiation was shown to scale with reach-scale stream power, reminiscent of slope-ratio thresholds in river avulsion. However, Delft3D simulations suggested that chute formation can exert negative feedback on shear stress and bank erosion in the adjacent mainstem bifurcate, such that the process of chute formation is also rate-limiting. Chute formation is activated iteratively in space and time in response to changes in river energy, selectively targeting sites of greatest change, and thereby mediating the river response.

Strickland River floodplain sedimentation rates derived through Pb-210 alpha-geochronology were found to be substantially higher adjacent to single-thread bends than adjacent to bifurcate bends, potentially due to an observed increase in channel capacity (and reduction in floodplain inundation frequency) associated with bend bifurcation. Further research is needed to determine whether this observation is significant in light of high uncertainty in the spatial variability of sedimentation rate estimates, but the data presented highlighted a need for carefully considered stratified sampling approaches in floodplain coring campaigns, and illustrated the complexity of possible sediment dispersal mechanisms, and associated ecological responses.

6.2. Research Forecast: Large River Processes

A full understanding of pattern dynamics in large rivers is only possible through analyses of process. If the bifurcate meander bends studied in this thesis were viewed at a single point in time, the presence of 'stable' vegetated islands at meander bends might prompt the observer to classify the channel pattern as low-order anabranching, implying lateral channel stability. However, this would belie the tumultuous origin of the chute channels at rapidly extending bends, and would misrepresent the nature of the river energy environment. Researchers must therefore document channel dynamics to

understand planform pattern – pattern is an outcome of process, not a static channel characteristic.

Recent advancements in process measurement instrumentation such as shallower-water sub-bed profiling, acoustic Doppler current profiling, multi-beam bathymetric mapping, and terrestrial laser scanning, will allow researchers to attain unprecedented views of the large river environment. Image analyses will continue to feature strongly in studies of large river dynamics, as image data provide a system-level overview of channel dynamics. In addition, advancements in modelling software, and an increase in the availability of this software, will allow researchers to add value to image and field datasets, and to rigorously test field-based hypotheses. Perhaps the greatest advancements in understanding large river dynamics will stem from research approaches that combine GIS, field, laboratory, and modelling techniques.

Understanding what sets large rivers apart from small rivers is one of the key paths of inquiry guiding large rivers research. There are clear points of difference in patterning processes and process-pattern feedbacks, which may be conditioned in some settings by the nature of the floodplain environment. As Ferguson (1981: 90) notes; channels may be "viewed as the outcome of a continuous struggle between the erosive potential of the river and the resistive forces of the valley-floor setting". In the large tropical rivers studied in this thesis, high sediment loads and aggressive sediment-vegetation interactions play a fundamental role in shaping the channel pattern, but further research is needed to document these interactions. Further research is also needed to understand the implications of sediment-vegetation interactions for large river floodplain ecology and ecosystem service provision, especially in highly populous systems where livelihoods may be directly affected by river channel dynamics. Geomorphology provides a fundamental template for these interactions, and should form a basis of multidisciplinary investigations.

REFERENCES

Aalto R. 2002. Geomorphic form and process of sediment flux within an active orogen: denudation of the Bolivian Andes and sediment conveyance across the Beni foreland. PhD Dissertation, University of Washington, Seattle.

Aalto R, Dunne T, Nittrouer CA, Maurice-Bourgoin L, Montgomery DR. 2002. Fluvial transport of sediment across a pristine tropical foreland basin: channel-flood plain interaction and episodic flood plain deposition. In: Dyer FJ, Thoms MC, Olley JM (eds). Symposium on the Structure, Function and Management Implications of Fluvial Sedimentary Systems, Alice Springs, Australia. International Association of Hydrological Sciences, 339-344.

Aalto R, Maurice-Bourgoin L, Dunne T, Montgomery DR, Nittrouer CA, Guyot JL. 2003. Episodic sediment accumulation on Amazonian flood plains influenced by El Niño/Southern Oscillation. *Nature* **425**: 493-497.

Aalto R, Lauer JW, Dietrich WE. 2008. Spatial and temporal dynamics of sediment accumulation and exchange along Strickland River floodplains (Papua New Guinea) over decadal-to-centennial timescales. *Journal of Geophysical Research-Earth Surface* **113**: F01S04 doi: 10.1029/2006jf000627.

Aalto R, Nittrouer CA. 2012. [210]Pb geochronology of flood events in large tropical river systems. *Philosophical Transactions of the Royal Society A* **370**: 1-35.

Alabyan AM, Chalov RS. 1998. Types of river channel patterns and their natural controls. *Earth Surface Processes and Landforms* **23**: 467-474.

Amsler ML, Drago EC. 2009. A review of the suspended sediment budget at the confluence of the Paraná and Paraguay Rivers. *Hydrological Processes* **23**: 3230-3235.

Ashmore PE. 1991. How do gravel-bed rivers braid? *Canadian Journal of Earth Sciences* **28**: 326-341.

Aslan A, Autin WJ, Blum MD. 2005. Causes of River Avulsion: Insights from the Late Holocene Avulsion History of the Mississippi River, U.S.A. *Journal of Sedimentary Research* **75**: 650-664.

Assine ML, Soares PC. 2004. Quaternary of the Pantanal, west-central Brazil. *Quaternary International* **114**: 23-34.

Assine ML, Silva A. 2009. Contrasting fluvial styles of the Paraguay River in the northwestern border of the Pantanal wetland, Brazil. *Geomorphology* **113**: 189-199.

Aufdenkampe AK, Mayorga E, Raymond PA, Melack JM, Doney SC, Alin SR, Aalto RE, Yoo K. 2011. Riverine coupling of biogeochemical cycles between land, oceans, and atmosphere. *Frontiers in Ecology and the Environment* **9**: 53-60.

Bak P. 1996. *How nature works*. Springer: New York, 205pp.

Barkdoll BD. 2004. Discussion of ''Subcritical 90° Equal-Width Open-Channel Dividing Flow'' by Hsu, C.C., Tang, C.J. and Shieh, M.Y. *Journal of Hydraulic Engineering* **130**: 171-172.

Barros V, Chamorro L, Coronel G, Baez J. 2004. The major discharge events in the Paraguay River: Magnitudes, source regions, and climate forcings. *Journal of Hydrometeorology* **5**: 1161-1170.

Begin ZB. 1981. The relationship between flow-shear stress and stream pattern. *Journal of Hydrology* **52**: 307-319.

Berry WD, Feldman S. 1985. *Multiple Regression in Practice.* SAGE Publications Ltd., Beverly Hills, CA.

Bertoldi W, Tubino M. 2007. River bifurcations: Experimental observations on equilibrium configurations. *Water Resources Research* **43**: W10437 doi: 10.1029/2007WR005907.

Blake DH, Ollier CD. 1971. Alluvial plains of the Fly River, Papua. *Zeitschrift für Geomorphologie Supplement Bände* **12**: 1-17.

Bledsoe BP, Watson CC. 2001. Logistic analysis of channel pattern thresholds: meandering, braiding, and incising. *Geomorphology* **38**: 281-300.

Blondeaux P, Seminara G. 1985. A unified bar-bend theory of river meanders. *Journal of Fluid Mechanics* **157**: 449-470.

Blum MD. 2007. Large River Systems and Climate Change. In: Gupta A (ed). *Large Rivers: Geomorphology and Management*. John Wiley and Sons: Chichester, 627-659.

Bolla Pittaluga M, Repetto R, Tubino M. 2003. Channel bifurcation in braided rivers: Equilibrium configurations and stability. *Water Resources Research* **39**: 1046 doi: 10.1029/2001wr001112.

Bolla Pittaluga M, Nobile G, Seminara G. 2009. A nonlinear model for river meandering. *Water Resources Research* **45**: W04432 doi: 10.1029/2008WR007298.

Braudrick CA, Dietrich WE, Leverich GT, Sklar LS. 2009. Experimental evidence for the conditions necessary to sustain meandering in coarse-bedded rivers. *Proceedings of the National Academy of Sciences of the United States of America* **106**: 16936-16941.

Brewer PA, Lewin J. 1998. Planform cyclicity in an unstable reach: complex fluvial response to environmental change. *Earth Surface Processes and Landforms* **23**: 989-1008.

Brice JC. 1975. Air photo interpretation of the form and behaviour of alluvial rivers. Final Report, US Army Research Office, Durham, Grant no. DA-ARD-D-31-124-70-G89.

Brice JC. 1982. Stream Channel Stability Assessment. Federal Highway Administration, Report No. FHWA/RD-82/021.

Bridge JS. 1993. The interaction between channel geometry, water flow, sediment transport and deposition in braided rivers. In: Best JL, Bristow CS (eds). *Braided Rivers.* Geological Society Special Publication 75, 13-71.

Bridge JS, Smith ND, Trent F, Gabel SL, Bernstein P. 1986. Sedimentology and morphology of a low-sinuosity river: Calamus River, Nebraska Sand Hills. *Sedimentology* **33**: 851-870.

Bridge JS, Demicco RV. 2008. *Earth Surface Processes, Landforms and Sediment Deposits.* Cambridge University Press, New York.

Brierley GJ. 1989. River planform facies models: the sedimentology of braided, wandering and meandering reaches of the Squamish River, British Columbia. *Sedimentary Geology* **61**: 17-35.

Brierley GJ. 1991. Bar sedimentology of the Squamish River, British Columbia: definition and application of morphostratigraphic units. *Journal of Sedimentary Petrology* **61**: 211-225.

Brierley G. 2008. Geomorphology and river management. *Kemanusiaan* **15**: 13-26.

Brierley GJ, Hickin EJ. 1991. Channel planform as a non-controlling factor in fluvial sedimentology: the case of the Squamish River floodplain, British Columbia. *Sedimentary Geology* **75**: 67-83.

Brierley GJ, Fryirs KA. 2005. *Geomorphology and river management: applications of the river styles framework*. Blackwell, Oxford, 398pp.

Bristow CS, Best JL. 1993. Braided rivers: perspectives and problems. In: Best JL, Bristow CS (eds). *Braided Rivers*. Geological Society Special Publication 75, 1-11.

Brooks AP, Brierley GJ. 2002. Mediated equilibrium: the influence of riparian vegetation and wood on the long-term evolution and behaviour of a near-pristine river. *Earth Surface Processes and Landforms* **27**: 343-367.

Bulle H. 1926. Untersuchungen über die Geschiebeableitung bei der Spaltung von Wasserläufen (*Investigations of sediment diversion at the division of channels)*. VDI Verlag, Berlin.

Burge LM. 2006. Stability, morphology and surface grain size patterns of channel bifurcation in gravel-cobble bedded anabranching rivers. *Earth Surface Processes and Landforms* **31**: 1211-1226.

Camporeale C, Perona P, Porporato A, Ridolfi L. 2005. On the long-term behaviour of meandering rivers. *Water Resources Research* **41**: W12403 doi: 10.1029/2005WR004109.

Camporeale C, Perucca E, Ridolfi L. 2008. Significance of cutoff in meandering river dynamics. *Journal of Geophysical Research-Earth Surface* **113**: F01001 doi: 10.1029/2006jf000694.

Camporeale C, Ridolfi L. 2010. Interplay among river meandering, discharge stochasticity and riparian vegetation. *Journal of Hydrology* **382**: 138-144.

Carson MA. 1984. The meandering-braided river threshold: A reappraisal. *Journal of Hydrology* **73**: 315-334.

Carson MA. 1986. Characteristics of high-energy "meandering" rivers: the Canterbury Plains, New Zealand. *Geological Society of America Bulletin* **97**: 886-895.

Constantine JA, Dunne T. 2008. Meander cutoff and the controls on the production of oxbow lakes. *Geology* **36**: 23-26.

Constantine JA, Dunne T, Piegay H, Kondolf GM. 2010a. Controls on the alluviation of oxbow lakes by bed-material load along the Sacramento River, California. *Sedimentology* **57**: 389-407.

Constantine JA, McLean SR, Dunne T. 2010b. A mechanism of chute cutoff along large meandering rivers with uniform floodplain topography. *Geological Society of America Bulletin* **122**: 855-869.

Cox DR, Snell DJ. 1989. *The Analysis of Binary Data. 2nd Edition.* Chapman and Hall, London.

Crosato A. 2009. Physical explanations of variations in river meander migration rates from model comparison. *Earth Surface Processes and Landforms* **34**: 2078-2086.

Crosato A, Mosselman E. 2009. Simple physics-based predictor for the number of river bars and the transition between meandering and braiding. *Water Resources Research* **45**: W03424 doi: 10.1029/2008wr007242.

Crosato A, Saleh MS. 2011. Numerical study on the effects of floodplain vegetation on river planform style. *Earth Surface Processes and Landforms* **36**: 711-720.

Cui Y, Parker G. 1999. Sediment transport and deposition in the Ok Tedi-Fly River system, Papua New Guinea: The modelling of 1998-1999. Report submitted to Ok Tedi Mining Limited. Available online at http://www.oktedi.com/.

Dade WB, Friend PF. 1998. Grain-size, sediment-transport regime, and channel slope in alluvial rivers. *Journal of Geology* **106**: 661-675.

Davies HL. 2009. New Guinea, Geology. In: Gillespie R, Clague D (eds). *The Encyclopedia of Islands*. University of California Press, Berkeley, 659-664.

Day G, Dietrich WE, Rowland JC, Marshall A. 2008. The depositional web on the floodplain of the Fly River, Papua New Guinea. *Journal of Geophysical Research-Earth Surface* **113**: F01S02 doi: 10.1029/2006JF000622.

Dietrich WE, Day G, Parker G. 1999. The Fly River, Papua New Guinea: Inferences about River Dynamcis, Floodplain Sedimentation and Fate of Sediment. In: Miller AJ, Gupta A (eds). *Varieties of Fluvial Form*. John Wiley and Sons: Chichester, 345-376.

Dollar ESJ, Rowntree KM. 1995. Hydroclimatic trends, sediment sources and geomorphic response in the Bell River catchment, Eastern Cape Drakensberg, South Africa. *South African Geographical Journal* **77**: 21-32.

Drago EC, Amsler ML. 1988. Suspended sediment at a cross section of the Middle Paraná River: concentration, granulometry and influence of the main tributaries. Sediment Budgets, Proceedings of the Porto Alegre Symposium, IAHS Publication No. 174, 381-396.

Drago EC, Amsler ML. 1998. Bed Sediment Characteristics in the Paraná and Paraguay Rivers. *Water International* **23**: 174-183.

Eaton BC, Millar RG, Davidson S. 2010. Channel patterns: Braided, anabranching, and single-thread. *Geomorphology* **120**: 353-364.

Edmonds DA, Slingerland RL. 2008. Stability of delta distributary networks and their bifurcations. *Water Resources Research* **44**: W09426 doi: 10.1029/2008wr006992.

Ellery WN, Ellery K, Rogers KH, McCarthy TS, Walker BH. 1993. Vegetation, hydrology and sedimentation processes as determinants of channel form and dynamics in the northeastern Okavango Delta, Botswana. *African Journal of Ecology* **31**: 10-25.

Engelund F, Hansen E. 1967. A Monograph on Sediment Transport in Alluvial Streams. Teknisk Forlag, Kobenhavn, Denmark.

EOSDIS. 2009. Earth Observing System Clearing House (ECHO) / Warehouse Inventory Search Tool (WIST) Version 10.28 (online application). Earth Observing System Data and Information System, Goddard Space Flight Center (GSFC), National Aeronautics and Space Administration (NASA). Greenbelt, MD. URL: https://wist.echo.nasa.gov/api/.

EROS. 2009. USGS Global Visualization Viewer (online application). Earth Resources Observation and Science Center, US Geological Survey. Sioux Falls, SD. URL: http://glovis.usgs.gov.

Federici B, Paola C. 2003. Dynamics of channel bifurcations in noncohesive sediments, *Water Resources Research* **39**: 1162 doi:10.1029/ 2002WR001434.

Ferguson RI. 1975. Meander irregularity and wavelength estimation. *Journal of Hydrology* **26**: 315-333.

Ferguson RI. 1981. Channel form and channel changes. In: Lewin J (ed). *British Rivers*. Allen and Unwin, London, 90-125.

Ferguson R. 1987. Hydraulic and Sedimentary Controls of Channel Pattern. In: Richards K (ed). *River Channels, Environment and Process*. Blackwell, Oxford, 129-158.

Ferguson RI. 1993. Understanding braiding processes in gravel-bed rivers: progress and unsolved problems. In: Best JL, Bristow CS (eds). *Braided Rivers.* Geological Society Special Publication 75, 73-87.

Field A. 2009. *Discovering Statistics Using SPSS. 3rd Edition.* SAGE Publications Ltd., London.

Filgueira-Rivera M, Smith ND, Slingerland RL. 2007. Controls on natural levée development in the Columbia River, British Columbia, Canada. *Sedimentology* **54**: 905-919.

Fisk HN. 1944. Geological Investigation of the Alluvial Valley of the Lower Mississippi River. US Army Corps of Engineers, Mississippi River Commission, Vicksburg, MS.

Fisk HN. 1947. Fine-Grained Alluvial Deposits and their Effects on Mississippi River Activity. Waterways Experiment Station, Vicksburg, MS.

Frascati A, Lanzoni S. 2009. Morphodynamic regime and long-term evolution of meandering rivers. *Journal of Geophysical Research-Earth Surface* **114**: F02002 doi: 10.1029/2008jf001101.

Frascati A, Lanzoni S. 2010. Long-term river meandering as a part of chaotic dynamics? A contribution from mathematical modelling. *Earth Surface Processes and Landforms* **35**: 791-802.

Friedkin J. 1945. A Laboratory Study of the Meandering of Alluvial Rivers. Waterways Experiment Station, Vicksburg, MS.

Fuller IC, Large ARG, Milan DJ. 2003. Quantifying channel development and sediment transfer following chute cutoff in a wandering gravel-bed river. *Geomorphology* **54**: 307-323.

Furbish DJ. 1988. River-Bend Curvature and Migration - How are they Related? *Geology* **16**: 752-755.

Furbish DJ. 1991. Spatial Autoregressive Structure in Meander Evolution. *Geological Society of America Bulletin* **103**: 1576-1589.

Galatowitsch SM, van der Valk AG. 1998. *Restoring Prairie Wetlands. An Ecological Approach.* Iowa State University Press, Ames, Iowa.

García NO, Vargas WM. 1996. The spatial variability of runoff and precipitation in the Río de la Plata basin. *Hydrological Science* **41**: 279-299.

García NO, Vargas WM. 1998. The temporal climatic variability in the 'Río de la Plata' basin displayed by the river discharges. *Climatic Change* **38**: 359-379.

Gautier E, Brunstein D, Vauchel P, Roulet M, Fuertes O, Guyot JL, Darozzes J, Bourrel L. 2007. Temporal relations between meander deformation, water discharge and sediment fluxes in the floodplain of the Rio Beni (Bolivian Amazonia). *Earth Surface Processes and Landforms* **32**: 230-248.

Gay GR, Gay HH, Gay WH, Martinson HA, Meade RH, Moody JA. 1998. Evolution of cutoffs across meander necks in Powder River, Montana, USA. *Earth Surface Processes and Landforms* **23**: 651-662.

Gibling MR, Davies NS. 2012. Palaeozoic landscapes shaped by plant evolution. Nature Geoscience **5**: 99-105.

Gilbert GK. 1917. Hydraulic-mining debris in the Sierra Nevada. US Department of the Interior/US Geological Survey Professional Paper 105, 154pp.

Gomez B, Phillips JD, Magilligan FJ, James LA. 1997. Floodplain sedimentation and sensitivity: Summer 1993 flood, upper Mississippi River valley. *Earth Surface Processes and Landforms* **22**: 923-936.

Gomez B, Eden DN, Hicks DM, Trustrum NA, Peacock DH, Wilmshurst J. 1999. Contribution of floodplain sequestration to the sediment budget of the Waipaoa River, New Zealand. In: Marriott S, Alexander J (eds). *Floodplains: Interdisciplinary Approaches*. Geological Society of London Special Publication 163, 69-88.

Goodbred Jr. SL, Kuehl SA. 1998. Floodplain processes in the Bengal Basin and the storage of Ganges-Brahmaputra river sediment: an accretion study using ^{137}Cs and ^{210}Pb geochronology. *Sedimentary Geology* **121**: 239-258.

Gran K, Paola C. 2001. Riparian vegetation controls on braided stream dynamics. *Water Resources Research* **34**: 2365-2376 doi: doi:10.1029/2000WR000203.

Gretener B, Strömqvist L. 1987. Overbank Sedimentation Rates of Fine Grained Sediments. A Study of the Recent Deposition in the Lower River Fyrisån. *Geografiska Annaler. Series A, Physical Geography* **69**: 139-146.

Griffiths JS, Hutchinson JN, Brunsden D, Petley DJ, Fookes PG. 2004. The reactivation of a landslide during the construction of the Ok Ma tailings dam, Papua New Guinea. *The Quarterly Journal of Engineering Geology and Hydrogeology* **37**: 173-186.

Gupta A. 2002. Large rivers. *Geomorphology* **44**: 173-174.

Gupta A (ed). (2007). *Large Rivers: Geomorphology and Management*. John Wiley and Sons: Chichester, 712pp.

Guyot JL. 1993. Hydrogéochimie des Fleuves de l'Amazonie Bolivienne. PhD Dissertation, ORSTOM, Paris.

Guyot JL, Jouanneau JM, Wasson JG. 1999. Characterisation of river bed and suspended sediments in the Rio Madeira drainage basin (Bolivian Amazonia). *Journal of South American Earth Sciences* **12**: 401-410.

Guyot JL, Walling DE. 2009. Flow and sediment dynamics of large rivers. Preface. *Hydrological Processes* **23**: 3127-3130.

Hardy RJ, Lane SN, Yu D. 2011. Flow structures at an idealised bifurcation: a numerical experiment. *Earth Surface Processes and Landforms* **36**: 2083-2096.

Harmar OP, Clifford NJ. 2006. Planform dynamics of the Lower Mississippi River. *Earth Surface Processes and Landforms* **31**: 825-843.

He Q, Walling DE. 1996. Use of fallout Pb-210 measurements to investigate longer-term rates and patterns of overbank sediment deposition on the floodplains of lowland rivers. *Earth Surface Processes and Landforms* **21**: 141-154.

Hickin EJ. 1974. The development of meanders in natural river channels. *American Journal of Science* **274**: 414-442.

Hickin EJ, Nanson GC. 1975. The character of channel migration on the Beatton River, north-east British Columbia, Canada. *Geological Society of America Bulletin* **86**: 487-494.

Hickin EJ, Nanson GC. 1984. Lateral Migration Rates of River Bends. *Journal of Hydraulic Engineering* **110**: 1557-1567.

Hobo N, Makaske B, Middelkoop H, Wallinga J. 2010. Reconstruction of floodplain sedimentation rates: a combination of methods to optimize estimates. *Earth Surface Processes and Landforms* **35**: 1499-1515.

Hooke JM. 1977. An analysis of changes in river channel patterns. PhD Thesis, University of Exeter, Exeter.

Hooke J. 1984. Changes in river meanders: a review of techniques and results of analyses. *Progress in Physical Geography* **8**: 473-508.

Hooke JM. 1995. River channel adjustment to meander cutoffs on the River Bollin and River Dane, northwest England. *Geomorphology* **14**: 235-253.

Hooke J. 2003. River meander behaviour and instability: a framework for analysis. *Transactions of the Institute of British Geographers* **28**: 238-253.

Hooke JM. 2004. Cutoffs galore! Occurrence and causes of multiple cutoffs on a meandering river. *Geomorphology* **61**: 225-238.

Hooke JM. 2007. Complexity, self-organisation and variation in behaviour in meandering rivers. *Geomorphology* **91**: 236-258.

Hooke JM. 2008. Temporal variations in fluvial processes on an active meandering river over a 20-year period. *Geomorphology* **100**: 3-13.

Horton BK, DeCelles PG. 1997. The modern foreland basin system adjacent to the Central Andes. *Geology* **25**: 895-898.

Hosmer DW, Lemeshow S. 1989. *Applied Logistic Regression*. Wiley: New York.

Howard AD. 1996. Modelling channel evolution and floodplain morphology. In: Anderson MG, Walling DE, Bates PD (eds). *Floodplain Processes*. John Wiley, Hoboken, New Jersey, 15-62.

Howard AD. 2009. How to make a meandering river. *Proceedings of the National Academy of Sciences of the United States of America* **106**: 17245-17246.

Huang HQ, Nanson GC. 2007. Why some alluvial rivers develop an anabranching pattern. *Water Resources Research* **43**: W07441 doi: 10.1029/2006WR005223.

Hudson PF, Heitmuller FT. 2003. Local- and watershed-scale controls on the spatial variability of natural levee deposits in a large fine-grained floodplain: Lower Panuco Basin, Mexico. *Geomorphology* **56**: 255-269.

Ikeda S. 1982. Lateral bed load transport on side slopes. *Journal of the Hydraulics Division ASCE* **108**: 1369-1373.

Ikeda S, Parker G, Sawai K. 1981. Bend theory of river meanders. Part 1. Linear development. *Journal of Fluid Mechanics* **112**: 363-377.

Iriondo M. 1993. Geomorphology and late Quaternary of the Chaco (South America). *Geomorphology* **7**: 289-303.

Jerolmack DJ, Mohrig D. 2007. Conditions for branching in depositional rivers. *Geology* **35**: 463-466.

Jerolmack DJ, Paola C. 2007. Complexity in a cellular model of river avulsion. *Geomorphology* **91**: 259-270.

Jerolmack DJ, Paola C. 2010. Shredding of environmental signals by sediment transport. *Geophysical Research Letters* **37**: L19401 doi: 10.1029/2010GL044638.

Johnson RH, Paynter J. 1967. Development of a cutoff on the River Irk at Chadderton, Lancashire. *Geography* **52**: 41-49.

Junk JW. 1999. The flood pulse concept of large rivers: learning from the tropics. *Archiv für Hydrobiologie, Supplementband* **115**: 261-280.

Junk WJ, Bayley PB, Sparks RE. 1989. The flood pulse concept in river-floodplain systems. *Canadian Special Publication of Fisheries and Aquatic Sciences* **106**: 110-127.

Keller EA, Swanson FJ. 1979. Effects of large organic material on channel form and fluvial processes. *Earth Surface Processes* **4**: 361-380.

Kleinhans MG. 2010. Sorting out river channel patterns. *Progress in Physical Geography* **34**: 287-326.

Kleinhans MG, Jagers HRA, Mosselman E, Sloff CJ. 2008. Bifurcation dynamics and avulsion duration in meandering rivers by one-dimensional and three-dimensional models. *Water Resources Research* **44**: W08454 doi: 10.1029/2007wr005912.

Kleinhans M, Cohen KM, Hoekstra J, IJmker JM. 2011. Evolution of a bifurcation in a meandering river with adjustable channel widths, Rhine delta apex, The Netherlands. *Earth Surface Processes and Landforms* **36**: 2011-2027.

Kleinhans MG, van den Berg JH. 2011. River channel and bar patterns explained and predicted by an empirical and a physics-based method. *Earth Surface Processes and Landforms* **36**: 721-738.

Kleinhans MG, de Haas T, Lavooi E, Makaske B. 2012. Evaluating competing hypotheses for the origins and dynamics of river anastomosis. *Earth Surface Processes and Landforms* in press (cited in Chapter 1).

Kleinhans MG, Ferguson RI, Lane SN, Hardy RJ. 2012. Splitting rivers at their seams: bifurcations and avulsion. *Earth Surface Processes and Landforms* in press (cited in Chapter 3).

Knighton AD, Nanson GC. 1993. Anastomosis and the continuum of channel pattern. *Earth Surface Processes and Landforms* **18**: 613-625.

Krepper CM, Garcia NO, Jones PD. 2006. Paraguay river basin response to seasonal rainfall. *International Journal of Climatology* **26**: 1267-1278.

Lambert CP, Walling DE. 1987. Floodplain Sedimentation: A Preliminary Investigation of Contemporary Deposition within the Lower Reaches of the River Culm, Devon, UK. *Geografiska Annaler. Series A, Physical Geography* **69**: 393-404.

Lane EW. 1957. *A study of the shape of channels formed by natural streams flowing in erodible material*. MRD Sediment Series No. 9, US Army Engineer Division, Omaha, NE.

Larsen EW, Girvetz EH, Fremier AK. 2006. Assessing the effects of alternative setback channel constraint scenarios employing a river meander migration model. *Environmental Management* **37**: 880-897.

Latrubesse EM. 2008. Patterns of anabranching channels: The ultimate end-member adjustment of mega rivers. *Geomorphology* **101**: 130-145.

Latrubesse EM, Chen Z, Stevaux JC. 2009. Preface to the special volume short and long term processes, landforms and responses in large rivers. *Geomorphology* **113**: 127-128.

Lauer JW, Parker G. 2008a. Modeling framework for sediment deposition, storage, and evacuation in the floodplain of a meandering river: Theory. *Water Resources Research* **44**: W04425 doi: 10.1029/2006wr005528.

Lauer JW, Parker G. 2008b. Modeling framework for sediment deposition, storage, and evacuation in the floodplain of a meandering river: Application to the Clark Fork River, Montana. *Water Resources Research* **44**: W08404 doi: 10.1029/2006wr005529.

Lauer JW, Parker G. 2008c. Net local removal of floodplain sediment by river meander migration. *Geomorphology* **96**: 123-149.

Lauer JW, Parker G, Dietrich WE. 2008. Response of the Strickland and Fly River confluence to postglacial sea level rise. *Journal of Geophysical Research-Earth Surface* **113**: F01S06 doi: 10.1029/2006jf000626.

Leopold LB, Wolman MG. 1957. River Channel Patterns: Braided, Meandering and Straight. Geological Survey Professional Paper 282-B.

Lesser GR, Roelvink JA, van Kester JATM, Stelling G. 2004. Development and validation of a three-dimensional morphological model. *Journal of Coastal Engineering* **51**: 883-915.

Lewin J, Brindle BJ. 1977. Confined meanders. In: Gregory KJ (ed). *River Channel Changes.* John Wiley and Sons: Chichester, 221-234.

Lewin J, Davies BE, Wolfenden PJ. 1977. Interactions between channel change and historic mining sediments. In: Gregory KJ (ed). *River Channel Changes*, John Wiley and Sons: Chichester, 353-367.

Lewin J, Hughes D. 1980. Welsh floodplain studies: II. Application of a qualitative inundation model. *Journal of Hydrology* **46**: 35-49.

Lewin J, Bradley SB, Macklin MG. 1983. Historical valley alluviation in mid-Wales. *Geological Journal* **18**: 331-350.

Lewin J, Macklin MG. 1987. Metal mining and floodplain sedimentation in Britain. In: Gardiner V (ed). *International Geomorphology 1986 Part 1.* John Wiley and Sons: Chichester, 1009-1027.

Lewin J, Brewer PA. 2001. Predicting channel patterns. *Geomorphology* **40**: 329-339.

Lewin J, Brewer PA. 2003. Reply to Van den Berg and Bledsoe's comment on Lewin and Brewer (2001) "Predicting Channel Patterns", Geomorphology 40, 329-339. *Geomorphology* **53**: 339-342.

Lewin J, Macklin MG. 2010. Floodplain catastrophes in the UK Holocene: messages for managing climate change. *Hydrological Processes* **24**: 2900-2911.

Lewis GW, Lewin J. 1983. Alluvial cutoffs in Wales and the Borderlands. *Special Publications of the International Association of Sedimentologists* **6**: 145-154.

Lokhtin VM. 1897. *River Channel Processes.* Ministry of Internal Waterways, St. Petersburg, 80pp (in Russian).

Low N, Gleeson B. 1998. Situating justice in the environment: the case of BHP at the Ok Tedi Copper mine. *Antipode* **30**: 201-226.

Lu XX, Chen XQ. 2008. Larger Asian rivers and their interactions with estuaries and coasts. *Quaternary International* **186**: 1-3.

Lu X, Jiang T. 2009. Larger Asian rivers: Climate change, river flow and sediment flux. *Quaternary International* **208**: 1-3.

Luchi R, Hooke JM, Zolezzi G, Bertoldi W. 2010a. Width variations and mid-channel bar inception in meanders: River Bollin (UK). *Geomorphology* **119**: 1-8.

Luchi R, Zolezzi G, Tubino M. 2010b. Modelling mid-channel bars in meandering channels. *Earth Surface Processes and Landforms* **35**: 902-917.

Magilligan FJ. 1992. Sedimentology of a fine-grained aggrading floodplain. *Geomorphology* **4**: 393-408.

Makaske B. 2001. Anastomosing rivers: a review of their classification, origin and sedimentary products. *Earth-Science Reviews* **53**: 149-196.

Makaske B, Smith DG, Berendsen HJA, de Boer AG, van Nielen-Kiezebrink MF, Locking T. 2009. Hydraulic and sedimentary processes causing anastomosing morphology of the upper Columbia River, British Columbia, Canada. *Geomorphology* **111**: 194-205.

McCarthy TS, Ellery WN. 1998. The Okavango Delta. *Transactions of the Royal Society of South Africa* **53**: 157-182.

Meade RH. 1996. River-sediment inputs to major deltas. In: Milliman JD, Haq BU (eds). *Sea-level Rise and Coastal Subsidence: Causes, Consequences and Strategies.* Kluwer, Dordrecht, 63-85.

Mertes LAK, Dunne T, Martinelli LA. 1996. Channel-floodplain geomorphology along the Solimões-Amazon River, Brazil. *Geological Society of America Bulletin* **108**: 1089-1107.

Micheli ER, Larsen EW. 2010. River channel cutoff dynamics, Sacramento River, California, USA. *River Research and Applications* doi: 10.1002/rra.1360.

Middelkoop H, Asselman NEM. 1998. Spatial variability of floodplain sedimentation at the event scale in the Rhine–Meuse delta, The Netherlands. *Earth Surface Processes and Landforms* **23**: 561-573.

Middelkoop H, van der Perk M. 1998. Modelling Spatial Patterns of Overbank Sedimentation on Embanked Floodplains. *Geografiska Annaler. Series A, Physical Geography* **80**: 95-109.

Millennium Ecosystem Assessment (MEA). 2005. *Ecosystems and Human Well-being: Synthesis.* Island Press: Washington, DC, 155pp.

Milliman JD. 1995. Sediment discharge to the ocean from small mountainous rivers: The New Guinea example. *Geo-Marine Letters* **15**: 127-133.

Milliman JD, Meade RH. 1983. World-Wdie Delivery of River Sediment to the Oceans. *Journal of Geology* **91**: 1-21.

Milliman JD, Syvitski JPM. 1992. Geomorphic/Tectonic Control of Sediment Discharge to the Ocean: The Importance of Small Mountainous Rivers. *The Journal of Geology* **100**: 525-544.

Milliman JD, Farnsworth KL. 2011. *River Discharge to the Coastal Ocean: A Global Synthesis*. Cambridge University Press, New York.

Miori S, Repetto R, Tubino M. 2006. A one-dimensional model of bifurcations in gravel bed channels with erodible banks. *Water Resources Research* **42**: W11413 doi: 10.1029/2006wr004863.

Mosselman E, Huisink M, Koomen E, Seymonsbergen A. 1995. Morphological changes in a large braided sand-bed river. In: Hickin E (ed). *River Geomorphology*. John Wiley and Sons: Chichester, 235-247.

Nagelkerke NJD. 1991. A note on the general definition of the coefficient of determination. *Biometrika* **78**: 691-692.

Nanson GC. 1980. Point bar and floodplain formation on the meandering Beatton River, northeastern British Columbia, Canada. *Sedimentology* **27**: 3-29.

Nanson GC, Croke JC. 1992. A genetic classification of floodplains. *Geomorphology* **4**: 459-486.

Nanson GC, Knighton AD. 1996. Anabranching rivers: Their cause, character and classification. *Earth Surface Processes and Landforms* **21**: 217-239.

Nanson GC, Huang HQ. 2008. Least action principle, equilibrium states, iterative adjustment and the stability of alluvial channels. *Earth Surface Processes and Landforms* **33**: 923-942.

Nelson JM, Smith JD. 1989. Flow in Meandering Channels with Natural Topography. In: Ikeda S, Parker G (eds). *River Meandering*. AGU Water Resources Monograph 12, 69-102.

Nicholas AP, Ashworth PJ, Kirkby MJ, Macklin MG, Murray T. 1995. Sediment slugs: large-scale fluctuations in fluvial sediment transport rates and storage volumes. *Progress in Physical Geography* **19**: 500-519.

Nicholas AP, Walling DE. 1997. Modelling flood hydraulics and overbank deposition on river floodplains. *Earth Surface Processes and Landforms* **22**: 59-77.

Nilsson C, Reidy CA, Dynesius M, Revenga C. 2005. Fragmentation and Flow Regulation of the World's Large River Systems. *Science* **308**: 405-408.

Nittrouer CA, Sternberg RW. 1981. The formation of sedimentary strata in an allochthonous shelf environment: The Washington Continental Shelf. *Marine Geology* **42**: 210-232.

Parker G. 1978. Self-formed straight rivers with equilibrium banks and mobile bed: part 2. The gravel river. *Journal of Fluid Mechanics* **89**: 127-146.

Parker G, Muto T, Akamatsu Y, Dietrich WE, Lauer JW. 2008. Unravelling the conundrum of river response to rising sea-level from laboratory to field. Part II. The Fly-Strickland River system, Papua New Guinea. *Sedimentology* **55**: 1657-1686.

Parker G, Shimizu Y, Wilkerson GV, Eke EC, Abad JD, Lauer JW, Paola C, Dietrich WE, Voller VR. 2010. A new framework for modeling the migration of meandering rivers. *Earth Surface Processes and Landforms* **36**: 70-86.

Peakall J, Ashworth PJ, Best JL. 2007. Meander-bend evolution, alluvial architecture, and the role of cohesion in sinuous river channels: A flume study. *Journal of Sedimentary Research* **77**: 197-212.

Perucca E, Camporeale C, Ridolfi L. 2006. Influence of river meandering dynamics on riparian vegetation pattern formation. *Journal of Geophysical Research-Biogeosciences* **111**: G01001 doi: 10.1029/2005jg000073.

Perucca E, Camporeale C, Ridolfi L. 2007. Significance of the riparian vegetation dynamics on meandering river morphodynamics. *Water Resources Research* **43**: W03430 doi: 10.1029/2006wr005234.

Phillips JD. 2010. The job of the river. *Earth Surface Processes and Landforms* **35**: 305-313.

Pickup G. 1984. Geomorphology of Tropical Rivers 1: Landforms, Hydrology and Sedimentation in the Fly and Lower Purari, Papua New Guinea. *Catena Supplement* **5**: 1-17.

Pickup G, Higgins RJ, Warner RF. 1981. Erosion and sediment yield in the Fly River drainage basins, Papua New Guinea. *Erosion and Sediment Transport in Pacific Rim Steeplands.* IAHS Publication 132, 438-456.

Pickup G, Marshall AR. 2009. Geomorphology, Hydrology, and Climate of the Fly River System. In: Bolton B (ed). *The Fly River, Papua New Guinea: Environmental Studies in an Impacted Tropical River System*. Developments in Earth and Environmental Sciences 9, Elsevier, 3-49.

Pinter N, Miller K, Wlosinski JH, van der Ploeg RR. 2004. Recurrent shoaling and channel dredging, Middle and Upper Mississippi River, USA. *Journal of Hydrology* **290**: 275-296.

Pizzuto JE. 1987. Sediment diffusion during overbank flows. *Sedimentology* **34**: 301-317.

Potter PE. 1978. Significance and Origin of Big Rivers. *The Journal of Geology* **86**: 13-33.

Repetto R, Tubino M, Paola C. 2002. Planimetric instability of channels with variable width. *Journal of Fluid Mechanics* **457**: 79-109.

Richards KS, Chandra S, Friend P. 1993. Avulsive channel systems: characteristics and examples. In: Best JL, Bristow CS (eds). *Braided Rivers*, Geological Society Special Publication 75, 195-203.

Rohrer WLM. 1984. Effects of flow and bank material on meander migration in alluvial rivers. In: Elliott CM (ed). *River Meandering*. American Society of Civil Engineers, New York, 770-782.

Rowland JC, Lepper K, Dietrich WE, Wilson CJ, Sheldon R. 2005. Tie channel sedimentation rates, oxbow formation age and channel migration rate from optically stimulated luminescence (OSL) analysis of floodplain deposits. *Earth Surface Processes and Landforms* **30**: 1161-1179.

Rowntree KM, Dollar ESJ. 1996. Controls on channel form and channel change in the Bell River, Eastern Cape, South Africa. *South African Geographical Journal* **78**: 20-28.

Rowntree KM, Dollar ESJ. 1998. Vegetation controls on channel stability in the Bell River, Eastern Cape, South Africa. *Earth Surface Processes and Landforms* **24**: 127-134.

Russell RJ. 1954. Alluvial Morphology of Anatolian Rivers. *Annals of the Association of American Geographers* **44**: 363-391.

Schumm SA. 1963. Sinuosity of Alluvial Rivers on the Great Plains. *Geological Society of America Bulletin* **74**: 1089-1100.

Schumm SA. 1985. Patterns of Alluvial Rivers. *Annual Review of Earth and Planetary Sciences* **13**: 5-27.

Schumm SA. 2005. *River Variability and Complexity.* Cambridge University Press, Cambridge, 220pp.

Schumm SA, Khan HR. 1972. Experimental Study of Channel Patterns. *Geological Society of America Bulletin* **83**: 1755-1770.

Seminara G. 2006. Meanders. *Journal of Fluid Mechanics* **554**: 271-297.

Singer MB, Aalto R. 2009. Floodplain development in an engineered setting. *Earth Surface Processes and Landforms* **34**: 291-304.

Singh A, Fienberg K, Jerolmack DJ, Marr J, Foufoula-Georgiou E. 2009. Experimental evidence for statistical scaling and intermittency in sediment transport rates. *Journal of Geophysical Research-Earth Surface* **114**: F01025 doi:10.1029/2007JF000963.

Sinha R, Friend PF. 2007. Quaternary fluvial systems of India. *Quaternary International* **159**: 1-5.

Slingerland R, Smith ND. 1998. Necessary conditions for a meandering-river avulsion. *Geology* **26**: 435-438.

Smith CE. 1998. Modelling high sinuosity meanders in a small flume. *Geomorphology* **25**: 19-30.

Smith JD, Maclean SR. 1984. A Model for Flow in Meandering Streams. *Water Resources Research* **20**: 1031 doi: 10.1029/WR020i009p01301.

Soulsby R. 1997. *Dynamics of Marine Sands*. Thomas Telford Publications, London, 253pp.

Sparks RE. 1995. Need for Ecosystem Management of Large Rivers and Their Floodplains. *BioScience* **45**: 168-182.

Stølum HH. 1996. River meandering as a self-organization process. *Science* **271**: 1710-1713.

Stølum HH. 1998. Planform geometry and dynamics of meandering rivers. *Geological Society of America Bulletin* **110**: 1485-1498.

Storey AW, Marshall AR, Yarrao M, Barrie B. 2009. Effects of Mine-Derived River Bed Aggradation on Fish Habitat of the Fly River, Papua New Guinea. In: Bolton B (ed). *The Fly River, Papua New Guinea: Environmental Studies in an Impacted Tropical River System*. Developments in Earth and Environmental Sciences 9, Elsevier, 463-490.

Struiksma N, Olesen K, Flokstra C, De Vriend H. 1985. Bed deformation in curved alluvial channels. *Journal of Hydraulic Research* **23**: 57-79.

Swanson KM, Watson E, Aalto R, Lauer JW, Bera MT, Marshall A, Taylor MP, Apte SC, Dietrich WE. 2008. Sediment load and floodplain deposition rates: Comparison of the Fly and Strickland Rivers, Papua New Guinea. *Journal of Geophysical Research-Earth Surface* **113**: F01S03.

Syvitski JPM, Vörösmarty CJ, Kettner AJ, Green P. 2005. Impact of Humans on the Flux of Terrestrial Sediment to the Global Coastal Ocean. *Science* **308**: 376-380.

Tal M, Paola C. 2007. Dynamic single-thread channels maintained by the interaction of flow and vegetation. *Geology* **35**: 347-350.

Tal M, Paola C. 2010. Effects of vegetation on channel morphodynamics: results and insights from laboratory experiments. *Earth Surface Processes and Landforms* **35**: 1014-1028.

Talmon AM, Struiksma N, van Mierlo MCLM. 1995. Laboratory measurements of the direction of sediment transport on transverse alluvial-bed slopes *Journal of Hydraulic Research* **33**: 495-517.

Thompson DM. 2003. A geomorphic explanation for a meander cutoff following channel relocation of a coarse-bedded river. *Environmental Management* **31**: 385-400.

Thorne CR. 1997. Channel types and morphological classification. In: Thorne CR, Hey RD, Newson MD (eds). *Applied Fluvial Geomorphology for River Engineering and Management.* John Wiley and Sons: Chichester, 175-222.

Thorne CR. 2002. Geomorphic analysis of large alluvial rivers. *Geomorphology* **44**: 203-219.

Tooth S, McCarthy TS, Brandt D, Hancox PJ, Morris R. 2002. Geological controls on the formation of alluvial meanders and floodplain wetlands: The example of the Klip River, eastern Free State, South Africa. *Earth Surface Processes and Landforms* **27**: 797-815.

Törnqvist TE, Bridge JS. 2002. Spatial variation of overbank aggradation rate and its influence on avulsion frequency. *Sedimentology* **49**: 891-905.

Törnqvist TE, Bridge JS. 2006. Causes of River Avulsion: Insights from the Late Holocene Avulsion History of the Mississippi River, U.S.A. – Discussion. *Journal of Sedimentary Research* **76**: 959.

Tower WS. 1904. The development of cutoff meanders. *Bulletin of the American Geographical Society of New York* **36**: 589-599.

Uittenbogaard RE, van Kester JATM, Stelling GS. 1992. Implementation of three turbulence models in 3D-TRISULA for rectangular grids. Technical Report Z81, WL/Delft Hydraulics, Delft, The Netherlands.

van den Berg JH. 1995. Prediction of alluvial channel pattern of perennial rivers. *Geomorphology* **12**: 259-279.

van den Berg JH, Bledsoe BP. 2003. Comment on Lewin and Brewer (2001): "Predicting channel patterns", Geomorphology 40, 329-339. *Geomorphology* **53**: 333-337.

van Rijn LC. 1984. Sediment Transport, Part III: Bed Forms and Alluvial Roughness. *Journal of Hydraulic Engineering* **110**: 1733-1754.

van Rijn LC. 1993. *Principles of Sediment Transport in Rivers, Estuaries and Coastal Seas*. Aqua Publications, The Netherlands.

Vienna Declaration. 2011. Vienna Declaration on the Status and Future of the World's Large Rivers, Vienna, 13 April 2011, by Participants of the International Conference on the Status and Future of the World's Large Rivers.

Vörösmarty CJ, McIntyre PB, Gessner MO, Dudgeon D, Prusevich A, Green P, Glidden S, Bunn SE, Sullivan CA, Liermann CR, Davies PM. 2010. Global threats to human water security and river biodiversity. *Nature* **467**: 555-561.

Vörösmarty CJ, Meybeck M, Fekete B, Sharma K, Green P, Syvitski JPM. 2003. Anthropogenic sediment retention: major global impact from registered river impoundments. *Global and Planetary Change* **39**: 169-190.

Walling DE. 2006. Human impact on land-ocean sediment transfer by the world's rivers. *Geomorphology* **79**: 192-216.

Walling DE, He Q, Nicholas AP. 1996. Floodplains as suspended sediment sinks. In: Anderson MG, Walling DE, Bates PD (eds). *Floodplain Processes*. John Wiley and Sons: Chichester, 399-440.

Walling DE, Fang D. 2003. Recent trends in the suspended sediment loads of the world's rivers. *Global and Planetary Change* **39**: 111-126.

Walling DE, Owens PN, Carter J, Leeks GJL, Lewis S, Meharg AA, Wright J. 2003. Storage of sediment-associated nutrients and contaminants in river channel and floodplain systems. *Applied Geochemistry* **18**: 195-220.

Wang ZB, Fokkink RJ, DeVries M, Langerak A. 1995. Stability of river bifurcations in 1D morphodynamic models. *Journal of Hydraulic Research* **33**: 739-750.

Zinger JA, Rhoades BL, Best JL. 2011. Extreme sediment pulses generated by bend cutoffs along a large meandering river. *Nature Geoscience* **4**: 675-678.

Zolezzi G, Seminara G. 2001. Downstream and upstream influence in river meandering. Part 1. General theory and application to overdeepening. *Journal of Fluid Mechanics* **438**: 183-211.

Personal Communication

Aalto R. Observations on vegetation in chute channels during a field campaign on the Beni River, Bolivia, August 2011.